


Spring 2012

# The search for an optimal means of determining the minmax control parameter using sensitivity analysis

John Teye Brown

Follow this and additional works at: <https://digitalcommons.latech.edu/dissertations>

 Part of the [Applied Mathematics Commons](#), and the [Mechanical Engineering Commons](#)

---

**THE SEARCH FOR AN OPTIMAL MEANS  
OF DETERMINING THE MINMAX  
CONTROL PARAMETER  
USING SENSITIVITY  
ANALYSIS**

by

John Teye Brown, B.Eng., M.S.

A Dissertation Presented in Partial Fulfillment  
of the Requirements of the Degree  
Doctor of Philosophy

COLLEGE OF ENGINEERING AND SCIENCE  
LOUISIANA TECH UNIVERSITY

May 2012

UMI Number: 3515929

All rights reserved

INFORMATION TO ALL USERS

The quality of this reproduction is dependent upon the quality of the copy submitted.

In the unlikely event that the author did not send a complete manuscript and there are missing pages, these will be noted. Also, if material had to be removed, a note will indicate the deletion.



UMI 3515929

Published by ProQuest LLC 2012. Copyright in the Dissertation held by the Author.  
Microform Edition © ProQuest LLC.

All rights reserved. This work is protected against  
unauthorized copying under Title 17, United States Code.



ProQuest LLC  
789 East Eisenhower Parkway  
P.O. Box 1346  
Ann Arbor, MI 48106-1346

LOUISIANA TECH UNIVERSITY

THE GRADUATE SCHOOL

MAY 19, 2012

Date

We hereby recommend that the dissertation prepared under our supervision  
by John Teye Brown

entitled THE SEARCH FOR AN OPTIMAL MEANS OF DETERMINING  
THE MINMAX PARAMETER USING SENSITIVITY ANALYSIS

be accepted in partial fulfillment of the requirements for the Degree of  
Doctor of Philosophy

Kath A. Evans

Supervisor of Dissertation Research

Wizhong Shi

Head of Department

Computational Analysis and Modeling

Department

Recommendation concurred in:

Wizhong Shi

[Signature]

[Signature]

[Signature]

Advisory Committee

Approved:

Bala Ramachandran

Director of Graduate Studies

Approved:

William M. Connelly

Dean of the Graduate School

[Signature]

Dean of the College

## ABSTRACT

The use of computational methods for design and simulation of control systems allows for a cost-effective trial and error approach. In this work, we are concerned with the robust, real-time control of physical systems whose state space is infinite-dimensional. Such systems are known as Distributed Parameter Systems (DPS). A body whose state is heterogeneous is a distributed parameter. In particular, this work focuses on DPS systems that are governed by linear Partial Differential Equations, such as the heat equation. We specifically focus on the MinMax controller, which is regarded as being a very robust controller. The mathematical formulation of the MinMax controller involves a design parameter,  $\theta$ . This parameter provides a numerical measure of the robustness of the MinMax controller; hence it is very important. However, there exists no explicit formula for determining its value in advance of attempted control design. Currently, this parameter's optimal value- optimal in the sense of robustness- is determined experimentally using an iterative process that seeks to maintain stability in the closed loop control system as well as an always positive definite result for  $[I - \theta^2 P \Pi]$  (i.e.  $[I - \theta^2 P \Pi] > 0$ ) where  $I$  is the identity matrix, while  $P$  and  $\Pi$  are solutions to Algebraic Riccati Equations discussed in this dissertation. This process is obviously computationally expensive.

The search for a more efficient means of determining  $\theta$ , including the possibility of the emergence of an explicit formula based on some mathematically rigorous criteria,

is the driving force for this work. We use sensitivity analysis as a tool to mathematically investigate different criteria (such as the controller sensitivity, state sensitivity, Riccati equations' sensitivity, etc.) to help achieve our goal of formulating a more efficient means of determining an optimal value for  $\theta$ .

For each of the systems investigated, it was found that low  $\theta$  values (e.g. 0.05) are sufficient for adequate performance, robustness, and convergence of the MinMax controller.

## APPROVAL FOR SCHOLARLY DISSEMINATION

The author grants to the Prescott Memorial Library of Louisiana Tech University the right to reproduce, by appropriate methods, upon request, any or all portions of this Dissertation. It is understood that "proper request" consists of the agreement, on the part of the requesting party, that said reproduction is for his personal use and that subsequent reproduction will not occur without written approval of the author of this Dissertation. Further, any portions of the Dissertation used in books, papers, and other works must be appropriately referenced to this Dissertation.

Finally, the author of this Dissertation reserves the right to publish freely, in the literature, at any time, any or all portions of this Dissertation.

Author John Lee Brown

Date May 1, 2012

## **DEDICATION**

To my family in Ghana, Guyana, Belize, Canada, and the USA. Thanks for all your support. To my mother Rebecca: I wish I had gotten the chance to know you. Some day we will meet again. I love you.



## TABLE OF CONTENTS

ABSTRACT.....	iii
DEDICATION.....	vi
LIST OF FIGURES .....	x
ACKNOWLEDGMENTS .....	xvii
CHAPTER 1 INTRODUCTION .....	1
1.1    Control of Distributed Parameter Systems .....	1
1.2    The Finite Dimensional MinMax Controller in Brief.....	2
1.3    The MinMax Parameter Problem .....	3
1.4    Sensitivity Analysis .....	4
1.5    Heat in a Thin Rod.....	6
1.6    Overview of Dissertation .....	7
CHAPTER 2 THEORETICAL BACKGROUND AND CONTROL DESIGN .....	9
2.1    Problem Formulation .....	9
2.2    Semigroups .....	10
2.3    MinMax Controller design.....	11
2.4    Stability Analysis and Robustness.....	13
2.5    Riccati Sensitivity.....	14
2.6    Controller Sensitivity.....	15
2.7    Sensitivity of the Compensator state .....	16
2.8    Functional Gains.....	17

CHAPTER 3 HEAT EQUATION .....	19
3.1 1-D Heat Equation .....	19
3.2 Numerical Results .....	23
3.2.1 Uncontrolled Results .....	23
3.2.2 Controlled Results .....	24
3.2.3 Stability Analysis .....	26
3.2.4 Control Effort .....	30
3.2.5 Sensitivity Analysis .....	36
3.2.6 Riccati Sensitivity .....	47
3.3 2-D Heat Equation .....	49
3.4 Numerical Results .....	52
3.4.1 Uncontrolled Results .....	52
3.4.2 Controlled Results .....	53
3.4.3 Stability Analysis .....	57
3.4.4 Control Effort .....	59
3.4.5 Sensitivity Analysis .....	61
3.4.6 Riccati Sensitivity .....	67
CHAPTER 4 WAVE EQUATION .....	69
4.1 Problem Formulation .....	69
4.2 Numerical Results .....	73
4.2.1 Uncontrolled Results .....	73
4.2.2 Controlled Results .....	74
4.2.3 Stability Analysis .....	78
4.2.4 Control Effort .....	80
4.2.5 Sensitivity Analysis .....	87

4.2.6	Controller Sensitivity .....	90
4.2.7	Riccati Sensitivity .....	97
<b>CHAPTER 5 EULER-BERNOULLI CANTILEVER BEAM WITH A ROTATING HUB .....</b>		<b>99</b>
5.1	Problem Formulation .....	99
5.2	Numerical Results .....	105
5.2.1	Uncontrolled Results .....	105
5.2.2	Controlled Results .....	106
5.2.3	Stability Analysis .....	110
5.2.4	Control Effort .....	112
5.2.5	Sensitivity Analysis .....	113
5.2.6	Riccati Sensitivity .....	121
<b>CHAPTER 6 CONCLUSIONS AND FUTURE WORK .....</b>		<b>123</b>
6.1	Conclusions .....	123
6.2	Future Work .....	126
<b>APPENDIX A NUMERICAL MODELING OF EXACT SOLUTIONS .....</b>		<b>127</b>
A.1	Exact Solutions .....	128
A.1.1	Uncontrolled 1-dimension Heat Equation .....	128
A.1.2	2-Dimensional Heat Equation .....	129
A.1.3	1-Dimensional Wave Equation .....	130
<b>APPENDIX B FINITE DIFFERENCE SOLUTIONS .....</b>		<b>131</b>
B.1	Finite Difference Solutions .....	132
B.1.1	1-dimensional heat equation .....	132
B.1.2	2-Dimensional Heat Equation .....	133
B.1.3	1-Dimensional Wave Equation .....	135
<b>BIBLIOGRAPHY .....</b>		<b>137</b>

## LIST OF FIGURES

Figure 3-1: Heat flow in 1-d rod .....	20
Figure 3-2: Uncontrolled heat flow in 1-d rod.....	23
Figure 3-3: Functional gains, $\theta = 0.05$ Figure 3-4: Functional gains, $\theta = 0.2$ .....	24
Figure 3-5: Functional gains, $\theta = 0.5$ Figure 3-6: Functional gains, $\theta = 0.7$ .....	24
Figure 3-7: Controlled temperature, full state MinMax.....	25
Figure 3-8: Controlled temperature, state estimate MinMax.....	26
Figure 3-9: Eigenvalues of $\begin{bmatrix} A & -BK \\ FC & A_c \end{bmatrix}$ .....	28
Figure 3-10: Eigenvalues of $\begin{bmatrix} A & -BK \\ FC & A_c \end{bmatrix}$ .....	29
Figure 3-11: Control effort, full state MinMax.....	31
Figure 3-12: Control effort, full state MinMax.....	31
Figure 3-13: Control effort, full state MinMax.....	32
Figure 3-14: Control effort, full state MinMax.....	32
Figure 3-15: Control effort, state estimate MinMax.....	33
Figure 3-16: Control effort, state estimate MinMax.....	33
Figure 3-17: Control effort, state estimate MinMax.....	34
Figure 3-18: Control effort, state estimate MinMax.....	34
Figure 3-19: Sensitivity of state.....	39
Figure 3-20: Controller sensitivity, full state MinMax.....	40
Figure 3-21: controller sensitivity, full state MinMax.....	40

Figure 3-22: Controller sensitivity, full state MinMax .....	41
Figure 3-23: Controller sensitivity, full-state MinMax.....	41
Figure 3-24: Controller sensitivity, state estimate MinMax .....	42
Figure 3-25: Controller sensitivity, state estimate MinMax .....	42
Figure 3-26: Controller sensitivity, state estimate MinMax .....	43
Figure 3-27: Controller sensitivity, state estimate MinMax .....	43
Figure 3-28: Maximum absolute $S_u(t)$ values.....	46
Figure 3-29: Maximum absolute $S_u(t)$ values.....	47
Figure 3-30: Norm of $\Pi_\theta$ versus $\theta$ .....	48
Figure 3-31: Norm of $P_\theta$ versus $\theta$ .....	48
Figure 3-32: Two-dimensional heat surface .....	49
Figure 3-33: Uncontrolled heat flow along center of 2-d square surface .....	53
Figure 3-34: Functional gains .....	54
Figure 3-35: Functional gains .....	54
Figure 3-36: Functional gains .....	54
Figure 3-37: Functional gains .....	55
Figure 3-38: Controlled temperature, full state MinMax system .....	56
Figure 3-39: Controlled temperature, state estimate MinMax system.....	56
Figure 3-40: Eigenvalues of $\begin{bmatrix} A & -BK \\ FC & A_c \end{bmatrix}$ .....	57
Figure 3-41: Eigenvalues of $\begin{bmatrix} A & -BK \\ FC & A_c \end{bmatrix}$ .....	58
Figure 3-42: Control effort, full state MinMax.....	60
Figure 3-43: Control effort, state estimate MinMax.....	60
Figure 3-44: Sensitivity of state.....	64

Figure 3-45: Controller sensitivity, state estimate MinMax .....	65
Figure 3-46: Controller sensitivity, full state MinMax .....	65
Figure 3-47: Maximum absolute $S_u(t)$ values, full state MinMax .....	66
Figure 3-48: Maximum absolute values, state estimate MinMax .....	67
Figure 3-49: Norm of $\Pi_\theta$ versus $\theta$ .....	68
Figure 3-50: Norm of $P_\theta$ versus $\theta$ .....	68
Figure 4-1: Control input functions .....	73
Figure 4-2: Uncontrolled displacement .....	74
Figure 4-3: Functional gains for $\theta = 0.08$ .....	75
Figure 4-4: Functional gains for $\theta = 0.16$ .....	75
Figure 4-5: Functional gains for $\theta = 0.32$ .....	76
Figure 4-6: Controlled state position, full state MinMax .....	77
Figure 4-7: Controlled displacement, state estimate MinMax .....	78
Figure 4-8: Eigenvalues of $\begin{bmatrix} A & -BK \\ FC & A_c \end{bmatrix}$ .....	79
Figure 4-9: Eigenvalues of $\begin{bmatrix} A & -BK \\ FC & A_c \end{bmatrix}$ .....	79
Figure 4-10: Control effort for full state MinMax system ( $\theta = 0.04$ ): controller 1 (top left), controller 2 (top right), controller 3 (bottom left), controller 4 (bottom right).....	81
Figure 4-11: Control effort for full state MinMax system ( $\theta = 0.08$ ): controller 1 (top left), controller 2 (top right), controller 3 (bottom left), controller 4 (bottom right).....	81
Figure 4-12: Control effort for full state MinMax System ( $\theta = 0.16$ ): controller 1 (top left), controller 2 (top right), controller 3 (bottom left), controller 4 (bottom right).....	82

Figure 4-13: Control effort for full state MinMax system ( $\theta = 0.32$ ): controller 1 (top left), controller 2 (top right), controller 3 (bottom left), controller 4 (bottom right).....	82
Figure 4-14: Control effort for state estimate MinMax system ( $\theta = 0.04$ ): controller 1 (top left), controller 2 (top right), controller 3 (bottom left), controller 4 (bottom right).....	83
Figure 4-15: Control effort for state estimate MinMax system ( $\theta = 0.08$ ): controller 1 (top left), controller 2 (top right), controller 3 (bottom left), controller 4 (bottom right).....	84
Figure 4-16: Control effort for state estimate MinMax system ( $\theta = 0.16$ ): controller 1 (top left), controller 2 (top right), controller 3 (bottom left), controller 4 (bottom right).....	84
Figure 4-17: Control effort for state estimate MinMax system ( $\theta = 0.32$ ): controller 1 (top left), controller 2 (top right), controller 3 (bottom left), controller 4 (bottom right).....	85
Figure 4-18: Sensitivity of state position .....	89
Figure 4-19: Controller sensitivity for full state MinMax system ( $\theta = 0.04$ ): controller 1 (top left), controller 2 (top right), controller 3 (bottom left), controller 4 (bottom right).....	90
Figure 4-20: Controller sensitivity for full state MinMax system ( $\theta = 0.08$ ): controller 1 (top left), controller 2 (top right), controller 3 (bottom left), controller 4 (bottom right).....	91
Figure 4-21: Controller sensitivity for full state MinMax system ( $\theta = 0.16$ ): controller 1 (top left), controller 2 (top right), controller 3 (bottom left), controller 4 (bottom right).....	91
Figure 4-22: Controller sensitivity for full state MinMax system ( $\theta = 0.32$ ): controller 1 (top left), controller 2 (top right), controller 3 (bottom left), controller 4 (bottom right).....	92
Figure 4-23: Controller sensitivity for state est. MinMax system ( $\theta = 0.04$ ): controller 1 (top left), controller 2 (top right), controller 3 (bottom left), controller 4 (bottom right).....	92
Figure 4-24: Controller sensitivity for state est. MinMax system ( $\theta = 0.08$ ): controller 1 (top left), controller 2 (top right), controller 3 (bottom left), controller 4 (bottom right).....	93

Figure 4-25: Controller sensitivity for state est. MinMax system ( $\theta = 0.16$ ): controller 1 (top left), controller 2 (top right), controller 3 (bottom left), controller 4 (bottom right).....	93
Figure 4-26: Controller sensitivity for state est. MinMax system ( $\theta = 0.32$ ): controller 1 (top left), controller 2 (top right), controller 3 (bottom left), controller 4 (bottom right).....	94
Figure 4-27: Maximum absolute controller sensitivity for full state MinMax system: controller 1 (top left), controller 2 (top right), controller 3 (bottom left), controller 4 (bottom right) .....	96
Figure 4-28: Maximum absolute controller sensitivity for state est. MinMax system: controller 1 (top left), controller 2 (top right), controller 3 (bottom left), controller 4 (bottom right) .....	97
Figure 4-29: Norm of $\Pi_\theta$ versus $\theta$ .....	98
Figure 4-30: Norm of $P_\theta$ versus $\theta$ .....	98
Figure 5-1: Euler-Bernoulli cantilever beam with a rotating hub .....	99
Figure 5-2: Uncontrolled displacement .....	106
Figure 5-3: Functional gains .....	107
Figure 5-4: Functional gains .....	107
Figure 5-5: Functional gains .....	108
Figure 5-6: Controlled state position, full state MinMax .....	109
Figure 5-7: Controlled state position, state estimate MinMax.....	109
Figure 5-8: Eigenvalues of $A - BKFCAC$ .....	110
Figure 5-9: Eigenvalues of $\begin{bmatrix} A & -BK \\ FC & A_c \end{bmatrix}$ .....	111
Figure 5-10: Control effort, full state MinMax.....	112
Figure 5-11: Control effort, state estimate MinMax.....	113
Figure 5-12: Sensitivity of state .....	118
Figure 5-13: Controller sensitivity, state estimate MinMax .....	119



Figure 5-14: Maximum $S_v(t)$ Values, full state system .....	120
Figure 5-15: Maximum $S_v(t)$ values, state estimate system .....	120
Figure 5-16: Norm of $\Pi_\theta$ versus $\theta$ .....	121
Figure 5-17: Norm of $P_\theta$ versus $\theta$ .....	122
Figure A-1: Exact solution of uncontrolled heat in 1-d rod.....	128
Figure A-2: Exact solution of uncontrolled heat on 2-d surface (along horizontal center).....	129
Figure A-3: Exact solution of displacement for 1-d wave equation .....	130
Figure B-4: Uncontrolled heat in 1-dimensional rod (explicit finite difference).....	133
Figure B-5: 2-D Grid used to generate matrix A .....	134
Figure B-6: Uncontrolled heat distribution across horizontal center of 2-dimensional square plate .....	135
Figure B-7: Uncontrolled displacement (explicit finite difference scheme) .....	136

## LIST OF TABLES

Table 3-1: Stability margin and radius for controlled system ( $A_{mm}$ ).....	30
Table 3-2: Area under control effort curve (Simpson's rule) .....	36
Table 3-3: Area under controller sensitivity curve (Simpson's rule) .....	45
Table 3-4: Stability margin and radius for controlled system ( $A_{mm}$ ) .....	59
Table 3-5: Area under control effort curve (Simpson's rule).....	61
Table 3-6: Area under controller sensitivity curve (Simpson's rule).....	66
Table 4-1: Stability margin and radius for controlled system ( $A_{mm}$ ).....	80
Table 4-2: Area under control effort curve (Simpson's rule).....	86
Table 4-3: Area under controller sensitivity curve (Simpson's rule).....	95
Table 5-1: Stability margin and radius for controlled system ( $A_{mm}$ ).....	111
Table 5-2: Area under control effort curve (Simpson's rule).....	113
Table 5-3: Area under controller sensitivity curve (Simpson's rule).....	119

## ACKNOWLEDGMENTS

To my advisor, Dr. Katie Allison Evans. I truly appreciate you being patient with my ups and downs, and I have learned a lot from you both academically and professionally. Thank you.

To my committee members:

Thank you Dr. Weizhong Dai for agreeing to be a member on my committee. I have not taken more classes with any other professor in my long and fruitful academic career as I have with you. The knowledge gained from Finite Difference methods and Numerical Analysis will forever guide my career.

To Dr. Dexter Cahoy: On short notice you agreed to participate on my committee. I thank you very much. I especially appreciate the knowledge gained in your Time Series class. It was great.

To Dr. Travis Atkison: Thank you for agreeing to be on my committee. You were very busy but accepted the offer to help me make my dreams come true. I am forever grateful.

To Dr. Lee Sawyer: I knew ever since I took Nuclear Physics with you that I wanted you to be on my committee. Your input is always greatly appreciated. I thank you very much for making yourself available

To Dr. Dave Meng. Thank you for participating in my oral defense despite your busy schedule. I appreciate it greatly.

To my Friends and Family. Thank you for being supportive. To my big brother Daniel. Thank you for showing me at an uncertain time in my young academic days, that Mathematics is simple because there is a solution to every Math problem and there are numerous ways to solve most problems. It really pushed my career on the path to this dissertation.

To Oneka. Without you I would not have made it through all the tough times. I only wish I could bless you someday in some way.

To my younger brother Donald. All your encouragements have helped greatly. Thank you.

To my mom and Dad. Thank you for everything. I love you.

To Richard. My 'brother from another mother'. Thanks for all your help. I want to especially thank God, with whom my mother and brother walk today. Keep them safe until I can see them.

# CHAPTER 1

## INTRODUCTION

### 1.1 Control of Distributed Parameter Systems

The design of control systems can be an expensive endeavor. However, the use of computational methods of design and simulation allows for a cost-effective trial and error approach. In this work, we are concerned with the robust real-time control of physical systems whose state space is infinite-dimensional. Such systems are known as Distributed Parameter Systems (DPS). A body whose state is heterogeneous is a distributed parameter system. In particular, this work focuses on DPS systems that are governed by linear Partial Differential Equations (PDEs). Examples of such systems include the heat equation, Euler-Bernoulli cantilevered beam, wave equation, etc.

Control design applied to a DPS also results in an infinite-dimensional PDE controller. For the purpose of computation and numerical simulation, we apply a discretization algorithm to approximate the PDE models by finite-dimensional systems. Controllers are designed for the finite-dimensional systems, resulting in finite-dimensional controllers, though they are known to converge to the infinite-dimensional, theoretical controllers [1].

There are many controllers that can be used for DPS control. The most classical of these controllers is the Linear Quadratic Regulator (LQR). The LQR and the Linear Quadratic Gaussians (LQG) are two of the most fundamental DPS control problems.

Their design and application are discussed fully in [2; 3]. The primary difference between the LQG and the LQR systems is that LQR is an example of full state feedback control (i.e. the entire state of the system is known at all time values), whereas the LQG is an example of state estimate feedback control (an observer or compensator is used to provide an estimate of the state based on measurements). Another example of DPS controller is the Central controller discussed at length in [4; 5]. This controller is known to stabilize the system it is applied to with a guaranteed robustness margin. The Central controller involves a control parameter that provides a measurement of its robustness. This parameter's value is given by a mathematically rigorous deterministic formula. Finally, another example of a DPS controller is the MinMax controller, which is the controller investigated in this dissertation.

### 1.2 The Finite Dimensional MinMax Controller in Brief

The following is a summarized excerpt from [6]. Consider a linear system described by

$$\dot{x}(t) = A(t)x(t) + B(t)u(t) + \Gamma(t)w(t), \quad \text{Eq. 1-1}$$

$$z(t) = H(t)x(t) + \Gamma_1(t)v(t), \quad \text{Eq. 1-2}$$

where  $x$  is the  $n \times 1$  state vector,  $u$  is the  $m \times 1$  input vector,  $z$  is the  $p \times 1$  measurement vector,  $w$  and  $v$  are the  $q \times 1$  and  $p \times 1$  input disturbance vectors, respectively. It is assumed that  $\Gamma_1$  is nonsingular. The measurement history up to  $t$  is defined as

$$Z_t = \{Z(s), 0 \leq s \leq t\}. \quad \text{Eq. 1-3}$$

The deterministic linear quadratic game problem under consideration is to obtain an optimal control strategy  $u(t) = u(Z_t)$ , for the worst case disturbances  $w(\cdot), v(\cdot)$  and

initial condition  $x(0)$  such that  $\min_u \max_v \max_w \max_{x(0)} J(u, v, w, x(0))$  subject to the constraints

in Eq. (1.1) and Eq. (1.2) where

$$J(u, v, w, x(0)) = \frac{1}{2} \left[ \frac{1}{\theta} \|x(0) - \hat{x}_0\|_{P_0^{-1}}^2 + \|x(T)\|_{Q_T}^2 + \int_0^T \left\{ \|x\|_{Q(t)}^2 + \|u\|_{R(t)}^2 + \frac{1}{\theta} \left( \|w\|_{W^{-1}(t)}^2 + \|v\|_{V^{-1}(t)}^2 \right) \right\} dt \right], \quad \text{Eq. 1-4}$$

$\theta$  is the control parameter,  $\hat{x}_0$  and the terminal time  $T$  are fixed, and all matrices have appropriate dimensions. It is assumed that  $R$ ,  $P_0$ ,  $W$  and  $V$  are positive definite, and  $Q$  and  $Q_T$  are nonnegative definite. Here  $\|x\|_A$  denotes  $\sqrt{x^T A x}$ . The minimization of the above cost function with respect to  $u$ , after it is already maximized with respect to the disturbances  $v, w$  and the initial state  $x_0$  is widely called the MinMax control problem.

### 1.3 The MinMax Parameter Problem

The MinMax controller is regarded as being a very robust controller. It has been implemented for such problems as the design of a fault detection filter [7] and flow control in a driven cavity [8]. Much work has been done in the past on the design and application of the MinMax controller e.g. [9; 10; 11; 12].

The MinMax controller is a state-space formulation of the well known  $H_\infty$  controller. The mathematical formulation of the  $H_\infty$  controller involves a control parameter whose optimal value remains an open problem in robust control theory [13]. In order to design a meaningful  $H_\infty$  control law for a system, the optimal control parameter,  $\theta^*$ , should be available before hand. In the literature, this value is determined by iterative schemes only. One such iterative scheme is as follows: start with a value  $\theta$  and determine whether  $\theta > \theta^*$  by solving two "indefinite" algebraic Riccati equations and checking the positive semi-definiteness and stabilizing properties of these solutions. If a

positive semi-definite solution exists, then  $\theta > \theta^*$  and the process is repeated with a lower  $\theta$ . This is clearly a computationally expensive process. Even more importantly, as  $\theta$  approaches  $\theta^*$ , numerical solutions of the algebraic Riccati equations become ill-conditioned. Secondly, as  $\theta$  decreases, evaluation of the coupling condition generally involves finding eigenvalues of stiff matrices. The iterative process is therefore inefficient and unreliable.

The search for a more efficient means of determining  $\theta$ , including the possibility of the emergence of an explicit formula, is the driving force for this work. We use sensitivity analysis as a tool to mathematically investigate different criteria such as the controller sensitivity, state sensitivity, Riccati equations' sensitivity, etc. to help achieve our aim of contributing towards the ultimate goal of determining a more efficient means of identifying  $\theta^*$ .

#### 1.4 Sensitivity Analysis

Sensitivity analysis provides a means of observing and analyzing the behavior or reactions of a system's output to variations in some input parameter. For instance, in many engineering applications, an in-depth analysis of the design may require efficient construction and manipulation of complicated geometries as well as accurate (though fast) numerical PDE solutions. In order to achieve the aim of optimizing the design, it may be very effective to alter the values of some of the design parameters. This alludes to the fact that the sensitivity of some output variables (such as variables that affect performance) to variations in some key parameters is critical.

Mathematically, the sensitivity of a function of a variable  $x$  with respect to that variable is the derivative of the function with respect to  $x$ , i.e.  $\frac{\partial f(x)}{\partial x}$ . In this work, we



seek to investigate the sensitivity of various functions (e.g., state position, control effort  $u$ , etc.) with respect to the MinMax control parameter  $\theta$ . We use a Galerkin finite element scheme in order to obtain a finite dimensional approximation of the solutions of the sensitivity equations.

There are two main classifications of numerical methods used to perform sensitivity analysis: the “discretize-then-differentiate” methods and the “differentiate-then-discretize” methods. The mechanisms of both methods are as their names suggest. An example of the former case is a method based on finite differences. This is the first and most prevalent method. There are issues with this method in the case of complex fluid flow problems as well as the typical issue of stability in finite difference schemes when dealing with step-size in the design variable (this is usually a trial-and-error process that leads to increased computational expense). These problems are discussed fully in [14; 15]. A second example of a “discretize-then-differentiate” method is Automatic Differentiation applied in [16; 17]. In this method a computer code is used to generate a finite dimensional state approximation. Specifically the program performs differentiation by repeatedly using the chain rule at the discrete level after the aforementioned finite dimensional state approximation is generated.

In this dissertation we apply Continuous Sensitivity Equation Methods (CSEMs) to the heat equation (1-dimensional and 2-dimensional), the wave equation, and the cantilevered Euler-Bernoulli beam that is attached to a rotating hub through which the control enters. The input parameter, which will be varied, is the MinMax parameter  $\theta$ . The CSEMs used here are categorized as the previously mentioned “differentiate-then-discretize” method. Examples of the usage of CSEMs are in [18; 19; 20]. A simple

example of the application of CSEMs is given in Section 2.2.1 of [21] and is presented here.

### 1.5 Heat in a Thin Rod

This example is for a steady state temperature distribution in a thin rod. A heat source is applied to only one section of the rod and the length of the rod is determined by the shape parameter. Let  $Q = (1,2)$  be the design space. For this discussion, let  $\Omega$  represent a bounded, connected, open subset of  $\mathfrak{R}^n$ , ( $n = 1,2,3$ ) satisfying the cone condition, see [22]. The state equation is an elliptic boundary value problem given as

$$-\frac{\partial^2 w(x)}{\partial x^2} = f(x), x \in \Omega(q) = (0, q), \quad \text{Eq. 1-5}$$

for a given  $q \in Q$ . Here  $\Omega(q)$  is defined as the interval  $(0, q)$ .  $f$  is the piecewise continuous function

$$f(x) = \begin{cases} 0, & 0 < x < 1 \\ -1, & 1 \leq x < q. \end{cases} \quad \text{Eq. 1-6}$$

We assume homogeneous Dirichlet boundary conditions, hence

$$w(0) = 0, w(q) = 0. \quad \text{Eq. 1-7}$$

These boundary conditions suggest that the two ends of the rod are insulated. The aim here is to solve Eq. 1-5 through Eq. 1-7 for the state  $w(x, q)$  and to then determine its sensitivity to small changes in  $q$ . The analytical solution can be verified to be

$$w(x, q) = \begin{cases} -\frac{(q-1)^2}{2q}x, & 0 < x < 1 \\ -\frac{(q-1)^2}{2q}x + \frac{1}{2}(x-1)^2, & 1 \leq x < q. \end{cases} \quad \text{Eq. 1-8}$$

We define the sensitivity

$$s(x, q) \triangleq \frac{\partial w(x, q)}{\partial q}. \quad \text{Eq. 1-9}$$

The sensitivity then is

$$s(x, q) = \frac{1 - q^2}{2q^2} x, \forall x \in \Omega(q) = (0, q). \quad \text{Eq. 1-10}$$

Discretization of this final sensitivity equation completes a “differentiate-then-discretize” example method.

In this work, we investigate the sensitivity of the controlled state, continuous algebraic Riccati equations’ solutions, and other variables with respect to variations in  $\theta$ . The potential end result is to be one step closer to having an efficient means of determining the optimal value of the parameter-optimal in terms of robustness, performance and even stability- that passes the test of some mathematically rigorous criteria.

## 1.6 Overview of Dissertation

In this dissertation, we perform sensitivity analysis on the heat equation, the Euler-Bernoulli cantilever beam with a rotating hub, as well as the wave equation. In Chapter 2 we discuss the MinMax controller design, stability analysis, Riccati sensitivity analysis and some theoretical background. In Chapter 3 we discuss the results of performing sensitivity and stability analyses for the 1 and 2-dimensional heat equations. In Chapter 4 we discuss the results for the 1-dimensional wave equation. In Chapter 5 we discuss the same results for the Euler-Bernoulli cantilevered beam with a rotating hub. In Chapter 6, we provide a conclusive analysis of the results and indications of the direction of future work. In Appendix A, we provide the exact solutions to the uncontrolled 1 and 2-dimensional heat equations, as well as the uncontrolled 1-dimensional wave equation.

This was done as a check for numerical accuracy of the simulations in Chapters 3 and 4.

Finally in Appendix B, we provide finite difference solutions to the uncontrolled 1-dimensional heat and wave equations, as well as the 2-dimensional heat equation.

# CHAPTER 2

## THEORETICAL BACKGROUND AND CONTROLLER DESIGN

### 2.1 Problem Formulation

As stated in Chapter 1, we are concerned with making progress towards the ultimate goal of determining a potential formula for choosing the MinMax parameter that is based on mathematically rigorous criteria. To this end, we work with physical systems that are governed by Partial Differential Equations (PDEs). Such systems are known as Distributed Parameter Systems. Based on the theory in [9; 10; 11], we assume that our PDE control system can be modeled in abstract form as

$$\dot{x}(t) = Ax(t) + Bu(t), x(0) = x_0. \quad \text{Eq. 2-1}$$

Here  $x(t) \in X$  is the state of the system and  $X$  is a Hilbert space. The operator  $A : X \rightarrow X$  describes the dynamics of the system,  $B : U \rightarrow X$  indicates how the controller is applied, and  $u(t)$  is the controller in Hilbert space  $U$ . The uncontrolled form of this equation is given as

$$\dot{x}(t) = Ax(t), x(0) = x_0. \quad \text{Eq. 2-2}$$

We further assume that there is less than complete knowledge of the system; hence we introduce a state measurement  $y(t) \in Y$ , which is a Hilbert space. The form taken by the measurement is given as

$$y(t) = Cx(t). \quad \text{Eq. 2-3}$$

The operator  $C: X \rightarrow Y$  determines how the state is measured. Since full state feedback is often impossible,  $C$  is generally not the identity operator.

## 2.2 Semigroups

For the purpose of this discussion we denote the state space system given by Eq. 2-2 and Eq. 2-3 as  $\Sigma(A, B, C)$ . The following definitions are cited from [23] and [24].

**Definition 2.1** Let  $X$  be a Hilbert space. A family  $T(t), 0 \leq t \leq \infty$ , of bounded linear operators from  $X$  into  $X$  is a **semigroup** of bounded linear operators on  $X$  if

1.  $T(0) = I$ , where  $I$  is the identity operator on  $X$
2.  $T(t+s) = T(s)T(t)$  for every  $t, s \geq 0$

**Definition 2.2** A semigroup  $T(t), 0 \leq t \leq \infty$ , of bounded linear operators on  $X$  is a **strongly continuous** semigroup, or  $C_0$ -semigroup, of bounded linear operators if

$$\lim_{t \downarrow 0} T(t)x = x, \text{ for every } x \in X. \quad \text{Eq. 2-4}$$

**Theorem 2.3** Let  $T(t)$  be a  $C_0$ -semigroup. There exist constants  $\omega \geq 0$  and  $M \geq 1$  such that

$$\|T(t)\| \leq Me^{\omega t}, \text{ for } 0 \leq t \leq \infty. \quad \text{Eq. 2-5}$$

If  $\omega < 0$  we say that  $T(t)$  is an **exponentially stable**  $C_0$ -semigroup. If  $\omega = 0$ ,  $T(t)$  is said to be **uniformly bounded**, and moreover, if  $M = 1$ ,  $T(t)$  is called a  $C_0$ -semigroup of **contractions**.

**Definition 2.4** An operator  $A$  is **exponentially stable** if and only if  $A$  generates an exponentially stable  $C_0$ -semigroup.

In this work, we assume  $A$  generates an exponentially stable  $C_0$  – semigroup which guarantees well-posedness of the control problem. This is true for the PDE's investigated in this work: heat equation as seen in [25; 26], the 1-dimensional wave equation [27] and the Euler-Bernoulli cantilevered beam with a rotating hub (also investigated in this work) [1; 28].

**Definition 2.5** The state linear system  $\Sigma(A, B, C)$  is **exponentially stable** if  $A$  is exponentially stable. We assume  $\Sigma(A, B, C)$  is exponentially stable for this work.

**Definition 2.6**  $\Sigma(A, B, C)$  is **stabilizable** if there exists a linear operator  $F: X \rightarrow U$  such that  $A + BF$  is exponentially stable. We refer to the pair  $(A, B)$  as being stabilizable.

**Definition 2.7**  $\Sigma(A, B, C)$  is **detectable** if there exists a linear operator  $L: Y \rightarrow X$  such that  $A + LC$  is exponentially stable. We refer to the pair  $(A, C)$  as being detectable.

### 2.3 MinMax Controller design

In attempting to achieve our aforementioned goal we design a MinMax controller for the 1 and 2-dimensional heat equations, the 1-dimensional wave equation and Euler-Bernoulli cantilevered beam with a rotating hub. The MinMax controller is a well-established control strategy (e.g. [6; 29]) and the equations for implementation are summarized here. We assume in this work that complete information about the controlled system is not available, hence a compensator is used. This compensator or observer incorporates the measurement of the state in Eq. 2-3 into its state equation:

$$\dot{x}_c(t) = A_c x_c(t) + Fy(t), x_c(0) = x_{c_0}, \quad \text{Eq. 2-6}$$

where  $x_c$  is the state of the compensator. In this work, we assume that  $(A, B)$  is stabilizable and that  $(A, C)$  is detectable (see definitions 2.6 and 2.7). Under these assumptions,

$$F = [I - \theta^2 P \Pi]^{-1} P C^*, \quad \text{Eq. 2-7}$$

and

$$A_c = A - BK - FC + \theta^2 M \Pi, \quad \text{Eq. 2-8}$$

where  $\Pi, P, M$  and  $K$  are defined in Eq. 2-9 and 2-10. There exists an optimal control of the form

$$u(t) = -Kx_c(t), \quad \text{Eq. 2-9}$$

where  $K$  is given as

$$K = R^{-1} B^* \Pi. \quad \text{Eq. 2-10}$$

In Eq. 2.7-2.10,  $\Pi$  and  $P$  are unique, positive definite solutions of the control and filter algebraic Riccati equations given as

$$A^* \Pi + \Pi A - \Pi [B R^{-1} B^* - \theta^2 M] \Pi + Q = 0, \quad \text{Eq. 2-11}$$

and

$$AP + PA^* - P [C^* C - \theta^2 Q] P + M = 0. \quad \text{Eq. 2-12}$$

Here,

$$Q = C^* C, \quad \text{Eq. 2-13}$$

and

$$M = B B^*. \quad \text{Eq. 2-14}$$

We are guaranteed minimal solutions  $\Pi$  and  $P$  such that



$$[I - \theta^2 P \Pi] > 0, \quad \text{Eq. 2-15}$$

for sufficiently small  $\theta$ . The final closed-loop control system is now

$$\begin{bmatrix} \dot{x} \\ \dot{x}_c \end{bmatrix} = \begin{bmatrix} A & -BR^{-1}B^*\Pi \\ A_c & FC \end{bmatrix} \begin{bmatrix} x \\ x_c \end{bmatrix}, \quad \begin{bmatrix} x(0) \\ x_c(0) \end{bmatrix} = \begin{bmatrix} x_0 \\ x_{c_0} \end{bmatrix}. \quad \text{Eq. 2-16}$$

## 2.4 Stability Analysis and Robustness

For a system that has bounded inputs, it is possible that the output maybe unbounded. This would render any solution useless; hence it is important that the controlled systems designed be stable. [30; 31] provide a simple criterion to determine stability of the systems under consideration. Consider the continuous-time system in Eq. 2-3:  $\dot{x}(t) = Ax(t)$ .

For a given initial condition  $x(0) = x_0$ , such a system has solution of the form

$$x(t) = e^{At}x_0, \quad \text{Eq. 2-17}$$

where  $t > 0$ . Using this solution the following theorem is provable

**Theorem 2.1** (Theorem 10.2 in [30])

The system in Eq. 2-2 is stable if and only if

$$\bigwedge_{i \in \overline{1, n}} \text{Re } s_i < 0, \quad \text{Eq. 2-18}$$

where  $s_i$  are the roots of the equation

$$\det(A - sI) = 0, \quad \text{Eq. 2-19}$$

i.e.  $s_i$  are eigenvalues of A. This theorem is used in stability plots in Chapters 3, and 4 and 5.

In order to further our search of an optimal means of choosing  $\theta$ , we compare robustness of the MinMax controllers implemented for different  $\theta$  values. Two measures of robustness are employed: stability margin and stability radius. The stability margin (as described in [32]) for a given matrix  $A$  is a measure of the distance from the imaginary axis to the nearest eigenvalue of matrix  $A$ . The stability radius, described in [32; 33], of matrix  $A$  is a measure of the distance from  $A$  to the nearest unstable matrix based on singular value computations.

## 2.5 Riccati Sensitivity

As previously stated, our goal is to contribute towards more efficient ways to determine the MinMax parameter  $\theta$ . Since the Algebraic Riccati Equations (ARE's) are essential to the design of the controller, and since their mathematical formulation is a function of  $\theta$ , we perform a sensitivity analysis of these equations. Consider the ARE's in Eq. 2-11 and Eq. 2-12:

$$A^*\Pi + \Pi A - \Pi[BR^{-1}B^* - \theta^2 M]\Pi + Q = 0,$$

$$AP + PA^* - P[C^*C - \theta^2 Q]P + M = 0.$$

We begin by finding the derivatives with respect to  $\theta$ ,

$$A^*\Pi_\theta + \Pi_\theta A - \Pi_\theta[BR^{-1}B^* - \theta^2 M]\Pi - \Pi[-2\theta M]\Pi$$

$$- \Pi[BR^{-1}B^* - \theta^2 M]\Pi_\theta = 0,$$

**Eq. 2-20**

$$AP_\theta + P_\theta A^* - P_\theta[C^*C - \theta^2 Q]P - P[-2\theta Q]P -$$

$$P[C^*C - \theta^2 Q]P_\theta = 0$$

**Eq. 2-21**

Here, let  $\Pi_\theta = \frac{\partial \Pi}{\partial \theta}$  and  $\frac{\partial P}{\partial \theta} = P_\theta$ . Now let  $\Pi_\theta = X$  and  $P_\theta = Y$ , then

$$A^*X + XA - X[BR^{-1}B^* - \theta^2 M]\Pi - \Pi[-2\theta M]\Pi$$

$$- \Pi[BR^{-1}B^* - \theta^2 M]X = 0,$$

**Eq. 2-22**

and

$$AY + YA^* - Y[C^*C - \theta^2Q]P - P[-2\theta Q]P - P[C^*C - \theta^2Q]Y = 0. \quad \text{Eq. 2-23}$$

Then factoring

$$\begin{aligned} [A^* - \Pi(BR^{-1}B^* - \theta^2M)]X + X[A - (BR^{-1}B^* - \theta^2M)\Pi] \\ - \Pi(-2\theta M)\Pi, \end{aligned} \quad \text{Eq. 2-24}$$

$$[A - P(C^*C - \theta^2Q)]Y + Y[A^* - (C^*C - \theta^2Q)P] - P(-2\theta Q)P. \quad \text{Eq. 2-25}$$

These final two equations are now in the form of Lyapunov equations which are solved numerically in Chapters 3, 4 and 5 of this work.

## 2.6 Controller Sensitivity

As previously stated in Chapter 1, we perform sensitivity analysis on the various PDE systems in this work. In doing so, we also investigate the sensitivity of the controller with respect to variations of the MinMax parameter,  $\theta$ . We know from Eq. 2-9 that  $u(t) = -Kx_c(t)$ . This can be re-written as

$$u(t, \theta) = -R^{-1}B^*\Pi x_c(t, \theta). \quad \text{Eq. 2-26}$$

Differentiating this with respect to  $\theta$  gives

$$\frac{\partial u(t, \theta)}{\partial \theta} = -R^{-1}B^* \frac{\partial \Pi}{\partial \theta} x_c(t, \theta) - R^{-1}B^*\Pi \frac{\partial x_c(t, \theta)}{\partial \theta}, \quad \text{Eq. 2-27}$$

or

$$u_\theta(t, \theta) = -R^{-1}B^*\Pi_\theta x_c(t, \theta) - R^{-1}B^*\Pi x_{c_\theta}(t, \theta). \quad \text{Eq. 2-28}$$

Let  $S_u(t) = u_\theta(t, \theta)$ , then

$$S_u(t, \theta) = -R^{-1}B^*\Pi_\theta x_c(t, \theta) - R^{-1}B^*\Pi x_{c_\theta}(t, \theta). \quad \text{Eq. 2-29}$$

## 2.7 Sensitivity of the Compensator state

The solution and subsequent simulations of Eq. 2-28 requires the definition of the sensitivity of the compensator's state variable  $x_{c_\theta}(t, \theta)$ . Recall that the compensator state is defined by Eq. 2-4 as

$$\dot{x}_c(t, \theta) = A_c x(t, \theta) + Fy(t, \theta). \quad \text{Eq. 2-30}$$

Substituting  $F$  and  $A_c$  into Eq. 2-30 gives

$$\begin{aligned} \dot{x}_c(t, \theta) = & Ax_c(t, \theta) - BR^{-1}B^*\Pi x_c(t, \theta) - [I - \theta^2 P\Pi]^{-1}PC^*Cx_c(t, \theta) \\ & + \theta^2 Mx_c(t, \theta) + [I - \theta^2 P\Pi]^{-1}PC^*Cx(t, \theta). \end{aligned} \quad \text{Eq. 2-31}$$

Differentiating this equation with respect to  $\theta$  gives

$$\begin{aligned} \dot{x}_{c_\theta}(t, \theta) = & Ax_{c_\theta}(t, \theta) - BR^{-1}B^*\Pi_\theta x_c(t, \theta) - \\ & BR^{-1}B^*\Pi_\theta x_{c_\theta}(t, \theta) + 2\theta M\Pi x_c(t, \theta) + \theta^2 M\Pi_\theta x_c(t, \theta) + \\ & [I - \theta^2 P\Pi]^{-1}[-2\theta P\Pi - \theta^2 P_\theta \Pi - \\ & \theta^2 P\Pi_\theta][I - \theta^2 P\Pi]^{-1}PC^*Cx_c(t, \theta) + \theta^2 M\Pi x_{c_\theta}(t, \theta) - \\ & [I - \theta^2 P\Pi]^{-1}PC^*Cx_c(t, \theta) - [I - \theta^2 P\Pi]^{-1}PC^*Cx_{c_\theta}(t, \theta) - \\ & [I - \theta^2 P\Pi]^{-1}[-2\theta P\Pi - \theta^2 P_\theta \Pi - \\ & \theta^2 P\Pi_\theta][I - \theta^2 P\Pi]^{-1}PC^*x(t, \theta) + [I - \theta^2 P\Pi]^{-1}P_\theta C^*Cx(t, \theta) + \\ & [I - \theta^2 P\Pi]^{-1}PC^*Cx_\theta(t, \theta) \end{aligned} \quad \text{Eq. 2-32}$$

Rearranging Eq. 2-32 gives

$$\begin{aligned} \dot{x}_{c_\theta}(t, \theta) = & (-[I - \theta^2 P\Pi]^{-1}[-2\theta P\Pi - \theta^2 P_\theta \Pi - \theta^2 P\Pi_\theta][I - \theta^2 P\Pi]^{-1} + \\ & [I - \theta^2 P\Pi]^{-1}P_\theta C^*C)x(t) + (-BR^{-1}B^*\Pi_\theta + [I - \theta^2 P\Pi]^{-1}[-2\theta P\Pi - \theta^2 P_\theta \Pi - \\ & \theta^2 P_\theta \Pi_\theta][I - \theta^2 P\Pi]^{-1}PC^*C - [I - \theta^2 P\Pi]^{-1}P_\theta C^*C + 2\theta M\Pi + \theta^2 M\Pi_\theta)x_c(t) + \\ & [I - \theta^2 P\Pi]^{-1}PC^*Cx_\theta(t, \theta) + (A - BR^{-1}B^*\Pi - [I - \theta^2 P\Pi]^{-1}PC^*C + \\ & \theta^2 M\Pi)x_{c_\theta}(t). \end{aligned} \quad \text{Eq. 2-33}$$

This can be re-written as

$$\dot{x}_{c\theta}(t, \theta) = A_{c1}x(t, \theta) + A_{c2}x_c(t) + A_{c3}S_x(t, \theta) + A_{c4}S_{x_c}(t) \quad \text{Eq. 2-34}$$

where

$$\begin{aligned} S_x(t, \theta) &= x_\theta(t, \theta), \\ S_{x_c}(t, \theta) &= x_{c\theta}(t, \theta), \\ A_{c1}(t, \theta) &= -[I - \theta^2 P \Pi]^{-1} [-2\theta P \Pi - \theta^2 P_\theta \Pi \\ &\quad - \theta^2 P \Pi_\theta] [I - \theta^2 P \Pi]^{-1} [I - \theta^2 P \Pi]^{-1} P_\theta C^* C, \\ A_{c2}(t, \theta) &= BR^{-1} B^* \Pi_\theta + [I - \theta^2 P \Pi]^{-1} [-2\theta P \Pi - \theta^2 P_\theta \Pi - \theta^2 P \Pi_\theta] [I - \\ &\quad \theta^2 P \Pi]^{-1} P C^* C - [I - \theta^2 P \Pi]^{-1} P_\theta C^* C + 2\theta M \Pi + \theta^2 M \Pi, \\ A_{c3}(t, \theta) &= [I - \theta^2 P \Pi]^{-1} P C^* C, \\ A_{c4}(t, \theta) &= A - BR^{-1} B^* \Pi - [I - \theta^2 P \Pi]^{-1} P C^* C + \theta^2 M \Pi. \end{aligned} \quad \text{Eq. 2-35}$$

## 2.8 Functional Gains

The following discussion of functional gains is a summary from [32]. The control law for some PDEs can be written in integral form. For example, if the control space  $U$  is finite dimensional, then from Riesz Representation theorem,

$$u(t) = -Kx_c(t) = -\langle k_i(s), x_c(t) \rangle, \quad \text{Eq. 2-36}$$

where  $s$  is a spatial variable and  $k_i(s) \in X$  for  $i = 1, 2, 3, \dots, m$ .  $k(s)$ , which is the kernel of the integral, is called a functional gain. Functional gains are important for many reasons. For example, the gains can be computed off-line, stored, and then multiplied by the state estimate before numerical integration, when computing the control. Also the functional gains can provide such information as the optimal locations for sensor placement (see for example [34]). In this work, we are using functional gains to verify that our Galerkin finite element scheme used to approximate the infinite dimensional PDE systems

converges. We also want to examine the effect of  $\theta$  on convergence of functional gains.

This is a way to assess the convergence of the controller and the finite element scheme.

## CHAPTER 3

### HEAT EQUATION

In this Chapter, we implement the MinMax controller and apply Continuous Sensitivity Equation Methods to the 1 and 2-dimensional heat equations. The goal here is to further our investigation of a more efficient means of choosing the MinMax parameter,  $\theta$ .

#### 3.1 1-D Heat Equation

Heat flow along a 1-dimensional structure, such as a rod, can be modeled by the diffusion equation:

$$U_t(t, x) - kU_{xx}(t, x) = \sum_{i=1}^m b_i(x)u(t), \quad \text{Eq. 3-1}$$

where  $0 < x < L$  and  $k = \frac{K_0}{c\rho}$  is the thermal diffusivity,  $K_0$  is the thermal conductivity,  $c$  is the specific heat capacity,  $\rho$  is the mass density,  $t$  represents time,  $x$  is the distance along the rod,  $U(t, x)$  is the temperature at time  $t$  and position  $x$ ,  $u(t)$  is the control input to the system, and  $b_i(x)$  describes how the control enters the system. Figure 3-1 shows the system under discussion.

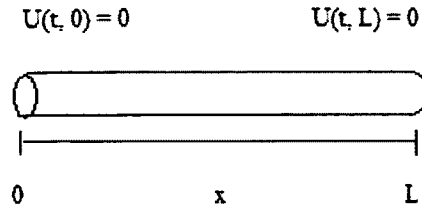


Figure 3-1: Heat flow in 1-d rod

We employ a Galerkin Finite Element scheme to Eq. 3-1. In order to determine the finite element approximation to Eq. 3-1, we first write the weak form of the PDE. In considering the weak form of the problem we seek to find a  $U(x) \in X = H_0^1(0, l)$  such that

$$\int_0^l \dot{U}(t, x)v(x)dx - k \int_0^l U''(t, x)v(x)dx = \int_0^l u(t) \sum_{i=1}^m b_i(x)v(x)dx. \quad \text{Eq. 3-2}$$

Here  $v(x) \in H_0^1(0, L)$  is the test function. Using integration by parts,

$$\int_0^l U''(t, x)v(x)dx = U'(t, x)v(x)|_0^l - \int_0^l U'(t, x)v'(t, x)dx = \int_0^l U'(t, x)v'(x)dx, \quad \text{Eq. 3-3}$$

since  $v(0) = v(l) = 0$ . Substituting this into Eq. (3.2) gives

$$\int_0^l \dot{U}(t, x)v(x)dx + k \int_0^l U'(t, x)v'(x)dx = \int_0^l u(t) \sum_{i=1}^m b_i(x)v(x)dx. \quad \text{Eq. 3-4}$$

Now let, where  $U(t, x) \approx U^N(t, x) = \sum_{i=1}^m e_i(t)\phi_i(x)$ ,  $\phi_i(x)$  are piecewise linear basis functions and  $e_i(t)$  are their coefficients. Then Eq. 3-4 becomes

$$\int_0^l \dot{U}^N(t, x)v(x)dx + k \int_0^l U'^N(t, x)v'(x)dx = \int_0^l u(t) \sum_{i=1}^m b_i(x)v(x)dx, \quad \text{Eq. 3-5}$$

or



$$\int_0^l \sum_{i=1}^N \dot{e}_i(t) \phi_i(x) v(x) dx + k \int_0^l \sum_{i=1}^N e_i(t) \phi'_i(x) v'(x) dx =$$

Eq. 3-6

$$\int_0^l u(t) \sum_{i=1}^m b_i(x) v(x) dx.$$

Now we let  $v(x)$  range over  $\phi_j(x)$  for  $j = 1, 2, \dots, N$ . Eq. 3-6 now becomes

$$\int_0^l \sum_{i=1}^N \dot{e}_i(t) \phi_i(x) \phi_j(x) dx + k \int_0^l \sum_{i=1}^N e_i(t) \phi'_i(x) \phi'_j(x) dx$$

Eq. 3-7

$$= u(t) \sum_{i=1}^m b_i(x) \phi_j(x) dx.$$

This can be rewritten as

$$M \begin{bmatrix} \dot{e}_1(t) \\ \vdots \\ \dot{e}_N(t) \end{bmatrix} + kK \begin{bmatrix} e_1(t) \\ \vdots \\ e_N(t) \end{bmatrix} = u(t) B_0,$$

Eq. 3-8

where

$$M = \left[ \int_0^l \phi_i(x) \phi_j(x) dx \right]_{i,j=1}^N, \quad K = \left[ \int_0^l \phi'_i(x) \phi'_j(x) dx \right]_{i,j=1}^N \quad \text{and} \quad B_0 = \left[ \int_0^l \sum_{i=1}^m b_i(x) \phi_j(x) dx \right]_{j=1}^N.$$

Here  $M$  and  $K$  are the mass and stiffness matrices respectively. Rearranging Eq. 3-8

gives

$$\begin{bmatrix} \dot{e}_1(t) \\ \vdots \\ \dot{e}_N(t) \end{bmatrix} = -kM^{-1}K \begin{bmatrix} e_1(t) \\ \vdots \\ e_N(t) \end{bmatrix} + u(t)M^{-1}B_0.$$

Eq. 3-9

Let  $X(t) = e(t)$ , then Eq. 3-9 becomes

$$\begin{bmatrix} \dot{X}_1(t) \\ \vdots \\ \dot{X}_N(t) \end{bmatrix} = -kM^{-1}K \begin{bmatrix} X_1(t) \\ \vdots \\ X_N(t) \end{bmatrix} + u(t)M^{-1}B_0.$$

Eq. 3-10

Since full knowledge of the system is not available, we take measurements in the form

$$y(t) = C[X(t)] \quad \text{Eq. 3-11}$$

where  $C$  is composed of four averaging measurements of the state position, resulting in the  $4 \times (2N - 2)$  matrix

$$\begin{bmatrix}
 \left[ \frac{4}{l} \int_0^{\frac{l}{4}} \phi_i^N(x) dx \right]_{i=1}^{N-1} & 0 \\
 \left[ \frac{4}{l} \int_{\frac{l}{4}}^{\frac{l}{2}} \phi_i^N(x) dx \right]_{i=1}^{N-1} & 0 \\
 \left[ \frac{4}{l} \int_{\frac{l}{2}}^{\frac{3l}{4}} \phi_i^N(x) dx \right]_{i=1}^{N-1} & 0 \\
 \left[ \frac{4}{l} \int_{\frac{3l}{4}}^l \phi_i^N(x) dx \right]_{i=1}^{N-1} & 0
 \end{bmatrix} \quad \text{Eq. 3-12}$$

Next, we define  $\{b_i\}_{i=1}^m$ . We begin by partitioning the spatial domain  $[0, l]$  as

$\{x_i\}_{i=1}^m$  where  $x_i = i \times \frac{l}{m}$ . The functions  $b_i$  are defined as  $b_i(x) = e^{-(x-x_i)^2}$  for

$x_{i-1} \leq x \leq x_i$ , where  $x_i^* = \frac{x_{i-1} + x_i}{2} = 1.25, 3.75, 6.25, 8.75$  since  $l = 10$  for the rod in

question. Finally,

$$B_0 = [B_1 \cdots B_m] \text{ and } \left[ B_i = \int_0^l b_i(x) \phi_j(x) dx \right]_{i,j=1}^{i=m, j=N-1} \quad \text{Eq. 3-13}$$

For this system,  $m = 4$ , hence

$$B_0 = [B_1 \quad B_2 \quad B_3 \quad B_4] \quad \text{Eq. 3-14}$$

### 3.2 Numerical Results

For all the simulations in this section  $N = 80, l = 10, R = I$  and

$$U(t, 0) = U(t, l) = 0. \quad \text{Eq. 3-15}$$

The results are presented in the following order: uncontrolled simulations, functional gains, controlled simulations, stability analysis and sensitivity analysis.

#### 3.2.1 Uncontrolled Results

For simulation purposes and to attain a solution to the system in Eq. 3-10 and Eq. 3-11 we apply the initial conditions

$$U_0 = U(0, x) = 100, U_{c_0} = U_c(0, x) = 0.75U_0. \quad \text{Eq. 3-16}$$

Figure 3-2 shows the uncontrolled state for this system. We desire the state to tend to the exponentially stable equilibrium position of zero (0). The MinMax controller is applied with the aim of achieving this goal.

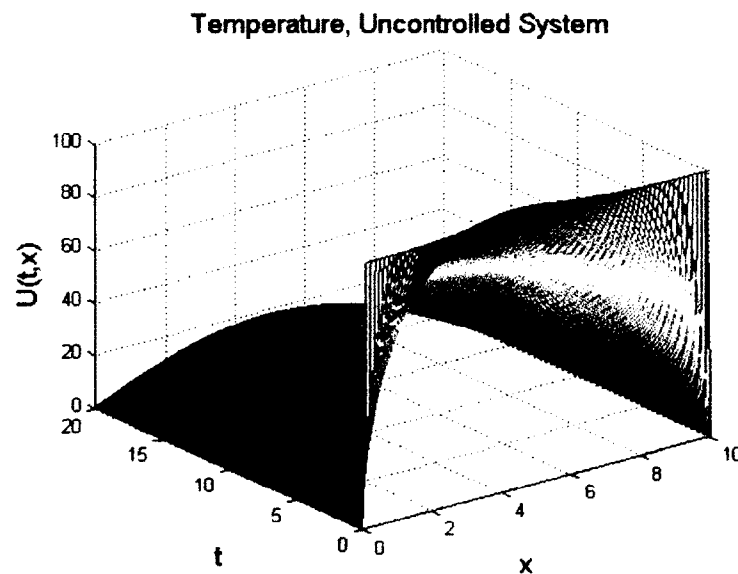


Figure 3-2: Uncontrolled heat flow in 1-d rod

### 3.2.2 Controlled Results

Figures 3-3 to 3-6 show the functional gains for the system in Eq. 3-10 and Eq. 3-11. The color legend in this plot is:  $N = 10$  blue,  $N = 20$  red,  $N = 40$  black,  $N = 80$  magenta. The results clearly show convergence of the functional gains, hence the Galerkin finite element scheme converges. More importantly, as  $\theta$  increases, there is no visual change in the functional gains. This suggests that, with respect to convergence of the functional gains and the MinMax controllers for this system, the choice of MinMax parameter is not pivotal.

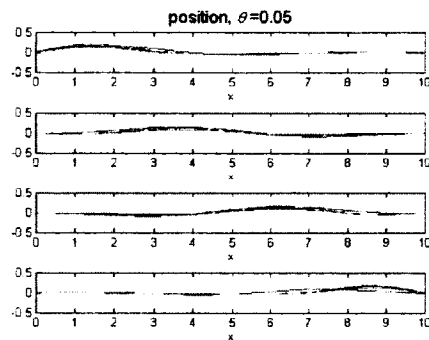


Figure 3-3: Functional gains,  $\theta = 0.05$

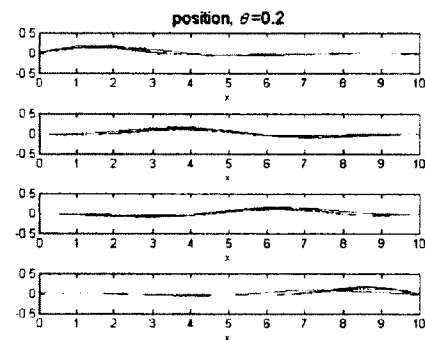


Figure 3-4: Functional gains,  $\theta = 0.2$

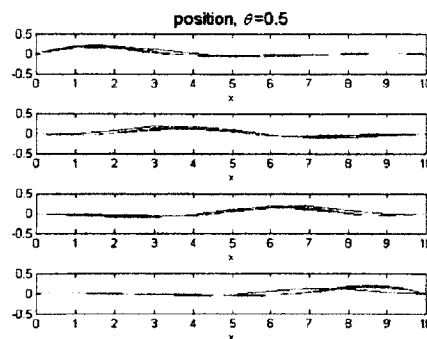


Figure 3-5: Functional gains,  $\theta = 0.5$

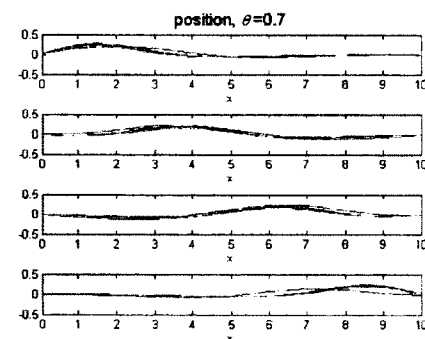


Figure 3-6: Functional gains,  $\theta = 0.7$

Figures 3-7 and 3-8 show the controlled temperature values along the rod for the full state ( $u(t) = -KU(t)$ ) and for the state estimate system ( $u(t) = -KU_c(t)$ ),

respectively. In each figure, the top left result is for  $\theta = 0.05$ , top right is for  $\theta = 0.2$ , bottom left is for  $\theta = 0.05$  and finally bottom right is for  $\theta = 0.7$ . The maximum  $\theta$  value that still results in  $[I - \theta^2 P \Pi] > 0$  and eigenvalues of  $\begin{bmatrix} A & -BK \\ FC & A_c \end{bmatrix}$  being in the left two quadrants of the complex plane as described in Chapter 2.

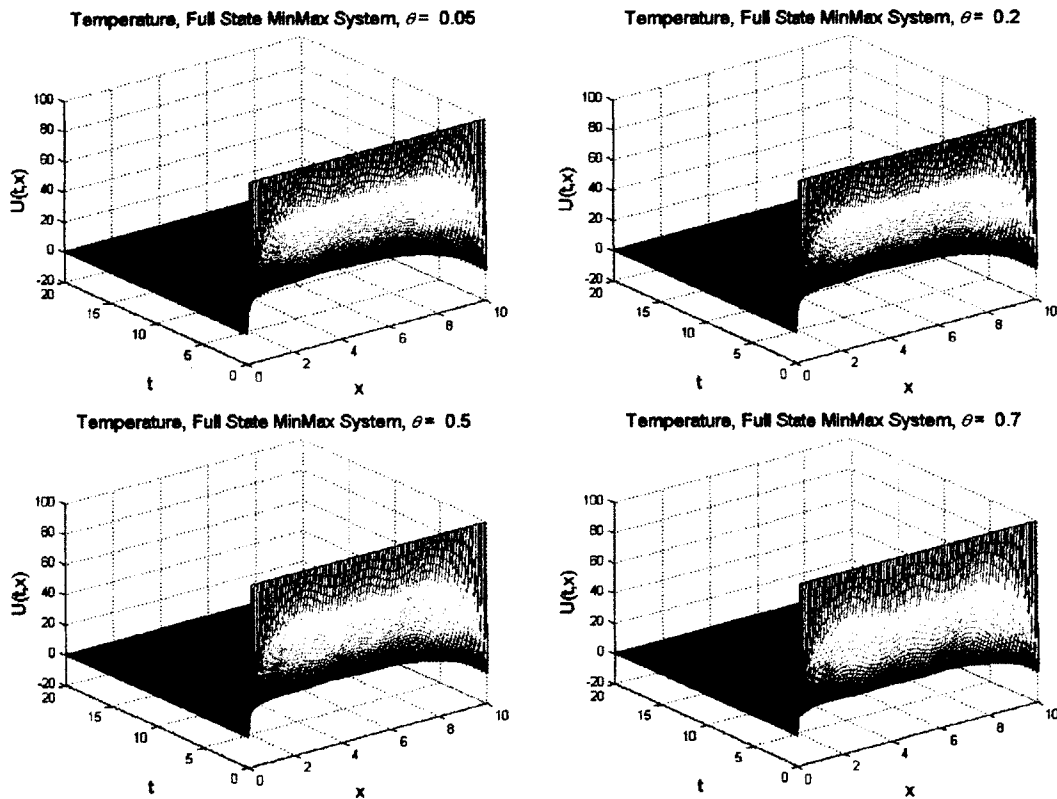


Figure 3-7: Controlled temperature, full state MinMax

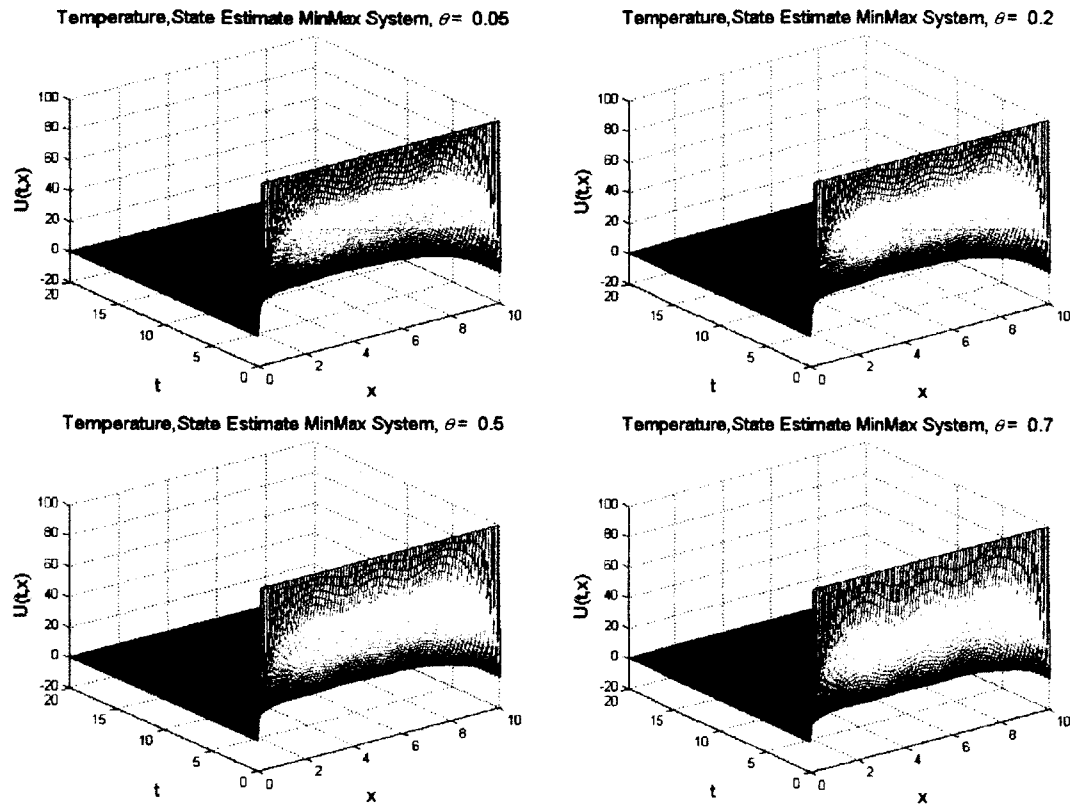


Figure 3-8: Controlled temperature, state estimate MinMax

The results show that, as  $\theta$  increases, there is an imperceptible difference in the performance of the controller. This would suggest that the choice of  $\theta$  in terms of performance is irrelevant. Both the full-state as well as the state estimate feedback systems do a great job in driving the system towards equilibrium. Although this is not our main goal, it is a necessary requirement.

### 3.2.3 Stability Analysis

The main aim of this dissertation is advance the search for a more refined means of choosing the optimal MinMax parameter. With this main goal in mind, it is necessary still to ensure stability in the control system without which our results will be invalid. In order to verify stability in the control system we investigate the eigenvalues of the matrix

$\begin{bmatrix} A & -BK \\ FC & A_c \end{bmatrix}$ . As described in Chapter 2, all the eigenvalues of this matrix must be on the left-hand side of the complex plane in order for the system to be stable. Figures 3-9 and 3-10 show the eigenvalue plots for varying  $\theta$  values. The graphs on the right side of each figure are a zoomed view showing the closest eigenvalues to the imaginary axis. As described in Chapter 2, this is known as the stability margin. The larger the stability margin, the higher the stability of the system. Two main conclusions can be drawn from the results:

1. Since all of the eigenvalues are on the left-hand side of the complex plane, the system is stable at all possible  $\theta$  values.
2. The stability margin increases slightly with increasing  $\theta$  (see Table 3-1). This suggests that as  $\theta$  increases the system's stability increases. However, since the difference in the stability margin is minute, we conclude that all possible  $\theta$  values can be chosen with respect to system stability.

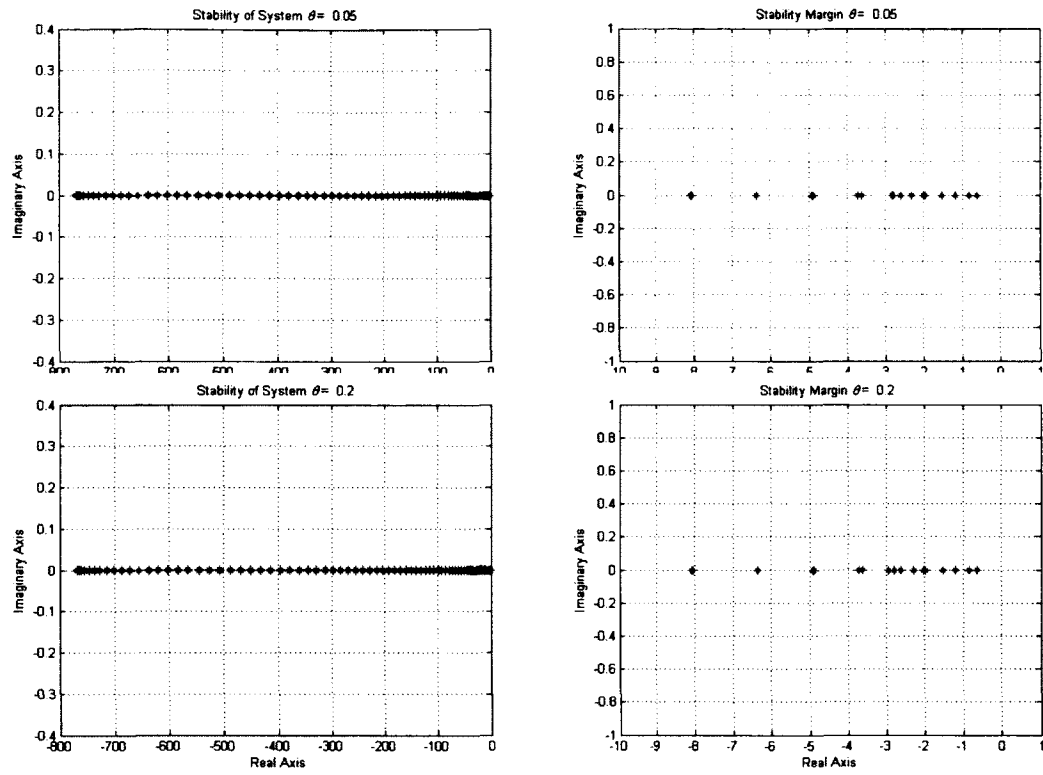


Figure 3-9: Eigenvalues of  $\begin{bmatrix} A & -BK \\ FC & A_c \end{bmatrix}$



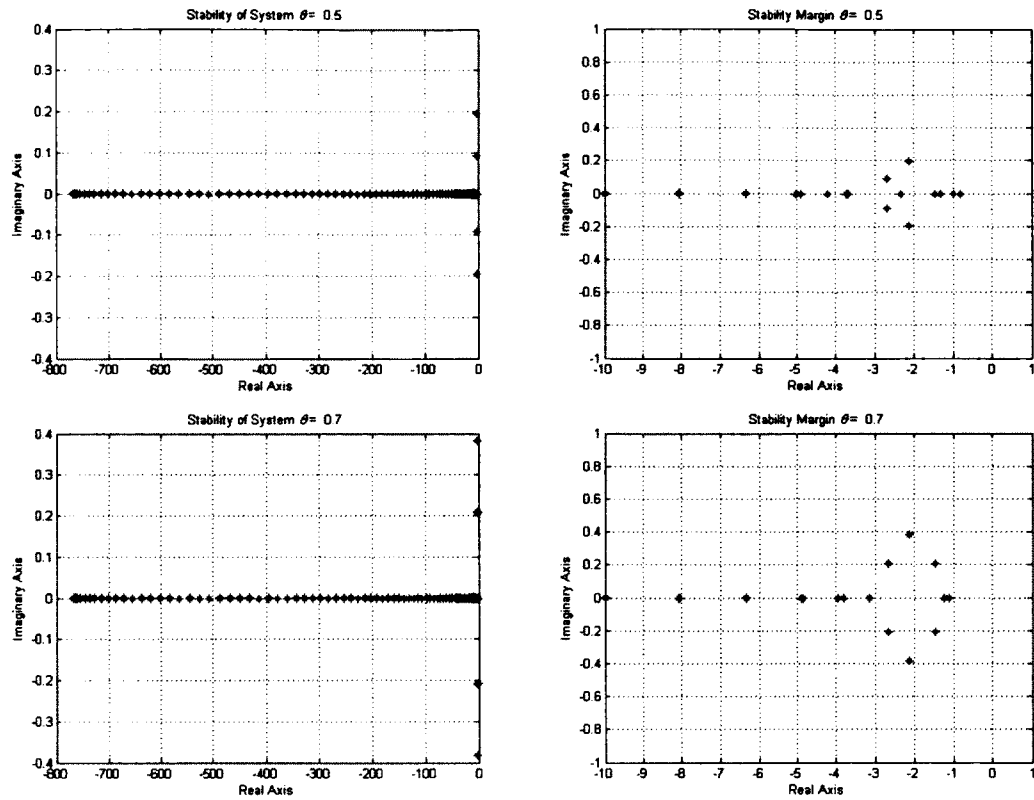


Figure 3-10: Eigenvalues of  $\begin{bmatrix} A & -BK \\ FC & A_c \end{bmatrix}$

Table 3-1 shows the stability margin and radius results for various  $\theta$  values.

Recall from Chapter 2, that the stability radius is a robustness measurement that indicates the distance of a particular matrix from the nearest unstable matrix. As a result the larger this distance, the more stable the system. The table shows that as  $\theta$  increases, the stability radius is virtually unchanged. This is in agreement with the previous results and hence the conclusion drawn is the same: the value of the MinMax parameter chosen is not critical based on the stability radius.

Table 3-1: Stability margin and radius for controlled system ( $A_{mm}$ )

$\theta$	Stability Margin	Stability Radius
0.05	0.106150912881119	0.0966256989626073
0.2	0.106242942442262	0.0966278024617770
0.5	0.106763979943028	0.0966337536956251
0.7	0.107351971099277	0.0966156352872341

### 3.2.4 Control Effort

As described in [4], an undesirable downside to the design of our controller is the idea that the controller's operation may require too much power. This is not cost-effective and hence one condition that we want to maintain is that the control effort, which is a direct indication of the power required, must be reasonable. We therefore provide in Figures 3-11 through 3-18 for  $\theta = 0.05, 0.2, 0.5, 0.7$ . In Figures 3-11 through 3-14, the system under investigation is the full state MinMax controlled system where no compensator/observer is used. In Figures 3-15 through 3-18, a compensator is implemented.

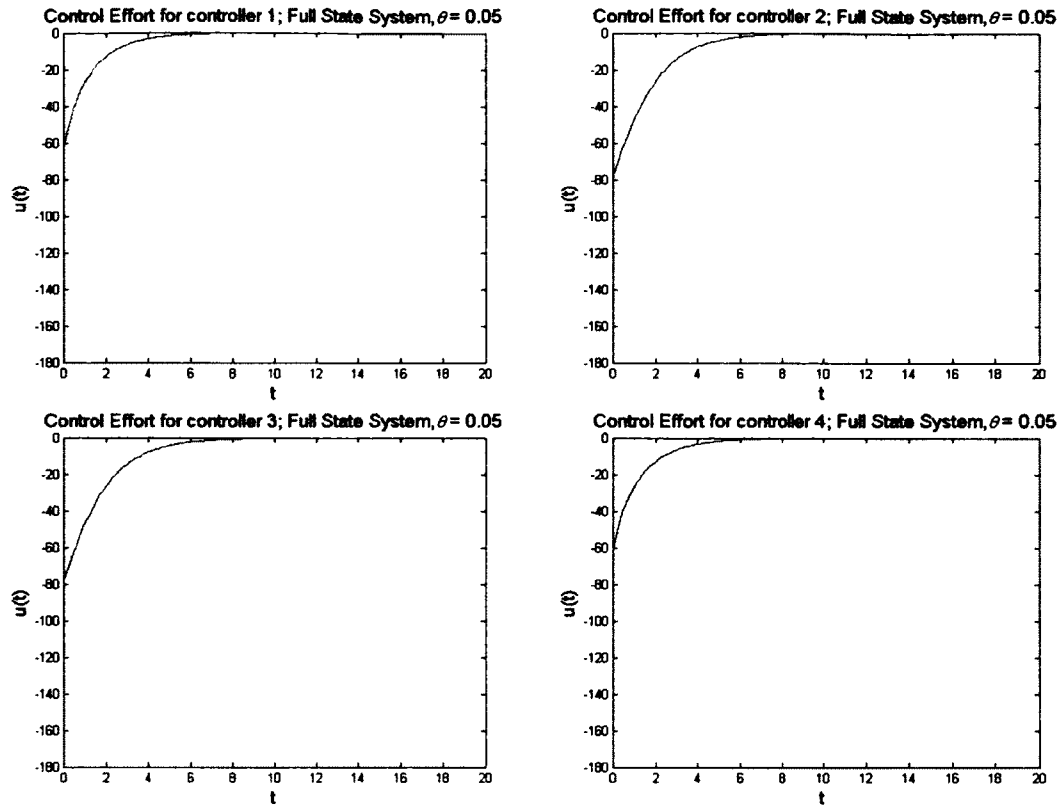


Figure 3-11: Control effort, full state MinMax

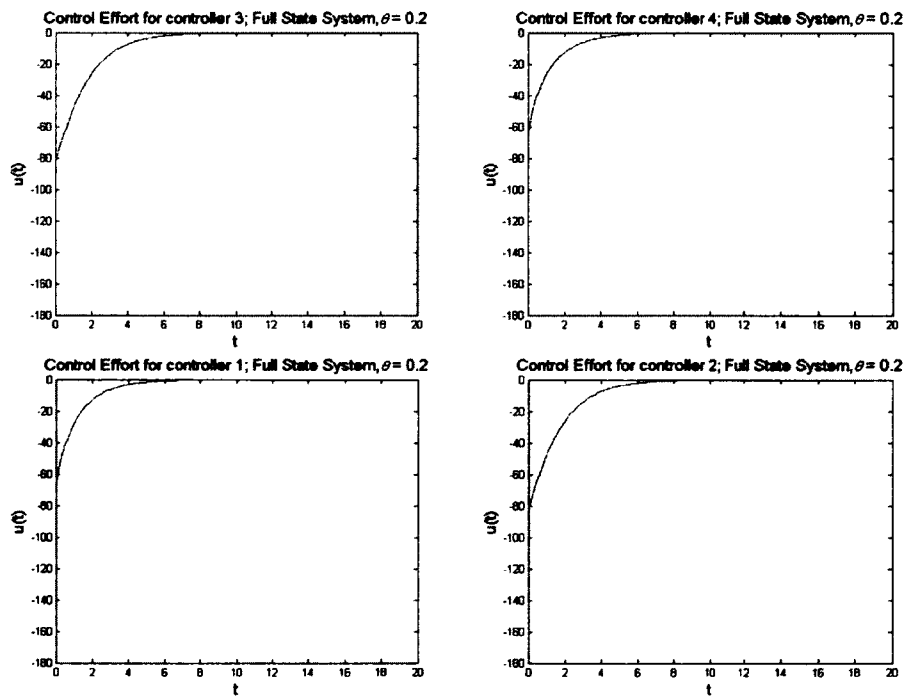


Figure 3-12: Control effort, full state MinMax

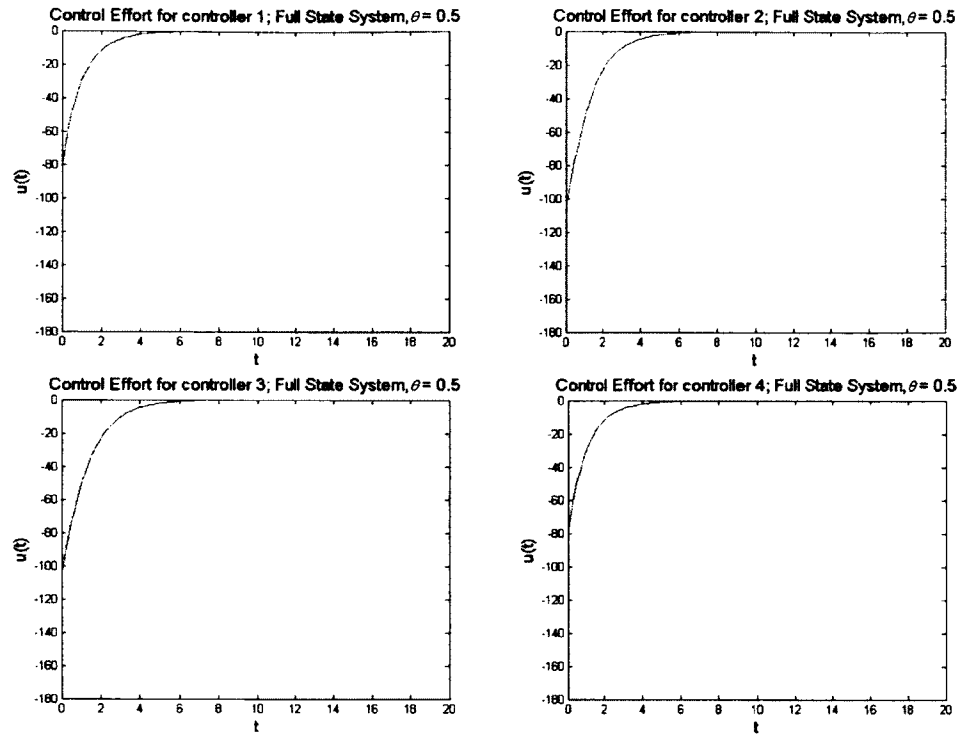


Figure 3-13: Control effort, full state MinMax

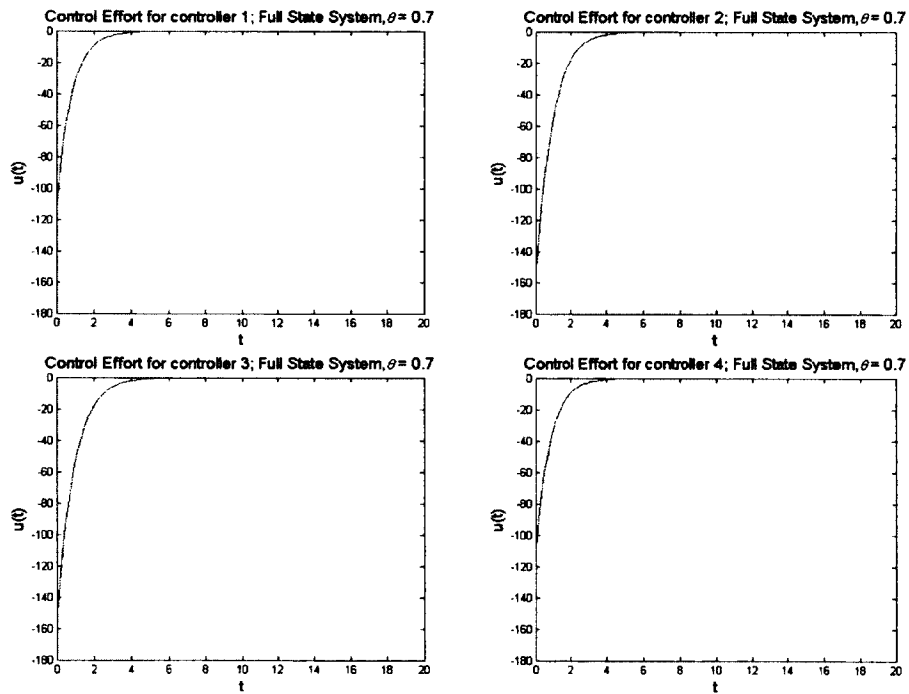


Figure 3-14: Control effort, full state MinMax

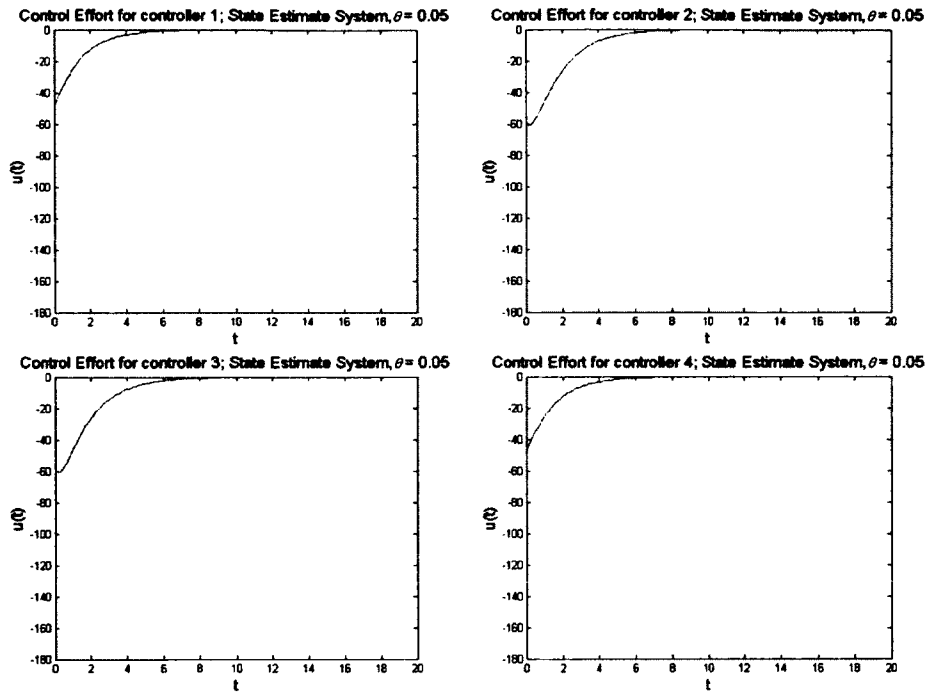


Figure 3-15: Control effort, state estimate MinMax

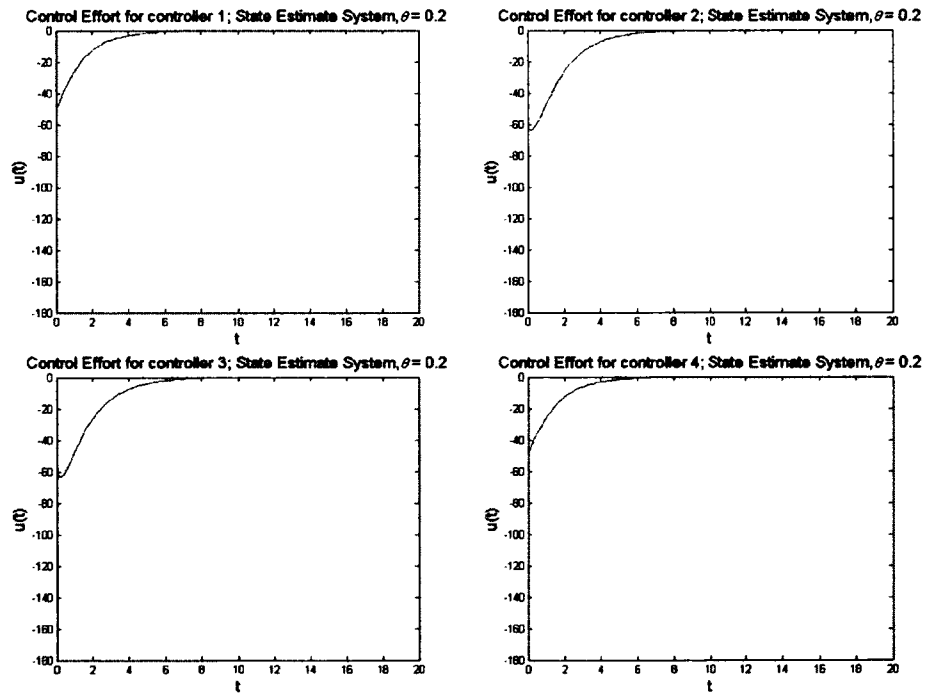


Figure 3-16: Control effort, state estimate MinMax

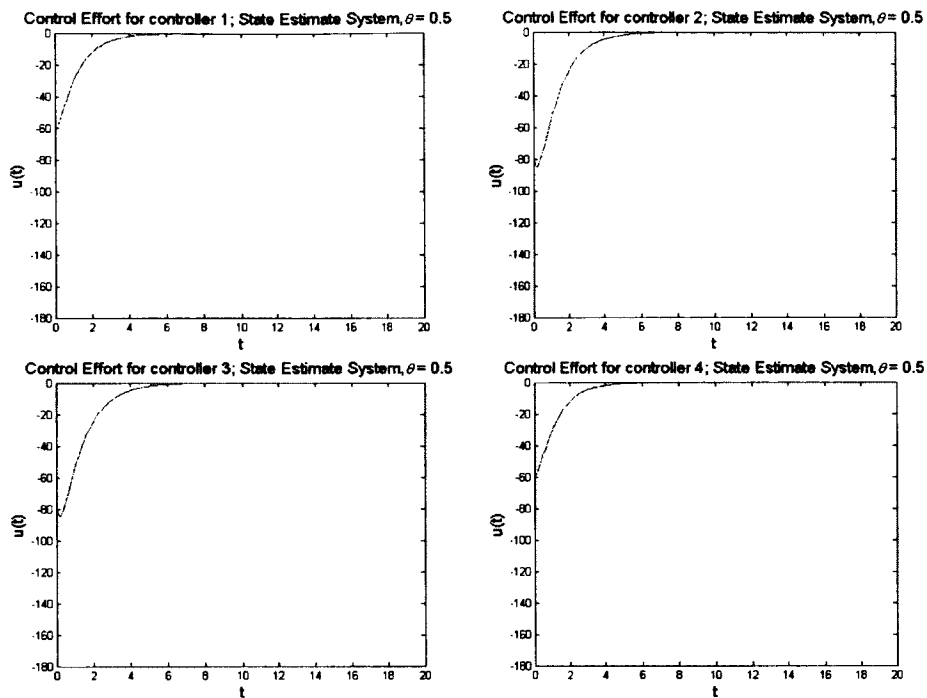


Figure 3-17: Control effort, state estimate MinMax

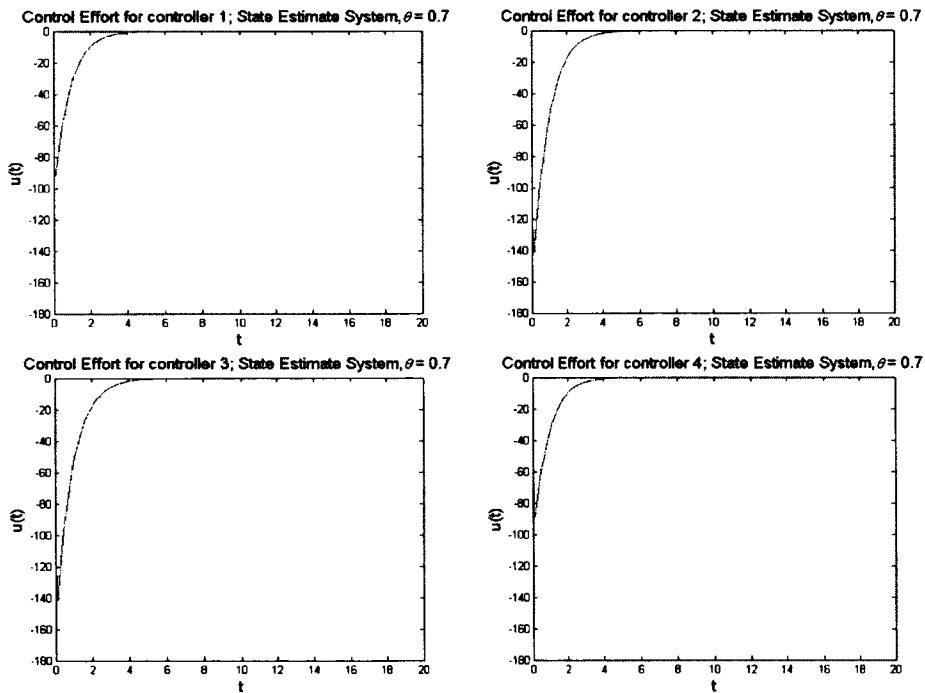


Figure 3-18: Control effort, state estimate MinMax

In order to better compare the control effort for different  $\theta$  values, we employ Simpson's rule to determine the area between the curve and the time axis. This area gives us the total control effort used. Table 3-2 summarizes the results where  $I$  gives the area obtained by Simpson's rule. The total area is calculated for each  $\theta$  value and recorded in the table. The results show two main trends:

1. The control effort for the full state system is higher than that of the state estimate system; however, this difference is small. This small difference is manifested in the similar controlled results for the two types of systems, as seen in Figures 3-7 and 3-8.
2. As  $\theta$  increases, the control effort increases for both types of systems. The percentage increase from  $\theta_1$  to  $\theta_2$ , is not insignificant (e.g. in the case of the state estimate system, the percentage difference is +11.19%). However, the actual values at  $\theta_1$  and  $\theta_2$  are of the same order of magnitude. Again we conclude that the value of  $\theta$  chosen is not critical based on the control

Table 3-2: Area under control effort curve (Simpson's rule)

<b>Area Under Curve</b>	$\theta_1 = 0.05$	$\theta_2 = 0.2$	$\theta_3 = 0.5$	$\theta_4 = 0.7$	<b>% change from <math>\theta_1</math> to <math>\theta_2</math></b>
$I_{controller\ 1}$ (full)	-80.530514	-80.945112	-83.641014	-89.030887	-10.55
$I_{controller\ 2}$ (full)	-141.407050	-141.210885	-140.174901	-142.835227	-1.01
$I_{controller\ 3}$ (full)	-141.514130	-141.327619	-140.349007	-143.066100	-1.09
$I_{controller\ 4}$ (full)	-78.885233	-79.322521	-82.162331	-87.718358	-11.19
<b>TOTAL</b>	<b>-442.34</b>	<b>-442.81</b>	<b>-446.33</b>	<b>-462.65</b>	<b>-4.59</b>
$I_{controller\ 1}$ (est.)	-74.223023	-75.117240	-80.628293	-88.171640	-18.79
$I_{controller\ 2}$ (est.)	-135.131386	-135.985626	-140.513787	-144.443766	-6.89
$I_{controller\ 3}$ (est.)	-135.216274	-136.077049	-140.650368	-144.653901	-6.98
$I_{controller\ 4}$ (est.)	-72.655741	-73.549363	-79.072485	-86.678280	-19.29
<b>TOTAL</b>	<b>-417.23</b>	<b>-420.73</b>	<b>-440.865</b>	<b>-463.95</b>	<b>+11.19</b>

### 3.2.5 Sensitivity Analysis

In order to perform sensitivity analysis of the 1-dimensional heat equation, we begin by differentiating Eq. 3-1 with respect to  $\theta$ , resulting in



$$U_{t_\theta}(t, x, \theta) - kU_{xx_\theta}(t, x, \theta) = \sum_{i=1}^m b_i(x)u_\theta(t, \theta), \quad \text{Eq. 3-17}$$

where, 
$$\frac{\partial U(t, x, \theta)}{\partial \theta} = U_\theta(t, x, \theta) \text{ and } \frac{\partial u(t, \theta)}{\partial \theta} = u_\theta(t, \theta).$$

Now let  $U_\theta(t, x, \theta) = S_U(t, x, \theta)$  and  $u_\theta(t, \theta) = S_u(t, \theta)$ . We then have

$$\dot{S}_U(t, x, \theta) - kS_{U_{xx}}(t, x, \theta) = \sum_{i=1}^m b_i(x)S_u(t, \theta). \quad \text{Eq. 3-18}$$

Now, let  $\frac{\partial S(t, x, \theta)}{\partial t} = \dot{S}(t, x, \theta)$  and  $\frac{\partial S(t, x, \theta)}{\partial x} = S'(t, x, \theta)$ , then

$$\dot{S}_U(t, x, \theta) - kS''_U(t, x, \theta) = \sum_{i=1}^m b_i(x)S_u(t, \theta). \quad \text{Eq. 3-19}$$

In order to determine the finite element approximation to Eq. 3-19, we first write the weak form of the PDE. In considering the weak form of the problem we seek to find a

$S_U(t, x) \in X = H_0^1(0, l)$  such that

$$\begin{aligned} \int_0^l \dot{S}_U(t, x, \theta)v(x)dx - k \int_0^l S''_U(t, x, \theta)v(x)dx = \\ \int_0^l \sum_{i=1}^m b_i(x)S_u(t, \theta)v(x)dx. \end{aligned} \quad \text{Eq. 3-20}$$

Using integration by parts,  $\int_0^l S''_U(t, x, \theta) = -\int_0^l S'_U v'(x)dx$ , hence the weak form is now

$$\begin{aligned} \int_0^l \dot{S}_U(t, x, \theta)v(x)dx + k \int_0^l S'_U(t, x, \theta)v'(x)dx = \\ \int_0^l \sum_{i=1}^m b_i(x)S_u(t, \theta)v(x)dx. \end{aligned} \quad \text{Eq. 3-21}$$

Let  $S_U(t, x, \theta) \approx S_U^N(t, x, \theta) = \sum_{i=1}^N e_i(t)\phi_i(x)$  where  $\phi_i(x)$  are piecewise linear basis functions and  $e_i(t)$  are their coefficients. Then

$$\begin{aligned} \int_0^l \dot{S}_U^N(t, x, \theta)v(x)dx + k \int_0^l S_U'^N(t, x, \theta)v'(x)dx = \\ \sum_{i=1}^m b_i(x)S_u(t, \theta)v(x)dx, \end{aligned} \quad \text{Eq. 3-22}$$

or

$$\int_0^l \sum_{i=1}^N \dot{e}_i(t) \phi_i(x) v(x) dx + k \int_0^l \sum_{i=1}^N e_i(t) \phi_i'(x) v'(x) dx = \int_0^l \sum_{i=1}^m b_i(x) S_u(t, \theta) v(x) dx. \quad \text{Eq. 3-23}$$

Now we let  $v(x)$  range over  $\phi_j(x)$  for  $j = 1, 2, \dots, N$ , hence

$$\int_0^l \sum_{i=1}^N \dot{e}_i(t) \phi_i(x) \phi_j(x) dx + k \int_0^l \sum_{i=1}^N e_i(t) \phi_i'(x) \phi_j'(x) dx = \int_0^l \sum_{i=1}^m b_i(x) S_u(t, \theta) \phi_j(x) dx. \quad \text{Eq. 3-24}$$

Eq. 3-24 can be written as

$$M \begin{bmatrix} \dot{e}_1(t) \\ \vdots \\ \dot{e}_N(t) \end{bmatrix} + kK \begin{bmatrix} e_1(t) \\ \vdots \\ e_N(t) \end{bmatrix} + S_u(t, \theta) B_0, \quad \text{Eq. 3-25}$$

where

$$M = \left[ \int_0^l \phi_i(x) \phi_j(x) dx \right]_{i,j=1}^N, \quad K = \left[ \int_0^l \phi_i'(x) \phi_j'(x) dx \right]_{i,j=1}^N \quad \text{are the mass and stiffness matrices}$$

$$\text{respectively and } B_0 = \left[ \int_0^l \sum_{i=1}^m b_i(x) \phi_j(x) dx \right]_{i,j=1}^{i=m, j=N}. \quad \text{Rearranging Eq. 3-25 gives}$$

$$\begin{bmatrix} \dot{e}_1(t) \\ \vdots \\ \dot{e}_N(t) \end{bmatrix} = -kKM^{-1} \begin{bmatrix} e_1(t) \\ \vdots \\ e_N(t) \end{bmatrix} + S_u(t, \theta) M^{-1} B_0, \quad \text{Eq. 3-26}$$

Recall that the derivation of  $S_u(t, \theta)$  is done in Chapter 2. The final complete system of equations (controlled and sensitivity equations) becomes

$$\begin{bmatrix} \dot{X}_1(t) \\ \dot{X}_c(t) \\ \dot{S}_X(t) \\ \dot{S}_{X_c}(t) \end{bmatrix} = \begin{bmatrix} A & -BK & 0 & 0 \\ FC & A_c & 0 & 0 \\ 0 & -BK_\theta & A & -BK \\ A_{c_1} & A_{c_2} & A_{c_3} & A_{c_4} \end{bmatrix} \begin{bmatrix} X_1(t) \\ X_c(t) \\ S_X(t) \\ S_{X_c}(t) \end{bmatrix}, \quad \text{Eq. 3-27}$$

where and  $K_\theta, A_{c_1}, A_{c_2}, A_{c_3}$ , and  $A_{c_4}$  are derived and defined in Chapter 2.

Figure 3-19 shows the sensitivity results for the 1-dimensional heat equation for varying  $\theta$ . The results show that the sensitivity of the state is initially high then rapidly decreases with increasing time. This suggests that the system is closer to its desired

equilibrium state as time elapses. More importantly, the results show that there is no significant change in the sensitivity of the state with respect to  $\theta$  as  $\theta$  increases. The conclusion then is that the actual value of  $\theta$  chosen is not critical based on the sensitivity analysis.

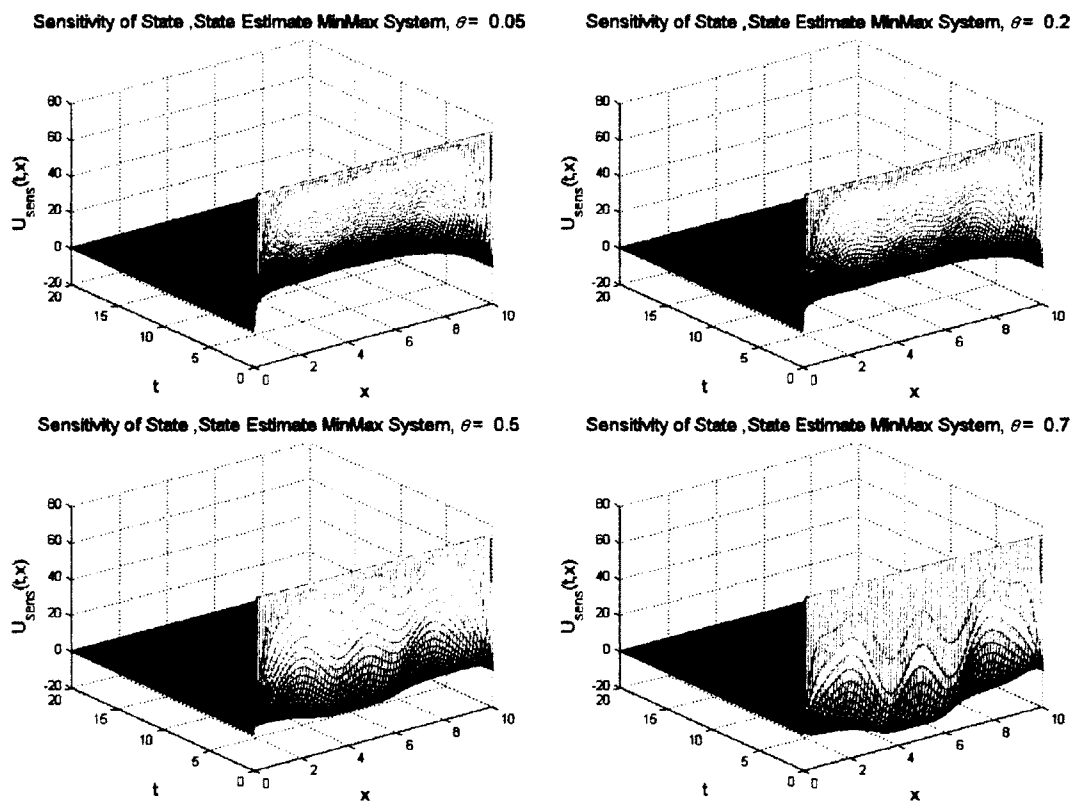


Figure 3-19: Sensitivity of state

Figures 3-20 through 3-27 show the results for the controller sensitivity for various  $\theta$  values.

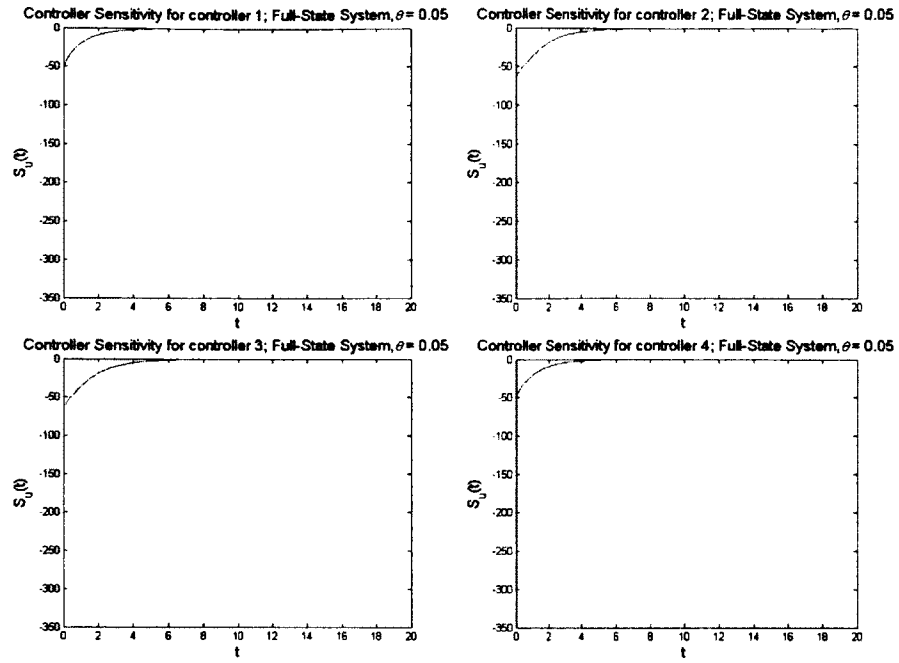


Figure 3-20: Controller sensitivity, full state MinMax

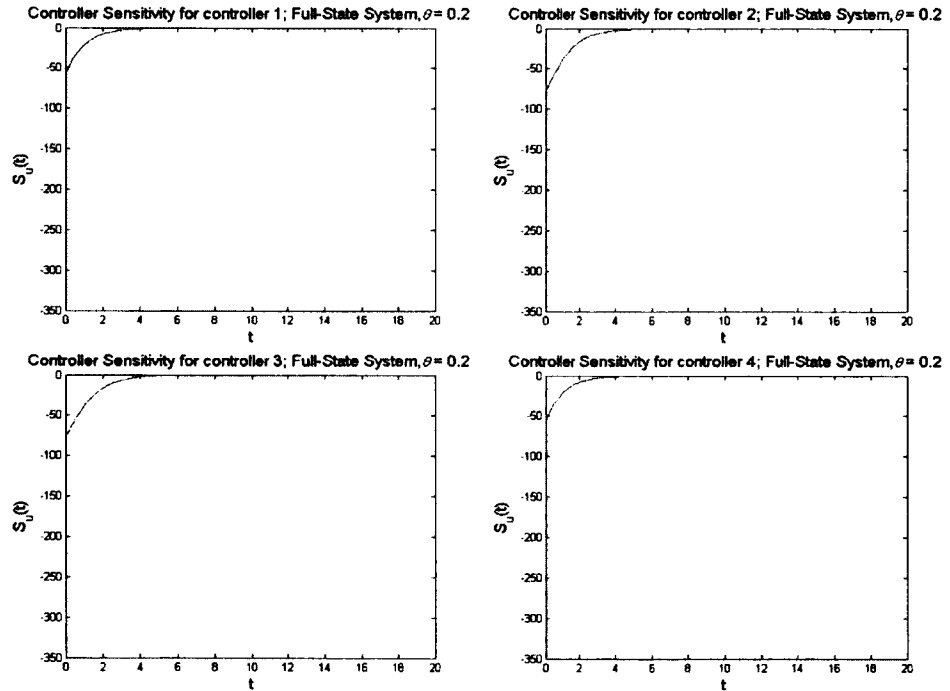


Figure 3-21: controller sensitivity, full state MinMax

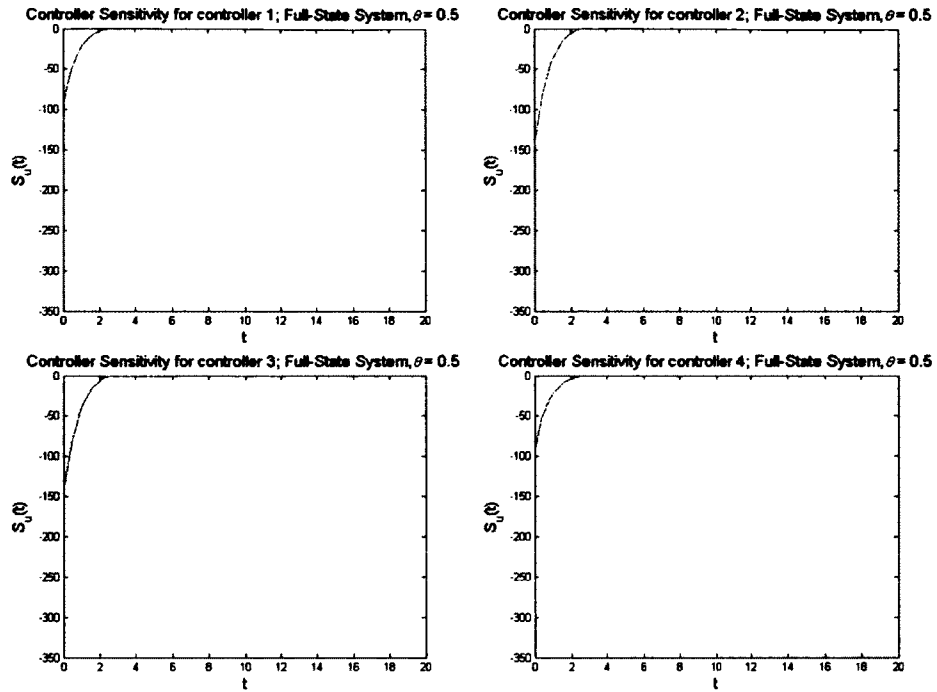


Figure 3-22: Controller sensitivity, full state MinMax

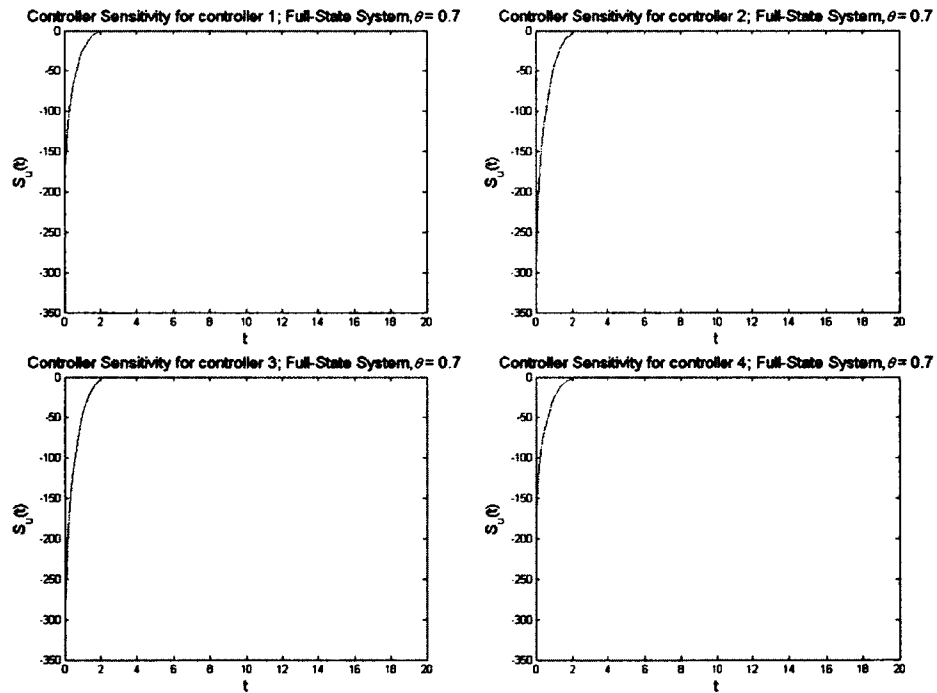


Figure 3-23: Controller sensitivity, full-state MinMax

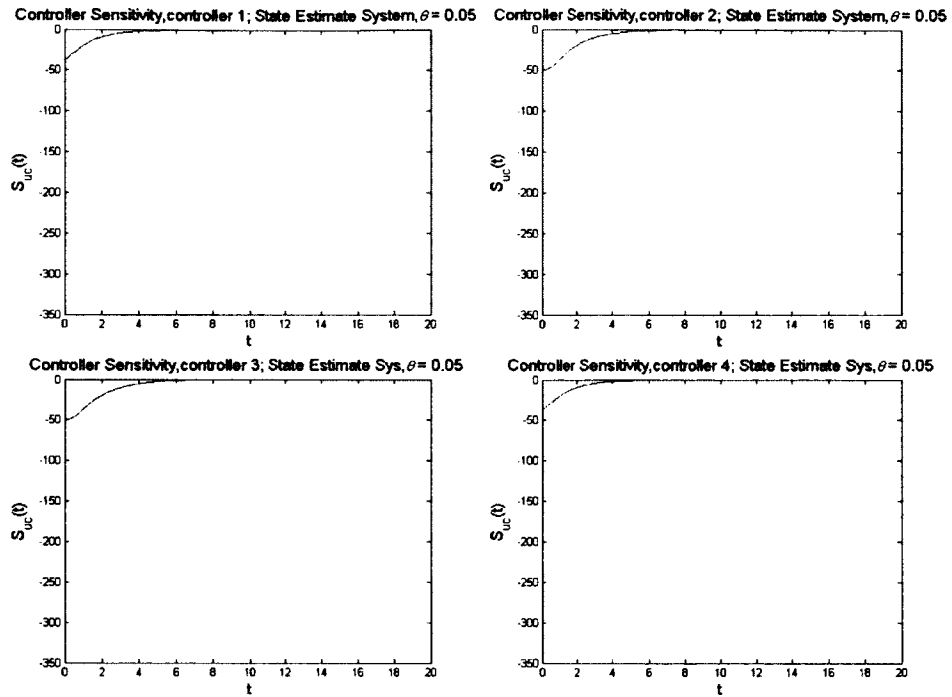


Figure 3-24: Controller sensitivity, state estimate MinMax

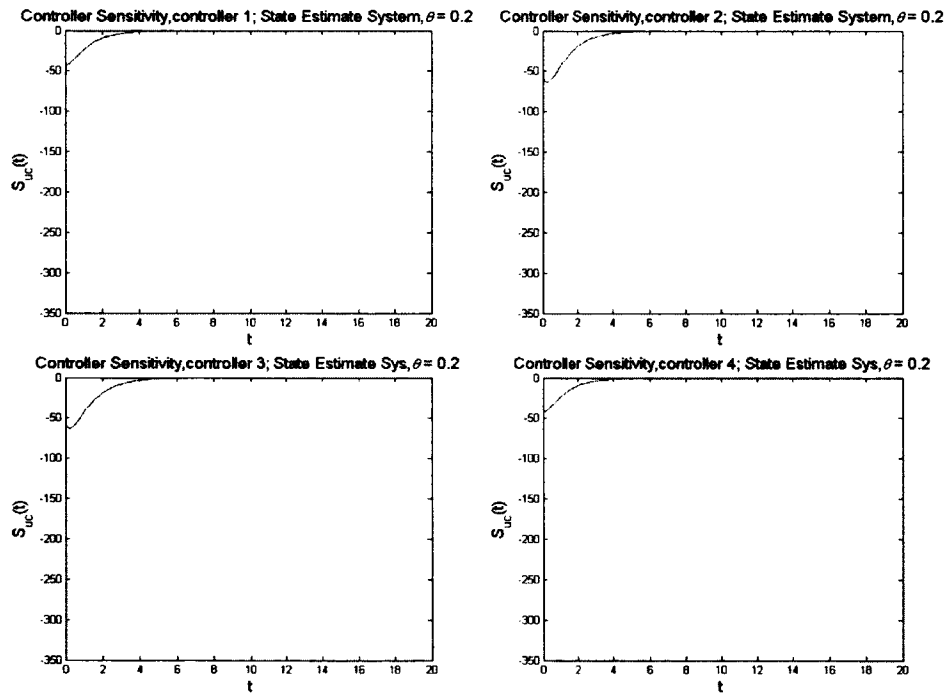


Figure 3-25: Controller sensitivity, state estimate MinMax

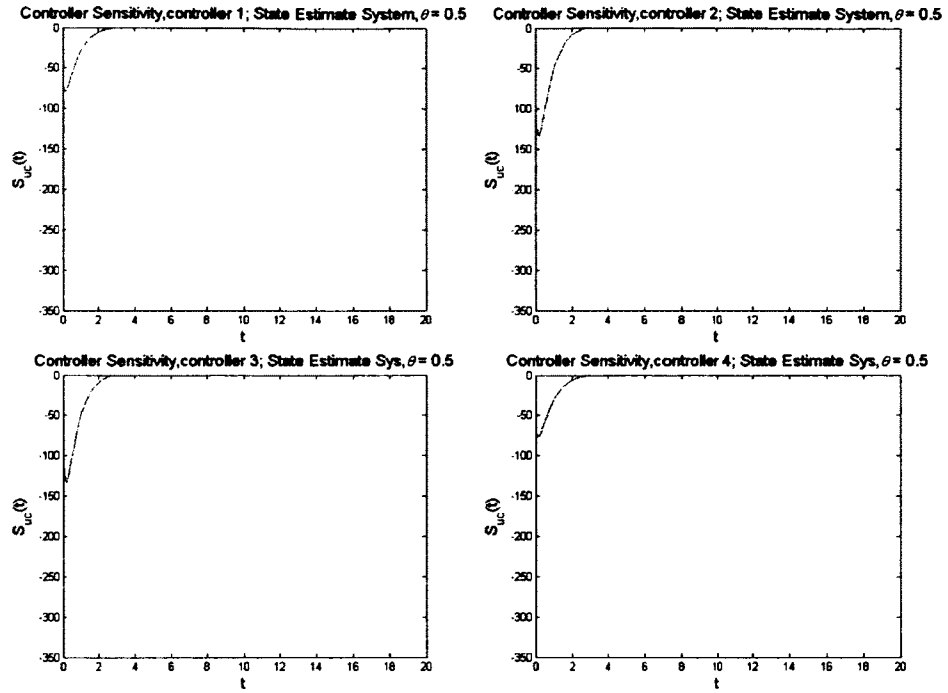


Figure 3-26: Controller sensitivity, state estimate MinMax

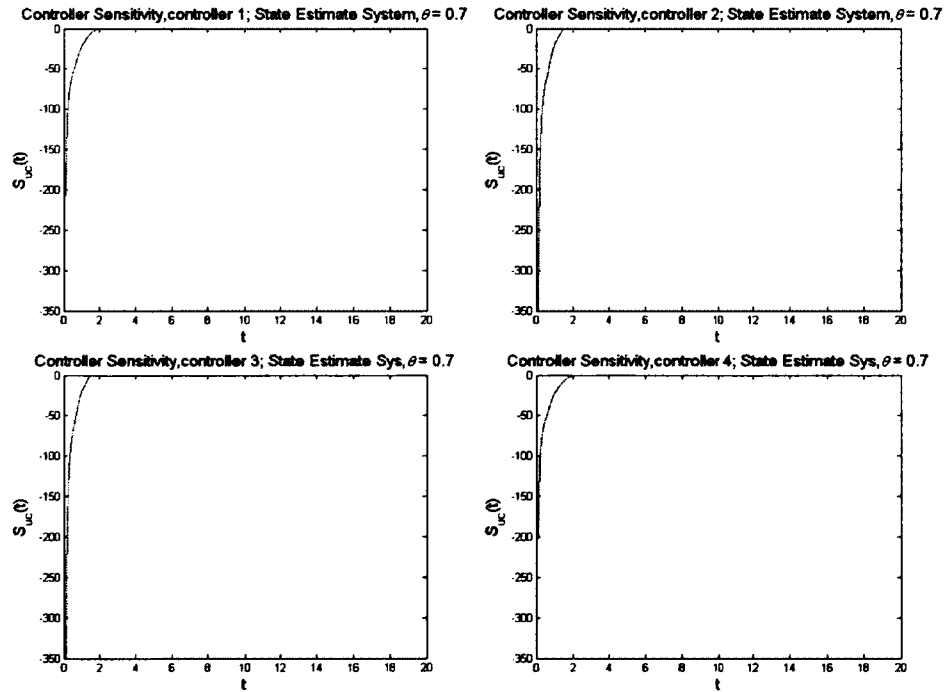


Figure 3-27: Controller sensitivity, state estimate MinMax

As was done in the case of the control effort, we employ Simpson's rule to determine the area between the curve and the time axis. This area gives us the total sensitivity of the controller. Table 3-3 summarizes the results where  $I$  gives the area obtained by Simpson's rule. The total area is calculated for each  $\theta$  value and recorded in the table.

As in the case of the control effort, the table shows that the change in the sensitivity results as  $\theta$  increases is not significant. The order of magnitude is the same (despite the fact that the percentage changes in controller sensitivity values were 38% and 18% respectively). We draw the same conclusion, the actual value of  $\theta$  chosen is not critical based on these sensitivity results.



Table 3-3: Area under controller sensitivity curve (Simpson's rule)

Area Under Curve	$\theta_1 = 0.05$	$\theta_2 = 0.2$	$\theta_3 = 0.5$	$\theta_4 = 0.7$	% change from $\theta_1$ to $\theta_2$
$I_{controller 1}$ (full)	-59.917206	-58.806556	-59.768889	-82.247312	-37.27
$I_{controller 2}$ (full)	-104.522587	-99.810961	-94.256909	-141.127601	-35.02
$I_{controller 3}$ (full)	-104.604629	-99.904745	-94.375426	-141.079794	-34.87
$I_{controller 4}$ (full)	-58.740397	-57.821848	-59.250787	-81.652895	-39.00
<b>TOTAL</b>	<b>-327.78</b>	<b>-316.34</b>	<b>-307.65</b>	<b>-446.11</b>	<b>-36.10</b>
$I_{controller 1}$ (est.)	-56.711188	-60.584871	-72.224398	-80.593801	-42.11
$I_{controller 2}$ (est.)	-102.642519	-107.079874	-116.267130	-107.437266	-4.67
$I_{controller 3}$ (est.)	-102.704091	-107.140862	-116.362847	-107.627948	-4.79
$I_{controller 4}$ (est.)	-55.532781	-59.401540	-71.117822	-79.883074	-43.85
<b>TOTAL</b>	<b>-317.59</b>	<b>-334.21</b>	<b>-375.97</b>	<b>-375.54</b>	<b>-18.25</b>

Figures 3-28 and 3-29 show the maximum absolute controller sensitivity values with respect to  $\theta$ . The results show that for both full-state and state estimate systems, as  $\theta$  increases, the maximum absolute controller sensitivity values increase. However, the

order of magnitude does not change. This suggests that the choice of  $\theta$  is again not critical in terms of maximum controller sensitivity.

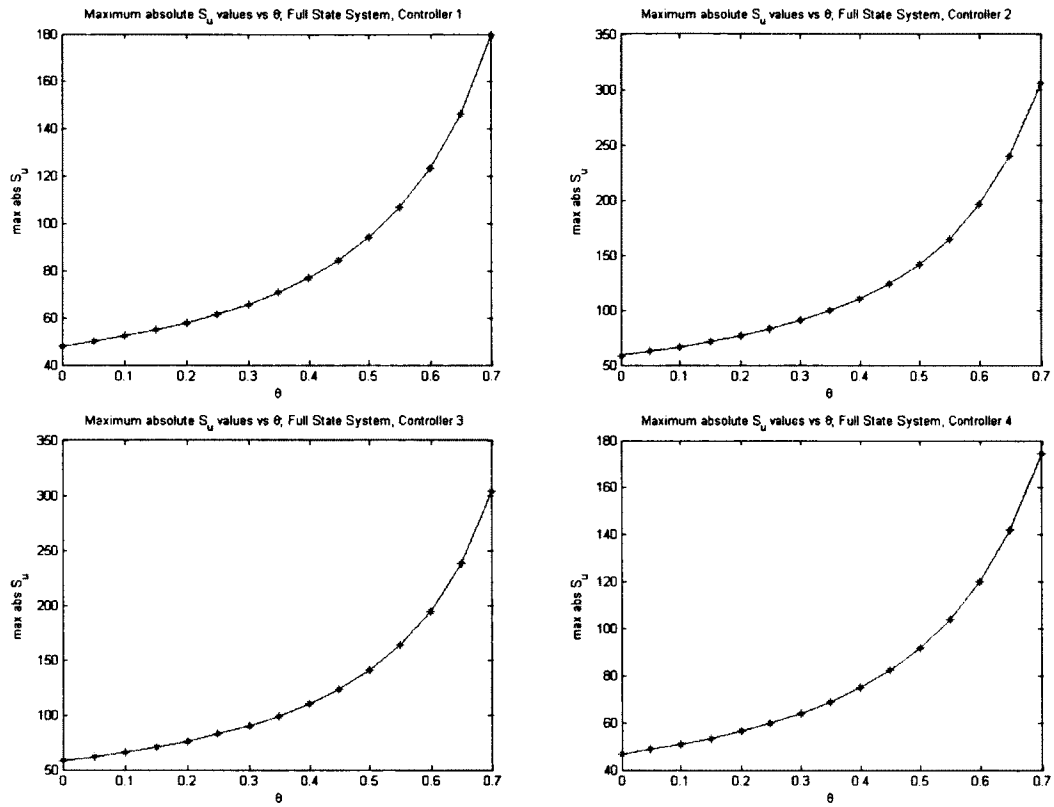


Figure 3-28: Maximum absolute  $S_u(t)$  values

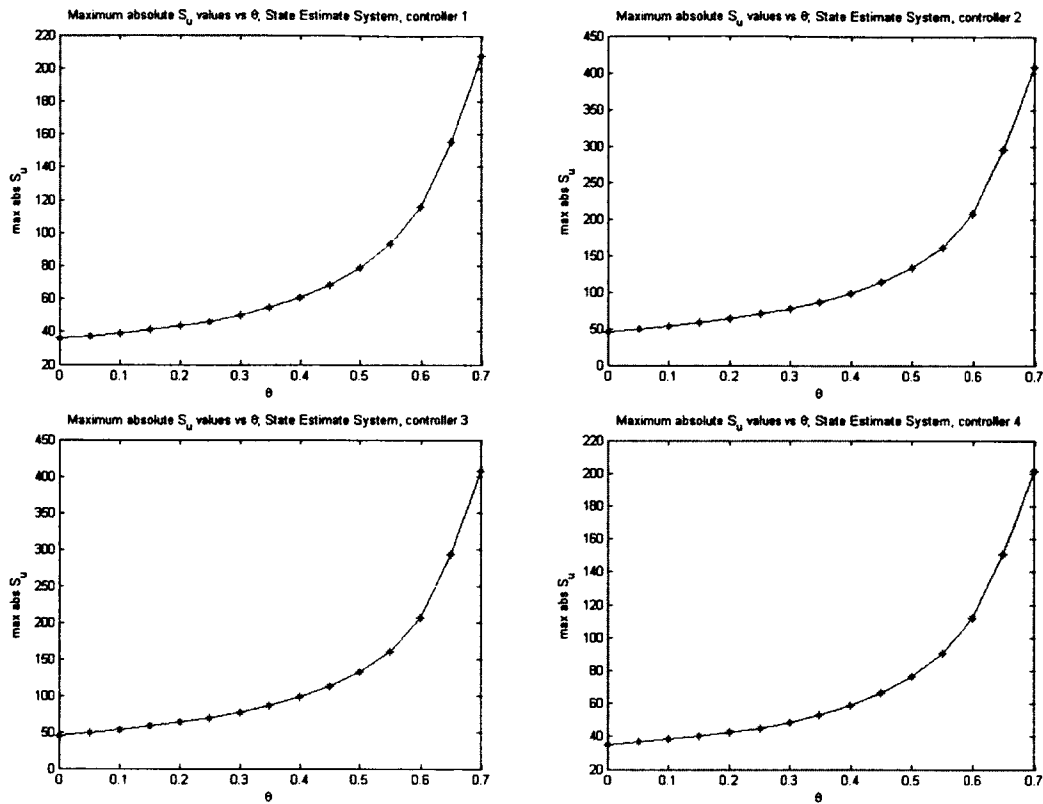


Figure 3-29: Maximum absolute  $S_u(t)$  values

### 3.2.6 Riccati Sensitivity

As stated in Chapter 2, in [35] and at the beginning of this chapter, a major issue in designing a MinMax controller is the determination of an optimal value for  $\theta$ . To this end, the main focus of this dissertation is the sensitivity analysis of the system with respect to  $\theta$ . The Algebraic Riccati Equations are a key component in the design of the controller as shown in Chapter 2. As a result we investigated the sensitivity of the Riccati equations with respect to  $\theta$ .

Figures 3-30 and 3-31 are plots of the maximum absolute values of the sensitivities of the Riccati equations' solutions ( $P$  and  $\Pi$ , described fully in Chapter 2) to the MinMax parameter  $\theta$ . The results show that both maximum sensitivities increase with increasing  $\theta$ . However the order of magnitude of the sensitivities for both results does not

change as  $\theta$  increases. This is in agreement with the controlled results which showed that increasing  $\theta$  has minimal effect on the controlled state. Again the conclusion to be drawn here is that the actual value of  $\theta$  is not critical.

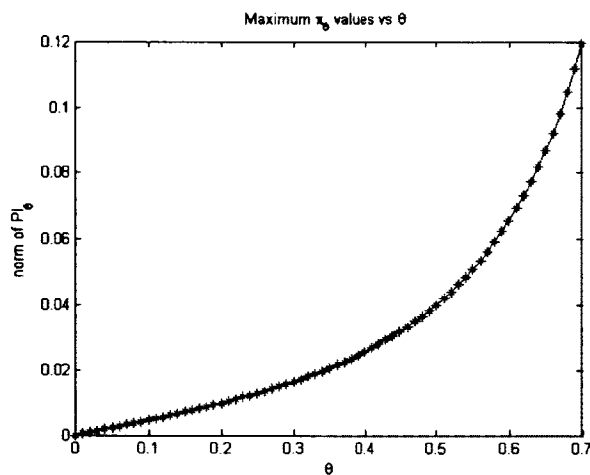


Figure 3-30: Norm of  $\Pi_\theta$  versus  $\theta$

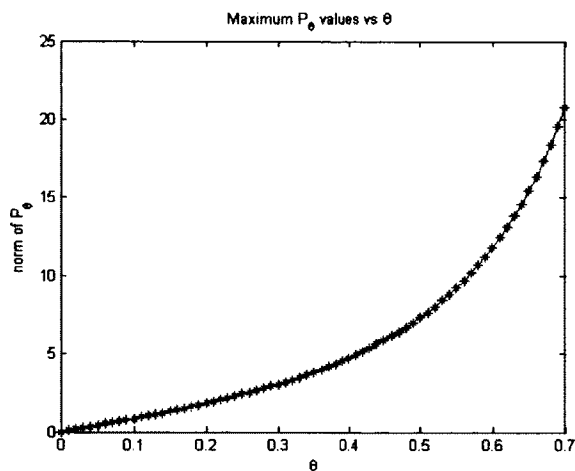


Figure 3-31: Norm of  $P_\theta$  versus  $\theta$

### 3.3 2-D Heat Equation

Heat flow in a 2D medium can be modeled by the equation:

$$U_t(t, x, y) = k[U_{xx}(t, x, y) + U_{yy}(t, x, y)] + \sum_{i=1}^m b_i(x)u(t), \quad \text{Eq. 3-28}$$

where  $0 < x, y < L$  and  $k$  is the aforementioned thermal diffusivity. Figure 3-32 shows the system under consideration.

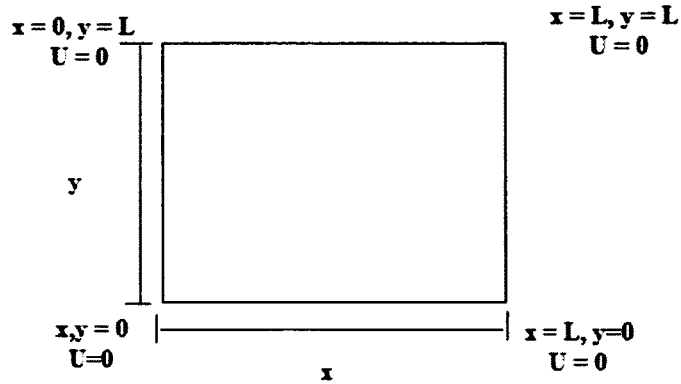


Figure 3-32: Two-dimensional heat surface

As in the previous case, we begin with the weak form of Eq. 3-28:

$$\begin{aligned} \int_0^L \int_0^L U_t(t, x, y)v(x, y)dx dy &= k \int_0^L \int_0^L U_{xx}(t, x, y)v(x, y)dx dy \\ &+ k \int_0^L \int_0^L U_{yy}(t, x, y)v(x, y)dx dy + \int_0^L \int_0^L \sum_{i=1}^m b_i(x, y)u(t)v(x, y)dx dy, \end{aligned} \quad \text{Eq. 3-29}$$

where  $v(x, y) \in H_0^1([0, L] \times [0, L])$  is the test function. Now integration by parts gives,

$$\begin{aligned} \int_0^L \int_0^L U_{xx}(t, x, y)v(x, y)dx dy &= U_x(t, x, y)v(x, y) \Big|_0^L \\ - \int_0^L \int_0^L U_x(t, x, y)v_x(x, y)dx dy &= - \int_0^L \int_0^L U_x(t, x, y)v_x(x, y)dx dy, \end{aligned} \quad \text{Eq. 3-30}$$

and

$$\begin{aligned}
\int_0^l \int_0^l U_{yy}(t, x, y) v(x, y) dx dy &= U_y(t, x, y) v(x, y) \Big|_0^l \\
- \int_0^l \int_0^l U_y(t, x, y) v_y(x, y) dx dy &= - \int_0^l \int_0^l U_y(t, x, y) v_y(x, y) dx dy
\end{aligned}$$

**Eq. 3-31**

Substituting these relationships into Eq. 3-29 gives

$$\begin{aligned}
\int_0^l \int_0^l U_t(t, x, y) v(x, y) dx dy &= -k \int_0^l \int_0^l U_x(t, x, y) v_x(x, y) dx dy \\
- k \int_0^l \int_0^l U_y(t, x, y) v_y(x, y) dx dy &+ \int_0^l \int_0^l \sum_{i=1}^m b_i(x, y) u(t) v(x, y) dx dy.
\end{aligned}$$

**Eq. 3-32**

Now as in the previous case, let  $U(t, x, y) \approx U^N(t, x, y) = \sum_{i=1}^N e_i(t) \phi_j(x, y)$ ,

hence Eq. 3-32 becomes

$$\begin{aligned}
\int_0^l \int_0^l U_t^N(t, x, y) v(x, y) dx dy &= -k \int_0^l \int_0^l U_x^N(t, x, y) v_x(x, y) dx dy \\
- k \int_0^l \int_0^l U_y^N(t, x, y) v_y(t, x, y) dx dy &+ \int_0^l \int_0^l \sum_{i=1}^m b_i(x, y) v(x) dx dy,
\end{aligned}$$

**Eq. 3-33**

or alternatively,

$$\begin{aligned}
&\int_0^l \int_0^l \sum_{i=1}^N \dot{e}_i(t) \phi_i(x, y) v(x, y) dx dy = \\
&-k \int_0^l \int_0^l \sum_{i=1}^N e_i(t) \phi_{i_x}(x, y) v_x(x, y) dx dy - \\
&k \int_0^l \int_0^l \sum_{i=1}^N e_i(t) \phi_{i_y}(x, y) v_y(x, y) dx dy + \\
&\int_0^l \int_0^l \sum_{i=1}^m b_i(x, y) u(t) v(x, y) dx dy.
\end{aligned}$$

**Eq. 3-34**

Now, let  $v(x, y)$  range over  $\phi_j$  for  $j = 1, 2, \dots, N$ , then Eq. 3-34 becomes

$$\begin{aligned}
& \int_0^l \int_0^l \sum_{i=1}^N \dot{e}_i(t) \phi_i(x, y) \phi_j(x, y) dx dy = \\
& -k \int_0^l \int_0^l \sum_{i=1}^N e_i(t) \phi_{i_x}(x, y) \phi_{j_x}(x, y) dx dy - \\
& k \int_0^l \int_0^l \sum_{i=1}^N e_i(t) \phi_{i_y}(x, y) \phi_{j_y}(x, y) dx dy + \\
& \int_0^l \int_0^l \sum_{i=1}^m b_i(x, y) u(t) \phi_j(x, y) dx dy.
\end{aligned}$$

**Eq. 3-35**

This can be rewritten as

$$M \begin{bmatrix} \dot{e}_1(t) \\ \vdots \\ \dot{e}_N(t) \end{bmatrix} = -kK \begin{bmatrix} e_1(t) \\ \vdots \\ e_N(t) \end{bmatrix} + B_0 u(t).$$

**Eq. 3-36**

where  $M = \left[ \int_0^l \int_0^l \phi_i(x, y) \phi_j(x, y) dx dy \right]_{i,j=1}^N$ ,  $B_0 = \left[ \sum_{i=1}^m b_i(x, y) \phi_j(x, y) dx dy \right]$  and

$$K = \left[ \int_0^l \int_0^l \phi_{i_x}(x, y) \phi_{j_x}(x, y) dx dy + \phi_{i_y}(x, y) \phi_{j_y}(x, y) dx dy \right]_{i,j=1}^N.$$

Finally, Eq. 3-36 becomes

$$\begin{bmatrix} \dot{e}_1(t) \\ \vdots \\ \dot{e}_N(t) \end{bmatrix} = -kM^{-1}K \begin{bmatrix} e_1(t) \\ \vdots \\ e_N(t) \end{bmatrix} + M^{-1}B_0 u(t).$$

**Eq. 3-37**

As in the 1-dimensional case, full knowledge of the system is not available so we take measurements in the form

$$y(t) = CX(t),$$

**Eq. 3-38**

where

$$C = [\text{zeros}(1, N) \ 0.05 \ \text{zeros}(1, N) \ 0.05 \ \dots \ \dots]$$

**Eq. 3-39**

Eq. 3-39 shows that measurements are taken at the interior nodes at intervals of  $N$ . In

this problem,  $m = 1$ , and  $b_i(x, y) = e^{-((x-x_0)^2 + (y-y_0)^2)}$  where  $(x_0, y_0)$  is the geometric center

of the 2-d surface.

### 3.4 Numerical Results

For all the simulations in this section,  $N = 18$ ,  $L_x = L_y = 10$ ,  $k = 1$ ,  $R = I$  and

$$U(t, 0, y) = U(t, x, 0) = U(t, L_x, y) = U(t, x, L_y) = 0. \quad \text{Eq. 3-40}$$

Note that  $N = 18$ , results in a total of 361 nodes (including boundary nodes, with 289 interior nodes) and 648 triangular elements in the Galerkin finite element scheme used to approximate the solutions to this problem. This Galerkin finite element scheme used for this 2-dimensional system is presented in [36]. This number  $N$  was limited due to computer memory problems. However, numerical results to be presented indicate convergence at this level of discretization. The results are presented in the following order: uncontrolled simulations, functional gains, controlled simulations, stability analysis and sensitivity analysis.

#### 3.4.1 Uncontrolled Results

In order to obtain a solution to the system in Eq. 3-37 and Eq. 3-38, we apply the following initial conditions

$$U_0 = U(0, x, y) = 100, \quad U_{c_0} = U_c(0, x, y) = 0.75U_0. \quad \text{Eq. 3-41}$$

Figure 3-3 shows the uncontrolled state for this system along the horizontal center line, i.e.  $U(t, x, \frac{L_y}{2})$ . The uncontrolled state along the vertical center line, i.e.  $U(t, y, \frac{L_x}{2})$ , is the same (due to symmetry) to the horizontal center results, and is therefore not presented here. As before, we desire the state to tend to the exponentially stable equilibrium position of zero (0).



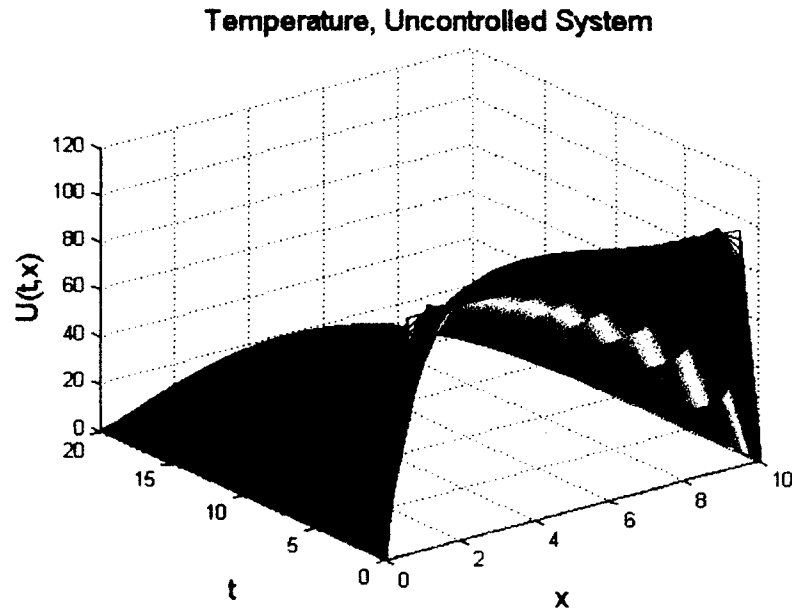


Figure 3-33: Uncontrolled heat flow along center of 2-d square surface

#### 3.4.2 Controlled Results

Figures 3-34 through 3-37 show the results for the functional gains for the system in Eq. 3-37 and Eq. 3-38. The color legend in this plot is:  $N = 6$  blue,  $N = 10$  red,  $N = 14$  black,  $N = 18$  magenta. The results show that the functional gains are converging to zero which suggests that the Galerkin finite element scheme employed is convergent. The results also show that as  $\theta$  increases, the convergence of the functional gains gets slightly slower. This implies that the lower the value of  $\theta$ , the faster the convergence of the controller.

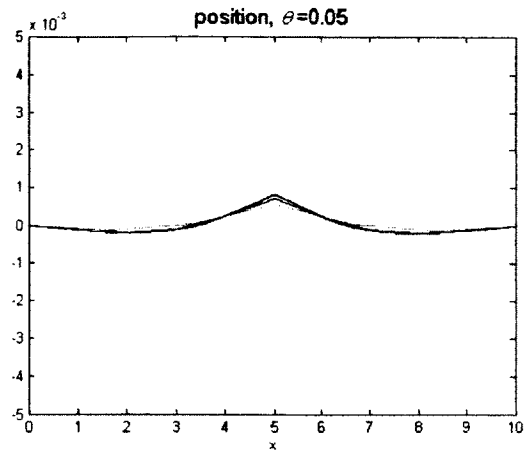


Figure 3-34: Functional gains

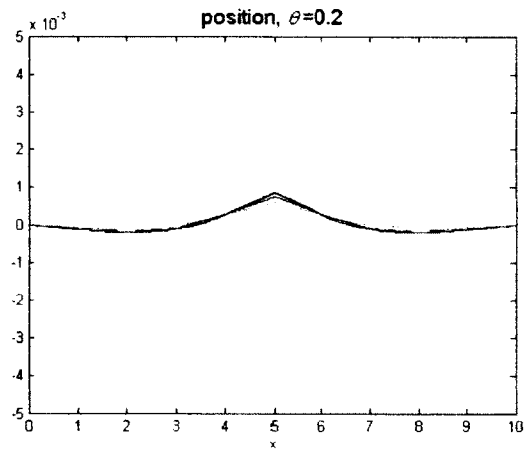


Figure 3-35: Functional gains

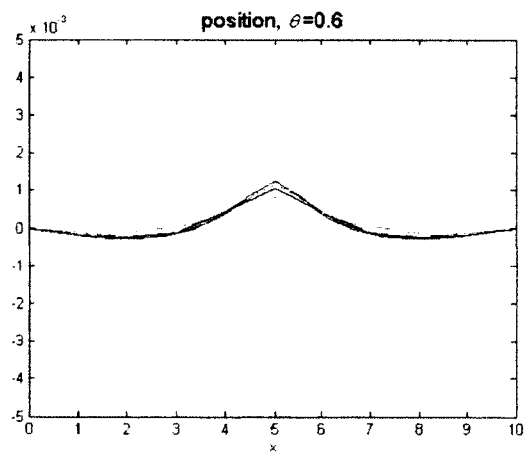


Figure 3-36: Functional gains

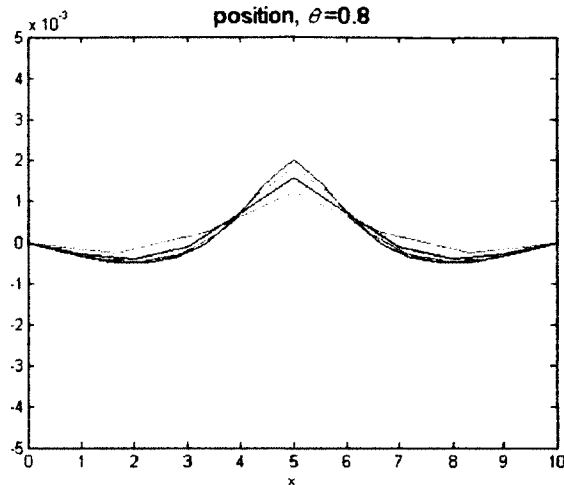


Figure 3-37: Functional gains

Figures 3-38 and 3-39 show the controlled temperature values along the horizontal center line of the square region for the full state ( $u(t) = -KU(t)$ ) and for the state estimate system ( $u(t) = -KU_c(t)$ ), respectively. In each figure, the top left result is for  $\theta = 0.05$ , top right is for  $\theta = 0.2$ , bottom left is for  $\theta = 0.6$  and finally bottom right is for  $\theta = 0.8$ . The maximum 0.8 is the maximum  $\theta$  value that still results in  $[I - \theta^2 P\Pi] > 0$  and eigenvalues of  $\begin{bmatrix} A & -BK \\ FC & A_c \end{bmatrix}$  being in the left two quadrants of the complex plane as described in Chapter 2. The state is driven to zero faster at the center of the rod. This is due to the Gaussian distribution of the control input operator. In general, however, the results show that as  $\theta$  increases, the controller's performance is virtually unchanging. This is in agreement with the 1-dimensional case and again suggests that the actual value of  $\theta$  chosen is not critical. In this 2-dimensional case, the difference between the full state system and the state estimate feedback system is not as salient as in the 1-dimensional case.

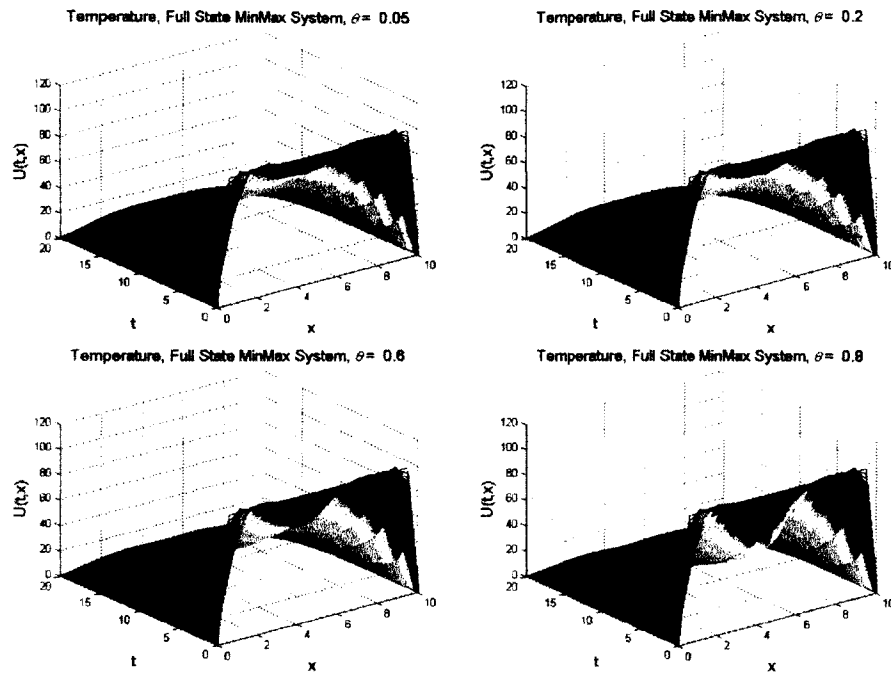


Figure 3-38: Controlled temperature, full state MinMax system

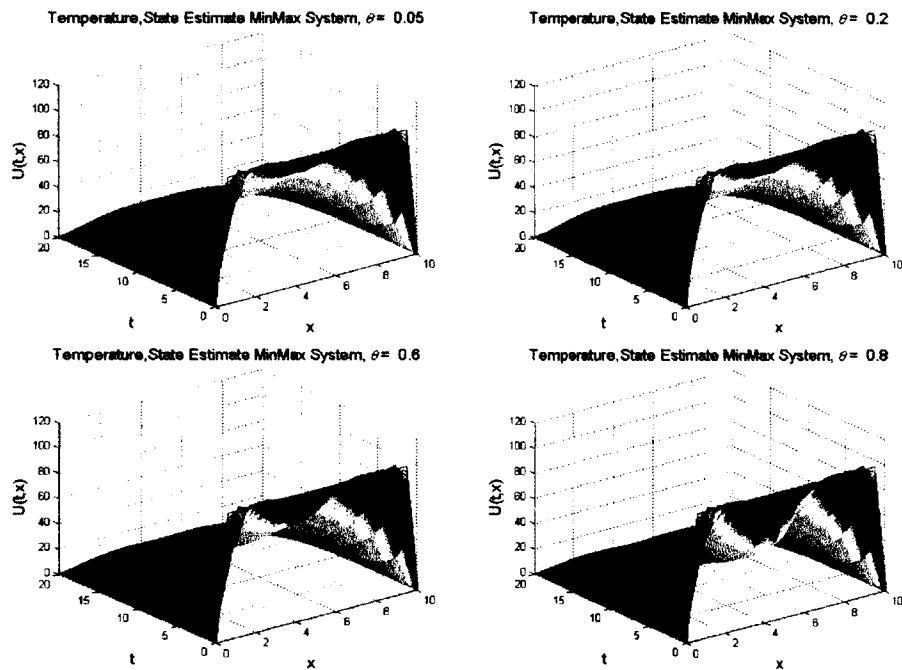


Figure 3-39: Controlled temperature, state estimate MinMax system

### 3.4.3 Stability Analysis

As in the 1-dimensional case, we investigate the eigenvalues of the following matrix  $\begin{bmatrix} A & -BK \\ FC & A_c \end{bmatrix}$ . Recall that all the eigenvalues of this matrix must be on the left-hand side of the complex plane in order for the system to be stable. Figures 3-40 and 3-41 show the eigenvalue plots for various  $\theta$  values. The results conclusively show that the controlled system is stable. Again the figures on the right show the closest eigenvalues to the imaginary axis. In these figures, the stability margin increases slightly with increasing  $\theta$  (see Table 3-4). The marginal increases again show that the actual value of  $\theta$  is not critical with respect to the stability of the system.

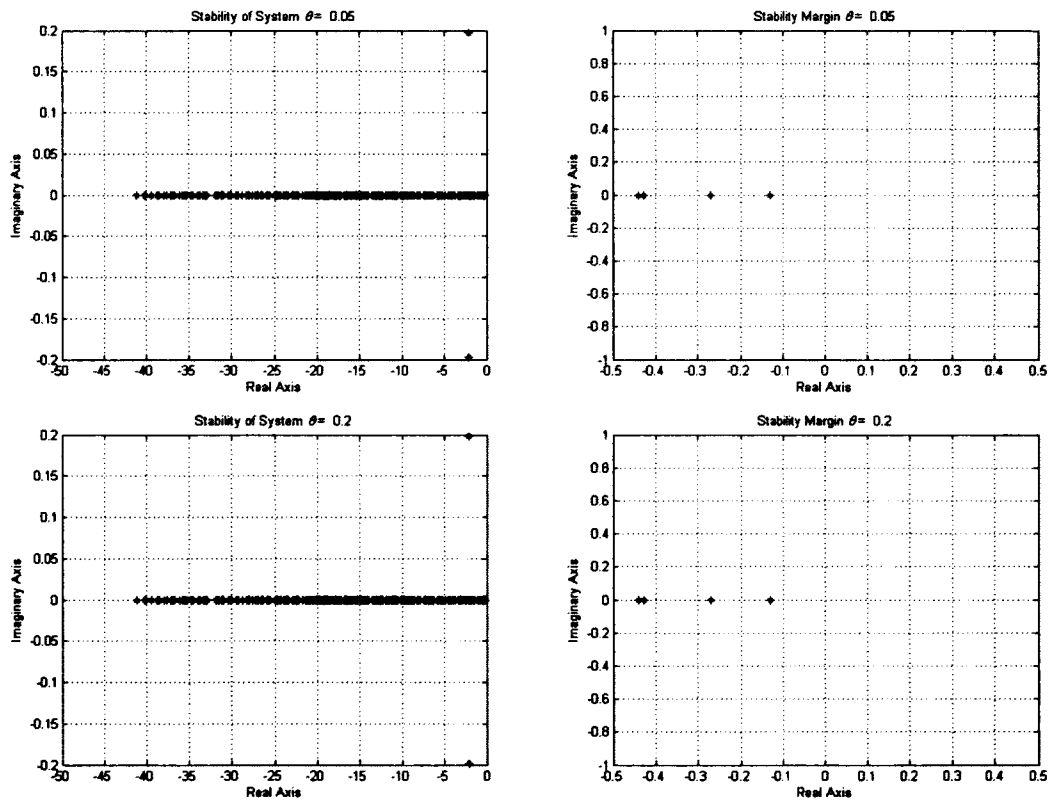


Figure 3-40: Eigenvalues of  $\begin{bmatrix} A & -BK \\ FC & A_c \end{bmatrix}$

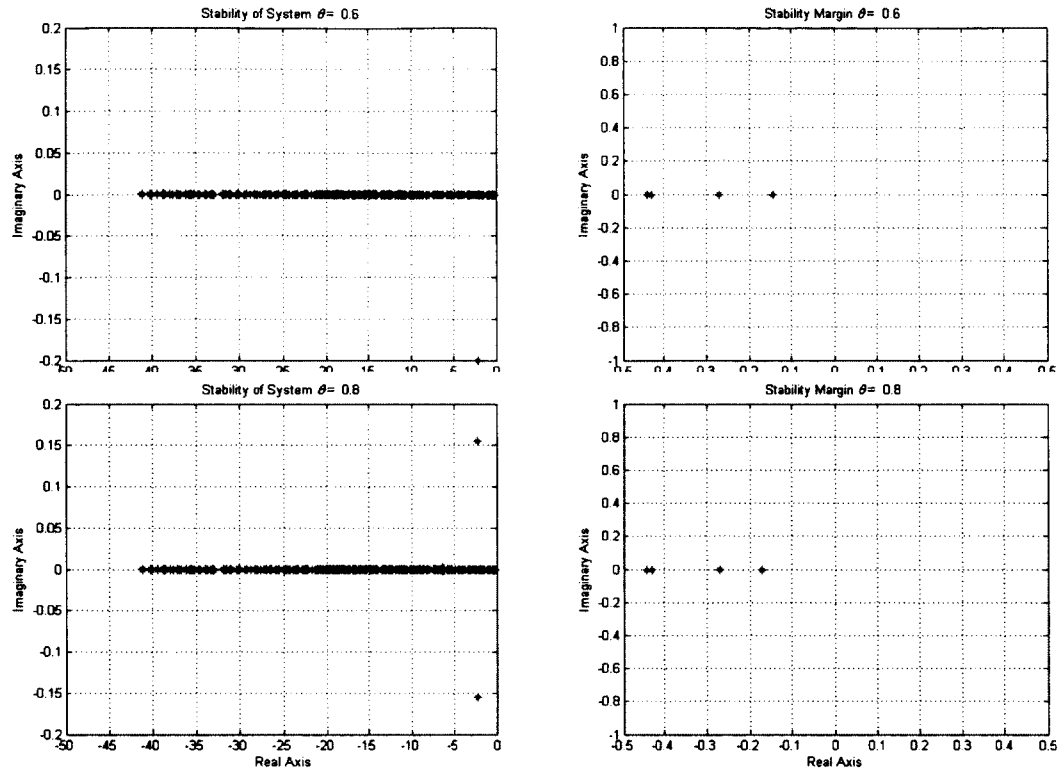


Figure 3-41: Eigenvalues of  $\begin{bmatrix} A & -BK \\ FC & A_C \end{bmatrix}$

Table 3-4 shows the stability margin and radius results for the controlled system.

The results show that as  $\theta$  increases, the stability radius increases slightly. The stability of the system, in terms of the stability radius increases. However, this increase is only slight; hence the choice of  $\theta$  is not critical in terms of the stability radius.

Table 3-4: Stability margin and radius for controlled system ( $A_{mm}$ )

$\theta$	Stability Margin	Stability Radius
0.05	0.131414815938655	0.116232872977096
0.2	0.132348858606243	0.116683248500507
0.6	0.144656368855594	0.122631778452644
0.8	0.172431522925289	0.135857785488283

#### 3.4.4 Control Effort

We provide Figures 3-42 and 3-43, the controlled effort for  $\theta = 0.05, 0.2, 0.6, 0.8$ . In Figure 3-42, the system under investigation is the Full State MinMax controlled system where no compensator/observer is used. In Figure 3-43 a compensator is implemented. As previously done, in order to better compare the control effort for varying  $\theta$  values, we employ Simpson's rule to find the area between the curve and the time axis. The results are shown in Table 3-5. The results show that the control effort increases (percentage) significantly from  $\theta_1$  to  $\theta_4$ , however, actual values are of the same order of magnitude. These results again re-enforce the conclusion that the actual value of  $\theta$  employed is not critical with respect to the effort required by the controller.

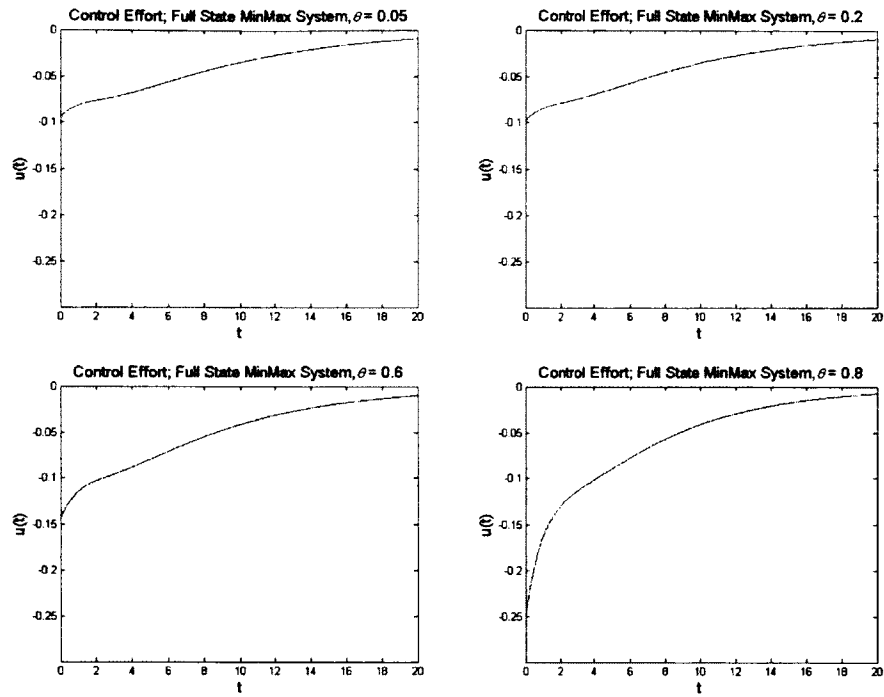


Figure 3-42: Control effort, full state MinMax

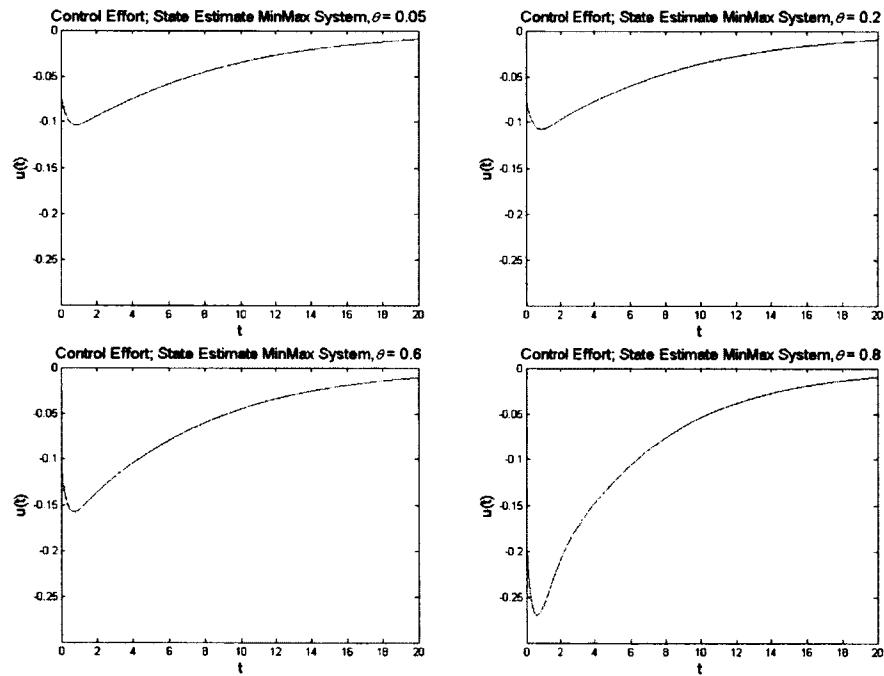


Figure 3-43: Control effort, state estimate MinMax



Table 3-5: Area under control effort curve (Simpson's rule)

Area Under Curve	$\theta_1 = 0.05$	$\theta_2 = 0.2$	$\theta_3 = 0.6$	$\theta_4 = 0.8$	%change from $\theta_1$ to $\theta_4$
$I_{controller 1}$ (full)	-0.808086	-0.827892	-1.030291	-1.180309	-46.06
$I_{controller 1}$ (est.)	-0.872973	-0.898834	-1.199288	-1.660371	-90.19

### 3.4.5 Sensitivity Analysis

In order to perform sensitivity analysis of the 2-dimensional heat equation, we begin by differentiating Eq. 3-28 with respect to  $\theta$ , resulting in

$$U_{t\theta}(t, x, y, \theta) - k[U_{xx\theta}(t, x, y, \theta) + U_{yy\theta}(t, x, y, \theta)] = \sum_{i=1}^m b_i(x, y)u_{\theta}(t, \theta). \quad \text{Eq. 3-42}$$

Here,  $\frac{\partial U(t, x, y, \theta)}{\partial \theta} = U_{\theta}(t, x, y, \theta)$  and  $\frac{\partial u(t, \theta)}{\partial \theta} = u_{\theta}(t, \theta)$ . Now let  $U_{\theta}(t, x, y, \theta) = S_U(t, x, y, \theta)$  and  $u_{\theta}(t, \theta) = S_u(t, \theta)$ . We then have

$$S_{U_t}(t, x, y, \theta) - k[S_{U_{xx}}(t, x, y, \theta) + S_{U_{yy}}(t, x, y, \theta)] = \sum_{i=1}^m b_i(x, y)S_u(t, \theta). \quad \text{Eq. 3-43}$$

The weak form of Eq. 3-43 is

$$\iint_0^t S_{U_t}(t, x, y, \theta)v(x, y)dxdy - k\left[\iint_0^t (S_{U_{xx}}(t, x, y, \theta) + S_{U_{yy}}(t, x, y, \theta))v(x, y)dxdy\right] = \iint_0^t \sum_{i=1}^m b_i(x, y)S_u(t, \theta)v(x, y)dxdy \quad \text{Eq. 3-44}$$

Using integration by parts,

$$\begin{aligned} & \iint_0^l \left( S_{U_{xx}}(t, x, y, \theta) + S_{U_{yy}}(t, x, y, \theta) \right) v(x, y) dx dy = \\ & - \iint_0^l \left( S_{U_x}(t, x, y, \theta) v_x(x, y) + \right. \end{aligned} \quad \text{Eq. 3-45}$$

$S_{U_y}(t, x, y, \theta) v_y(x, y) \Big) dx dy$ , hence the weak form is now

$$\begin{aligned} & \iint_0^l S_{U_t}(t, x, y, \theta) v(x, y) dx dy + k \left[ \iint_0^l \left( S_{U_x}(t, x, y, \theta) v_x(x, y) + \right. \right. \\ & \left. \left. S_{U_y}(t, x, y, \theta) v_y(x, y) \right) dx dy \right] = \iint_0^l \sum_{i=1}^m b_i(x, y) S_u(t, \theta) dx dy. \end{aligned} \quad \text{Eq. 3-46}$$

Let  $S_U(t, x, y, \theta) \approx S_U^N(t, x, y, \theta) = \sum_{i=1}^N e_i \phi_i(x, y, \theta)$  so that

$$\begin{aligned} & \iint_0^l S_{U_t}^N(t, x, y, \theta) v(x, y) dx dy + \\ & k \left[ \iint_0^l \left( S_{U_x}^N(t, x, y, \theta) v_x(x, y) + S_{U_y}^N(t, x, y, \theta) v_y(x, y) \right) dx dy \right] = \end{aligned} \quad \text{Eq. 3-47}$$

$\iint_0^l \sum_{i=1}^m b_i(x, y) S_u(t, \theta) dx dy$ , or

$$\begin{aligned} & \iint_0^l \sum_{i=1}^N \dot{e}_i(t) \phi_i(x, y) v(x, y) dx dy + \\ & k \iint_0^l \sum_{i=1}^N e_i(t) \left[ \phi_{i_x}(x, y) v_x(x, y) + \phi_{i_y}(x, y) v_y(x, y) \right] dx dy = \end{aligned} \quad \text{Eq. 3-48}$$

$\iint_0^l \sum_{i=1}^m b_i(x, y) S_u(t, \theta) v(x, y) dx dy$ .

Now we let  $v(x, y)$  range over  $\phi_j(x, y)$  for  $j = 1, 2, \dots, N$ , hence

$$\begin{aligned} & \iint_0^l \sum_{i=1}^N \dot{e}_i(t) \phi_i(x, y) \phi_j(x, y) dx dy + \\ & k \iint_0^l \sum_{i=1}^N e_i(t) \left[ \phi_{i_x}(x, y) \phi_{j_x}(x, y) + \phi_{i_y}(x, y) \phi_{j_y}(x, y) \right] dx dy = \end{aligned} \quad \text{Eq. 3-49}$$

$\iint_0^l \sum_{i=1}^m b_i(x, y) S_u(t, \theta) \phi_j(x, y) dx dy$ .

Eq. 3-49 can be written as

$$M \begin{bmatrix} \dot{e}_1(t) \\ \vdots \\ \dot{e}_N(t) \end{bmatrix} + kK \begin{bmatrix} e_1(t) \\ \vdots \\ e_N(t) \end{bmatrix} + S_u(t, \theta) B_0. \quad \text{Eq. 3-50}$$

where

$$M = \left[ \int_0^l \int_0^l \phi_i(x, y) \phi_j(x, y) dx dy \right]_{i,j=1}^N,$$

$$B_0 = \left[ \int_0^l \int_0^l \sum_{i=1}^m b_i(x, y) \phi_j(x, y) dx dy \right]_{i,j=1}^{i=m, j=N}$$

and **Eq. 3-51**

$$K = \left[ \int_0^l \phi_{ix}(x, y, \theta) \phi_{jx}(x, y, \theta) + \phi_{iy}(x, y, \theta) \phi_{jy}(x, y, \theta) \right]_{i,j=1}^N.$$

Rearranging Eq. 3-50 gives

$$\begin{bmatrix} \dot{e}_1(t) \\ \vdots \\ \dot{e}_N(t) \end{bmatrix} = -kM^{-1}K \begin{bmatrix} e_1(t) \\ \vdots \\ e_N(t) \end{bmatrix} + S_u(t, \theta)M^{-1}B_0.$$

**Eq. 3-52**

Recall that the derivation of  $S_u(t, \theta)$  is done in Chapter 2. The final complete system of equations (controlled and sensitivity equations) becomes

$$\begin{bmatrix} \dot{X}(t) \\ \dot{X}_c(t) \\ \dot{S}_X(t) \\ \dot{S}_{X_c}(t) \end{bmatrix} = \begin{bmatrix} A & -BK & 0 & 0 \\ FC & A_c & 0 & 0 \\ 0 & -BK_\theta & A & -BK \\ A_{c1} & A_{c2} & A_{c3} & A_{c4} \end{bmatrix} \begin{bmatrix} X(t) \\ X_c(t) \\ S_X(t) \\ S_{X_c}(t) \end{bmatrix}$$

**Eq. 3-53**

where  $K_\theta$ ,  $A_{c1}$ ,  $A_{c2}$ ,  $A_{c3}$ , and  $A_{c4}$  are derived and defined in Chapter 2.

Figure 3-44 shows the sensitivity results for the 2-dimensional heat equation for varying  $\theta$ . The results show that the sensitivity of the state is initially high then decreases with increasing time. This suggests that the system is closer to its desired equilibrium state as time elapses. More importantly, the results show that there is virtually no change in the sensitivity of the state with respect to  $\theta$  as  $\theta$  increases. Near the center of the spatial domain, there is a slight decrease in sensitivity as  $\theta$  increases. This increase is not significant, however. The conclusion then is that the actual value of  $\theta$  chosen is not critical based on the sensitivity analysis.

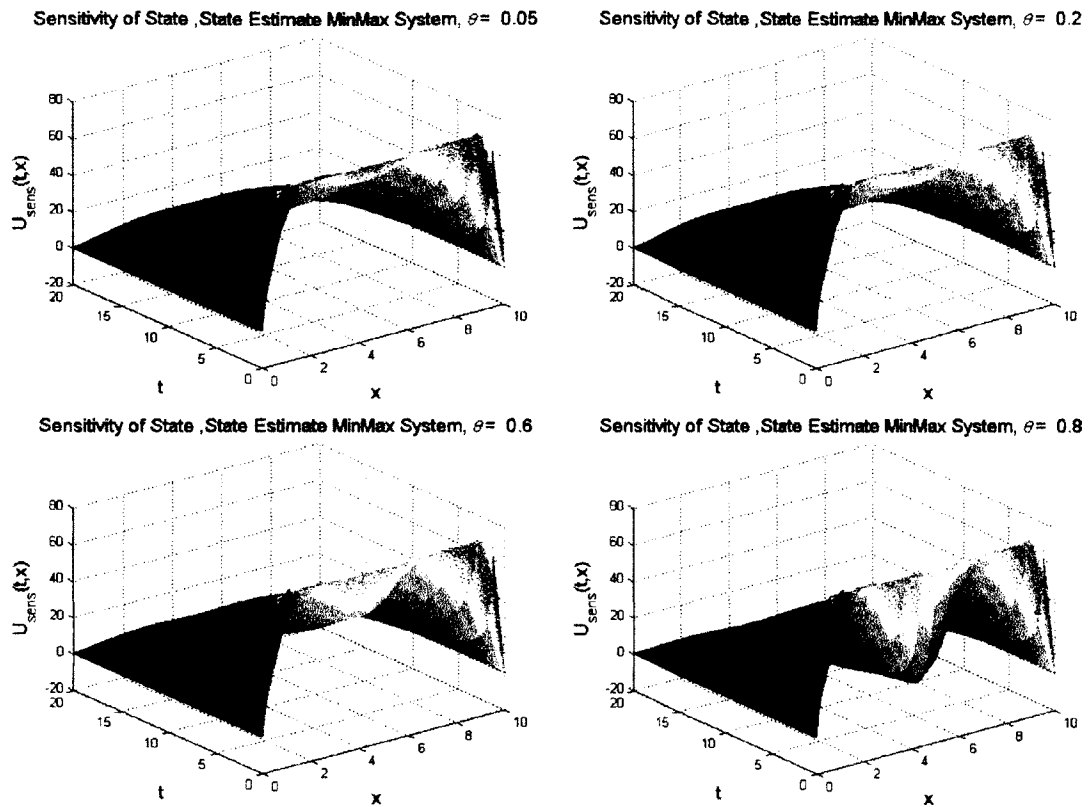


Figure 3-44: Sensitivity of state

Figures 3-45 and 3-46 show the results for the controller sensitivity for various  $\theta$  values. Table 3-6 shows the values of the areas between the curves and the time axis, giving the total sensitivity over the elapsed time. Although the sensitivity increases with increasing  $\theta$ , the change is not significant. The values are all of the same order of magnitude (despite the significant percentage increase from  $\theta_1$  to  $\theta_4$ ). We draw the same conclusion as in the 1-dimensional case: the actual value of  $\theta$  chosen is not critical based on these sensitivity results.

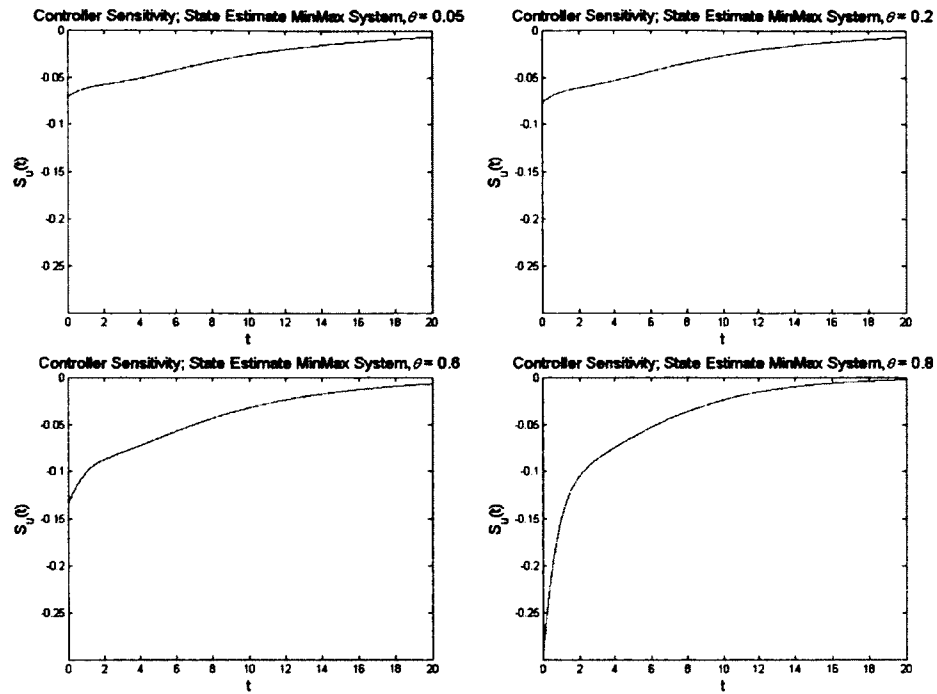


Figure 3-45: Controller sensitivity, state estimate MinMax

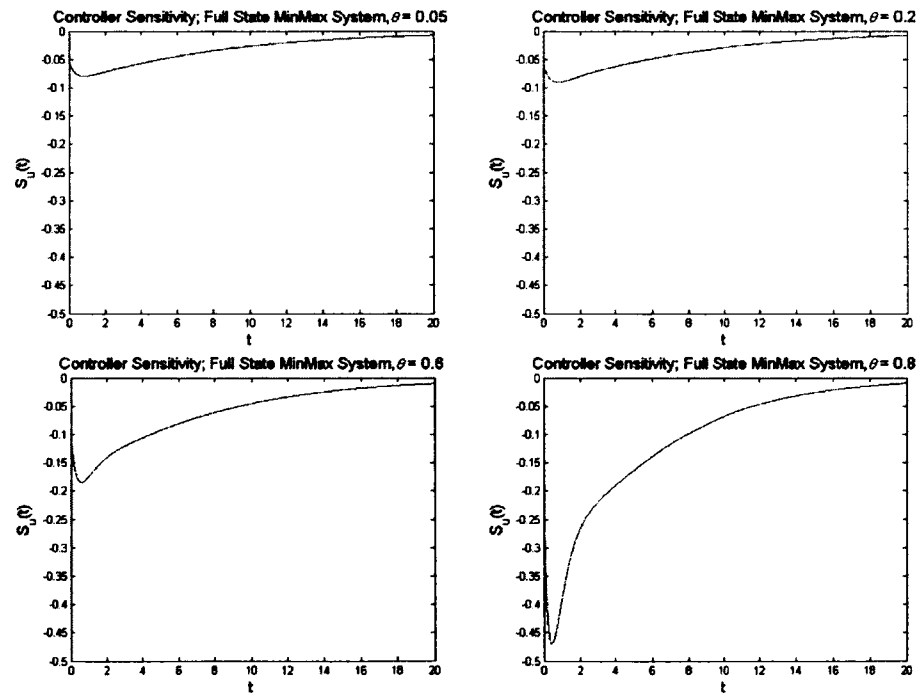
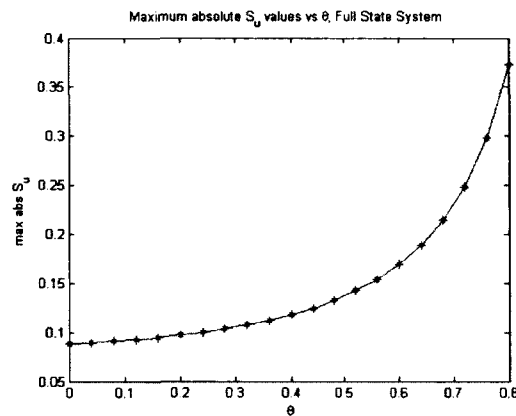


Figure 3-46: Controller sensitivity, full state MinMax

Table 3-6: Area under controller sensitivity curve (Simpson's rule)

Area Under Curve	$\theta_1 = 0.05$	$\theta_2 = 0.2$	$\theta_3 = 0.6$	$\theta_4 = 0.8$	%change from $\theta_1$ to $\theta_4$
$I_{controller\ 1}$ (full)	-0.610156	-0.637937	-0.838519	-0.883410	-44.78
$I_{controller\ 1}$ (est.)	-0.669111	-0.735296	-1.240240	-2.216588	-231.12

Figures 3-47 and 3-48 show the maximum absolute controller sensitivity values with respect to  $\theta$ . The results show that as  $\theta$  increases, the maximum absolute controller sensitivity increases. However, this increase is insignificant. This agrees with the previous results which showed that the controller's performance changes minimally with increasing  $\theta$ .

Figure 3-47: Maximum absolute  $S_u(t)$  values, full state MinMax

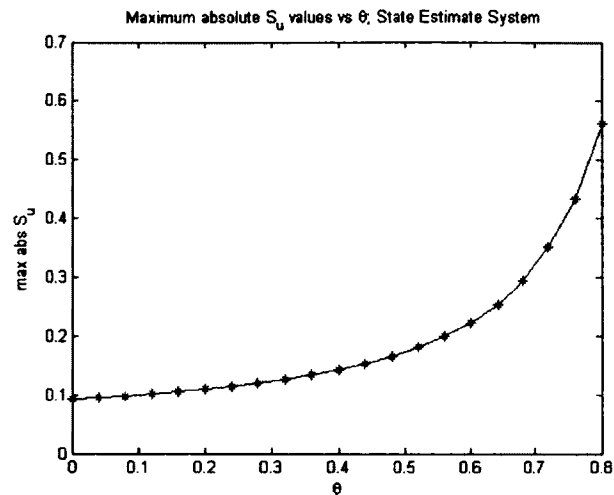
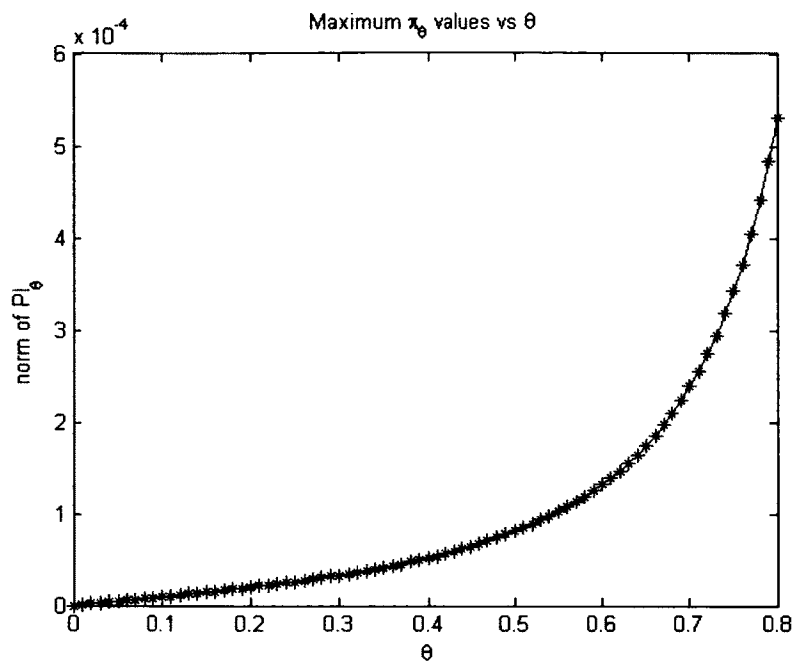
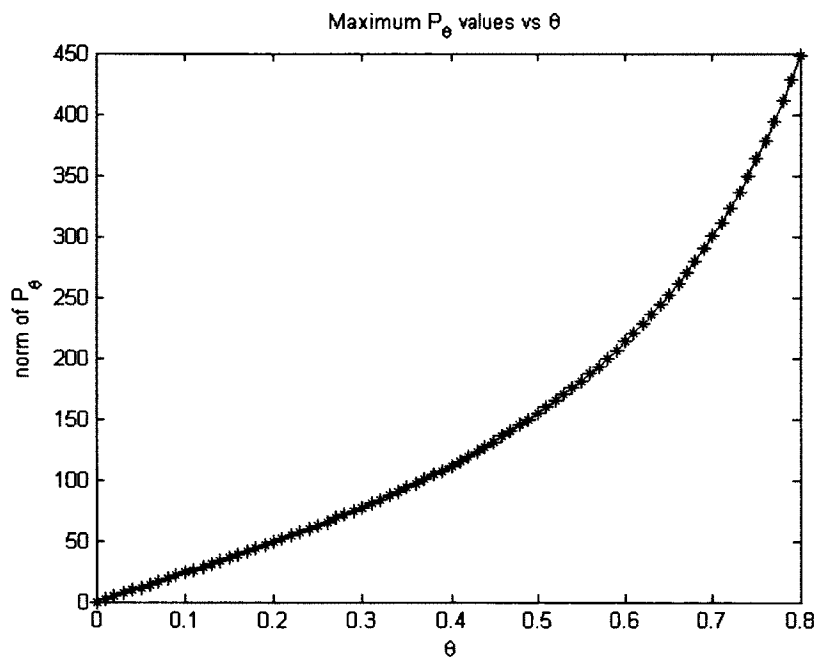


Figure 3-48: Maximum absolute values, state estimate MinMax

#### 3.4.6 Riccati Sensitivity

As in the case of the 1-dimensional heat equation, we investigated the sensitivity of the Riccati equations with respect to  $\theta$ . Figures 3-49 and 3-50 are plots of the maximum absolute values of the sensitivities of the Riccati equations' solutions ( $P$  and  $\Pi$ , described fully in Chapter 2) to the MinMax parameter  $\theta$ . The results show that both maximum sensitivities increase with increasing  $\theta$ . However the order of magnitude of the sensitivities for both results does not change as  $\theta$  increases. This is in agreement with the 1-dimensional heat equation results. Again the conclusion to be drawn here is that the actual value of  $\theta$  is not critical.

Figure 3-49: Norm of  $\Pi_\theta$  versus  $\theta$ Figure 3-50: Norm of  $P_\theta$  versus  $\theta$



## CHAPTER 4

### WAVE EQUATION

#### 4.1 Problem Formulation

In this Chapter, we implement the MinMax controller and apply Continuous Sensitivity Equation Methods (as described in Chapter 2) to the 1-dimensional wave equation. The goal here is to further our investigation of a more efficient means of choosing the MinMax parameter,  $\theta$ . The 1-dimensional wave equation with viscous damping can be written as

$$U_{tt}(t, x) - U_{xx}(t, x) + \gamma U_t(t, x) = \sum_{i=1}^m b_i(x)u(t), \quad \text{Eq. 4-1}$$

where  $U(t, x)$  represents the displacement at position  $x$  and time  $t$  for  $t \geq 0$ ,  $\gamma$  is the viscous damping coefficient,  $0 \leq x \leq l$  is the spatial dimension,  $b_i(x)$  are the control input functions which describe how the control is applied, and  $u(t)$  is the control input to the system. In this case, the speed of propagation of the wave is taken to be unity. We apply the following boundary conditions to this system:

$$U(t, 0) = U(t, l) = 0. \quad \text{Eq. 4-2}$$

In order to implement the MinMax controller on this system, we use distributed parameter control theory. This requires the formulation of a finite dimensional approximation of the PDE. A Galerkin finite element scheme is used. In order to determine the finite element approximation to Eq. (4.1), we first write the weak form of the PDE. In considering the weak form of the problem we seek to find

$U(x) \in X = H_0^1(0, l)$  such that

$$\int_0^l \ddot{U}(t, x)v(x)dx - \int_0^l U''(t, x)v(x)dx + \gamma \int_0^l \dot{U}(t, x)v(x)dx = \int_0^l \sum_{i=1}^m b_i(x)u(t)v(x)dx, \quad \text{Eq. 4-3}$$

where,  $v(x) \in V = H_0^1$ ,  $\dot{U}(t, x) = U_t(t, x)$ , and  $U'(t, x) = U_x(t, x)$ .

Using integration by parts,

$$\int_0^l U''(t, x)v(x)dx = U'(t, x)v(x) \Big|_0^l - \int_0^l U'(t, x)v'(x)dx = - \int_0^l U'(t, x)v'(x)dx, \text{ where}$$

$v(0) = v(l) = 0$ . Substituting this into Eq. (4.3) gives

$$\begin{aligned} & \int_0^l \ddot{U}(t, x)v(x)dx + \\ & \int_0^l U'(t, x)v'(x)dx + \gamma \int_0^l \dot{U}(t, x)v(x)dx = \\ & \int_0^l \sum_{i=1}^m b_i(x)u(t)v(x)dx. \end{aligned} \quad \text{Eq. 4-4}$$

Now we divide the spatial domain into  $N$  equidistant subintervals and approximate

$U(t, x)$  by  $U^N(t, x) = \sum_{i=1}^N e_i(t)\phi_i(x)$  where  $\phi_i(x)$  are piecewise linear basis functions and

$e_i(t)$  are the corresponding coefficients of these functions. We then have

$$\begin{aligned} & \int_0^l \ddot{U}^N(t, x)v(x)dx + \int_0^l U^{N'}(t, x)v'(x)dx + \\ & \gamma \int_0^l \dot{U}^N(t, x)v(x)dx = \int_0^l \sum_{i=1}^m b_i(x)u(t)v(x)dx, \end{aligned} \quad \text{Eq. 4-5}$$

which can be rewritten as

$$\begin{aligned} & \int_0^l \sum_{i=1}^N \ddot{e}_i(t)\phi_i(x)v(x)dx + \\ & \int_0^l \sum_{i=1}^N e_i(t)\phi_i'(x)v'(x)dx + \\ & \gamma \int_0^l \sum_{i=1}^N \dot{e}_i(t)\phi_i(x)v(x)dx = \int_0^l \sum_{i=1}^m b_i(x)u(t)v(x)dx. \end{aligned} \quad \text{Eq. 4-6}$$

Let  $v(x)$  range over the basis functions  $\phi_j(x)$  for  $j = 1, 2, \dots, N$ . Eq. 4-6 becomes

$$\int_0^l \sum_{i=1}^N \ddot{e}_i(t) \phi_i(x) \phi_j(x) dx + \int_0^l \sum_{i=1}^N e_i(t) \phi_i'(x) \phi_j'(x) dx + \gamma \int_0^l \sum_{i=1}^N \dot{e}_i(t) \phi_i(x) \phi_j(x) dx = \int_0^l \sum_{i=1}^m b_i(x) u(t) \phi_j(x) dx. \quad \text{Eq. 4-7}$$

This can be rewritten as

$$M \begin{bmatrix} \ddot{e}_1(t) \\ \vdots \\ \ddot{e}_N(t) \end{bmatrix} + \gamma M \begin{bmatrix} \dot{e}_1(t) \\ \vdots \\ \dot{e}_N(t) \end{bmatrix} + K \begin{bmatrix} e_1(t) \\ \vdots \\ e_N(t) \end{bmatrix} = B_0 u(t), \quad \text{Eq. 4-8}$$

where  $M = \left[ \int_0^l \phi_i(x) \phi_j(x) dx \right]_{i,j=1}^N$  and  $K = \left[ \int_0^l \phi_i'(x) \phi_j'(x) dx \right]_{i,j=1}^N$  are the mass and stiffness matrices, respectively, and  $B_0 = \left[ \int_0^l \sum_{i=1}^m b_i(x) \phi_j(x) dx \right]_{i,j=1}^N$  is the control input matrix.

Rearranging Eq. 4-8 gives

$$\begin{bmatrix} \ddot{e}_1(t) \\ \vdots \\ \ddot{e}_N(t) \end{bmatrix} = -\gamma I \begin{bmatrix} \dot{e}_1(t) \\ \vdots \\ \dot{e}_N(t) \end{bmatrix} - M^{-1} K \begin{bmatrix} e_1(t) \\ \vdots \\ e_N(t) \end{bmatrix} + M^{-1} B_0 u(t). \quad \text{Eq. 4-9}$$

As stated in Chapter 2, it is necessary for the system to be posed as a first order system of differential equations. To this end, we define  $x_1(t) = e(t)$  and  $x_2(t) = \dot{e}(t)$ . Eq. 4-9 now becomes

$$\begin{bmatrix} \dot{x}_1(t) \\ \dot{x}_2(t) \end{bmatrix} = \begin{bmatrix} 0 & I \\ -M^{-1}K & -\gamma I \end{bmatrix} \begin{bmatrix} x_1(t) \\ x_2(t) \end{bmatrix} + \begin{bmatrix} 0 \\ M^{-1}B_0 \end{bmatrix} u(t). \quad \text{Eq. 4-10}$$

Since full knowledge of the system is not available, we take measurements in the form

$$y(t) = C \begin{bmatrix} x_1(t) \\ x_2(t) \end{bmatrix}, \quad \text{Eq. 4-11}$$

where  $C$  is composed of four averaging measurements of both the position and velocity states, resulting in the following  $8 \times (2N - 2)$  matrix

$$\begin{bmatrix}
 \left[ \frac{4}{l} \int_0^{\frac{l}{4}} \phi_i^N(x) dx \right]_{i=1}^{N-1} & 0 \\
 \left[ \frac{4}{l} \int_{\frac{l}{4}}^{\frac{l}{2}} \phi_i^N(x) dx \right]_{i=1}^{N-1} & 0 \\
 \left[ \frac{4}{l} \int_{\frac{l}{2}}^{\frac{3l}{4}} \phi_i^N(x) dx \right]_{i=1}^{N-1} & 0 \\
 \left[ \frac{4}{l} \int_{\frac{3l}{4}}^l \phi_i^N(x) dx \right]_{i=1}^{N-1} & 0 \\
 0 & \left[ \frac{4}{l} \int_0^{\frac{l}{4}} \phi_i^N(x) dx \right]_{i=1}^{N-1} \\
 0 & \left[ \frac{4}{l} \int_{\frac{l}{4}}^{\frac{l}{2}} \phi_i^N(x) dx \right]_{i=1}^{N-1} \\
 0 & \left[ \frac{4}{l} \int_{\frac{l}{2}}^{\frac{3l}{4}} \phi_i^N(x) dx \right]_{i=1}^{N-1} \\
 0 & \left[ \frac{4}{l} \int_{\frac{3l}{4}}^l \phi_i^N(x) dx \right]_{i=1}^{N-1}
 \end{bmatrix}$$

Eq. 4-12

Next, we define  $\{b_i\}_{i=1}^m$ . We begin by partitioning the spatial domain  $[0, l]$  as  $\{x_i\}_{i=1}^m$  where  $x_i = i \times \frac{l}{m}$ . The functions  $b_i$  are defined as  $b_i(x) = e^{-(x-x_i^*)^2}$  for  $x_{i-1} \leq x \leq x_i$ , where  $x_i^* = \frac{x_{i-1} + x_i}{2} = 1.25, 3.75, 6.25, 8.75$  since  $L=10$  and  $m=4$  for this problem. Figure 4-1 shows the four control input functions.

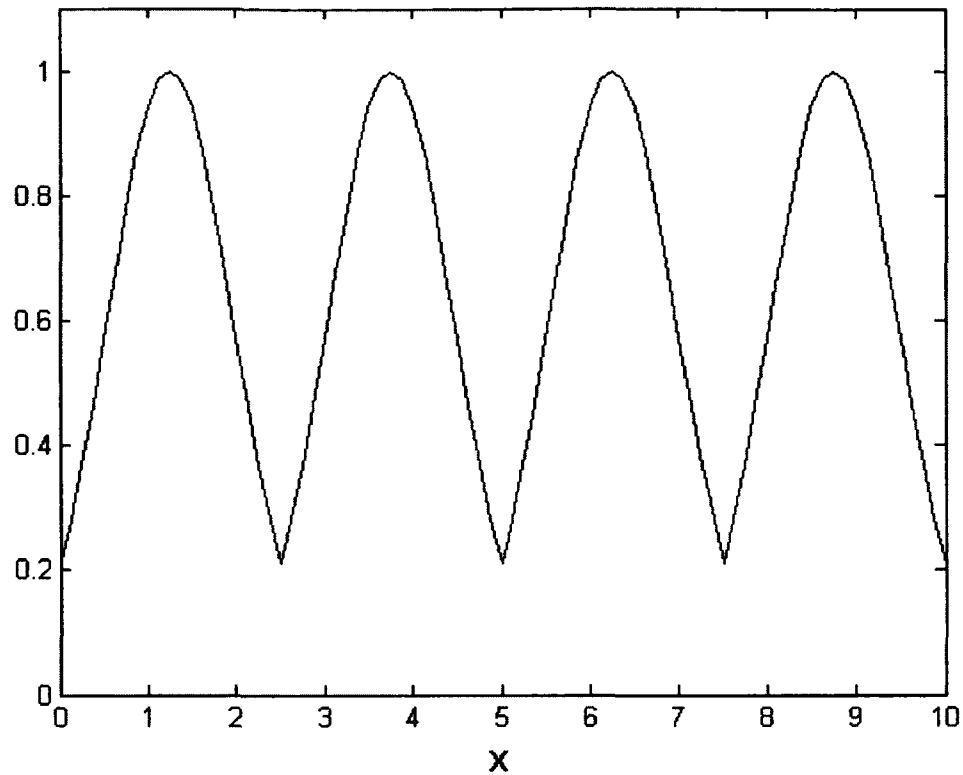


Figure 4-1: Control input functions

Finally,

$$B_0 = \begin{bmatrix} 0 & \dots & 0 \\ B_1 & \dots & B_m \end{bmatrix} \quad \text{and} \quad B_i = \begin{bmatrix} \int_0^l b_i(x)\phi_j(x)dx \\ \vdots \\ \int_0^l b_i(x)\phi_{N-1}(x)dx \end{bmatrix}_{i,j=1}^{i=m,j=N-1}. \quad \text{Eq. 4-13}$$

## 4.2 Numerical Results

For all simulations in this section,  $N = 60$  and  $R = 0.001 * I$ . The results are presented in the following order: Uncontrolled simulations, functional gains, controlled simulations, stability analysis, and sensitivity analysis.

### 4.2.1 Uncontrolled Results

For simulation purposes and to attain a solution to the system in Eq. 4-10 and Eq. 4-11, we apply the following initial conditions

$$X_0 = \left[ X(0, x), \frac{\partial}{\partial t} X(0, x) \right] = [\sin x, \cos x]$$

$$X_{c0} = \left[ X_c(0, x), \frac{\partial}{\partial t} X_c(0, x) \right] = 0.75X_0.$$

Eq. 4-14

Figure 4-2 shows the uncontrolled state displacement for the system in Eq. 4-10 and Eq. 4-11.

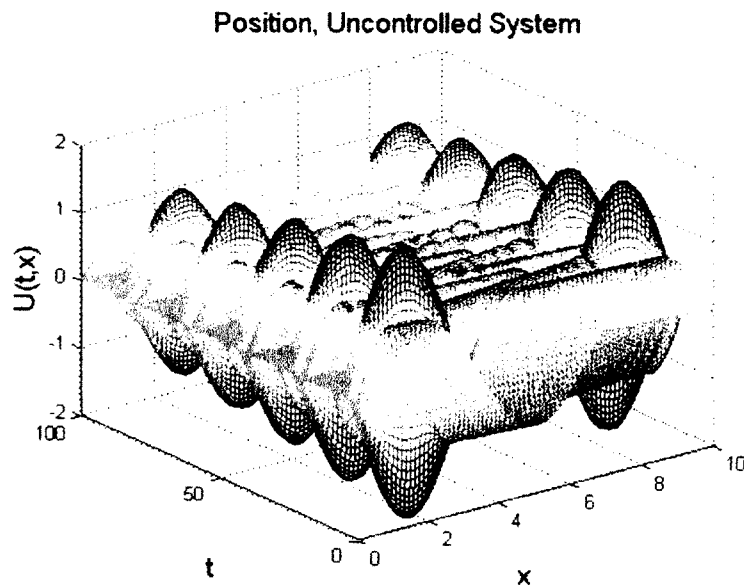


Figure 4-2: Uncontrolled displacement

The simulation was performed using as little damping as possible while ensuring that the system is controllable. In this case,  $\gamma = 0.01$ . The consequence is that after  $t = 100$ , the state position has not dissipated. We desire the state to tend to the exponentially stable equilibrium position of zero (0). The MinMax controller is applied with the aim of achieving this goal.

#### 4.2.2 Controlled Results

Figures 4-3 through 4-5 show the functional gains for the MinMax controller for  $\theta = 0.08, 0.16, 0.32$ . The color legend is as follows:  $N = 20$  red,  $N = 40$  black,  $N = 80$  cyan

and  $N = 160$  magenta. These results show that the functional gains are converging to zero. Furthermore, the results show that as  $\theta$  changes, the functional gain plots are similar. This indicates that there is convergence of the Galerkin finite element scheme and that the controller convergence is unaffected by the choice of  $\theta$ .

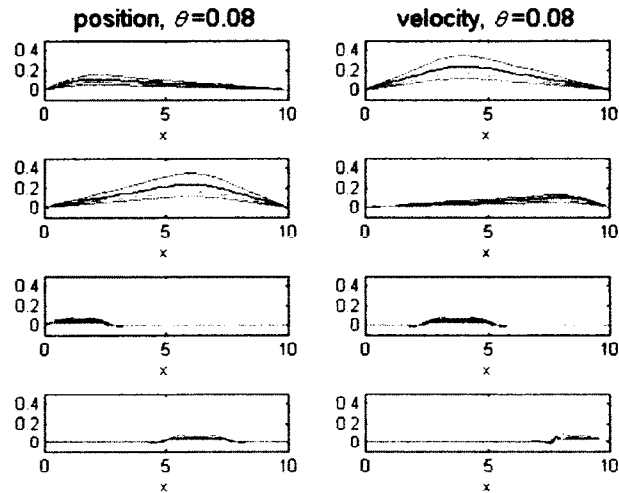


Figure 4-3: Functional gains for  $\theta = 0.08$

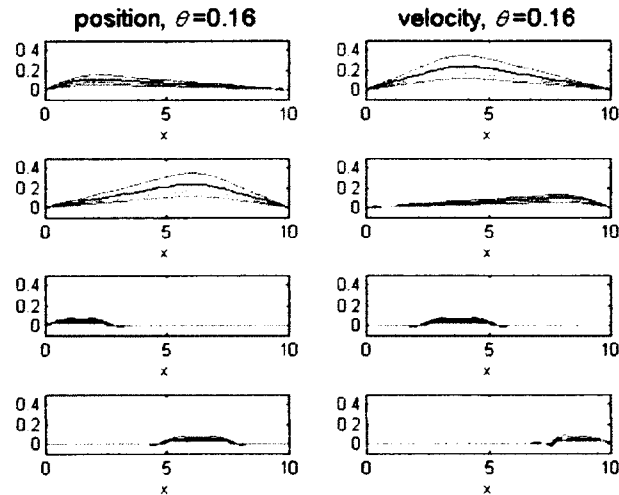


Figure 4-4: Functional gains for  $\theta = 0.16$

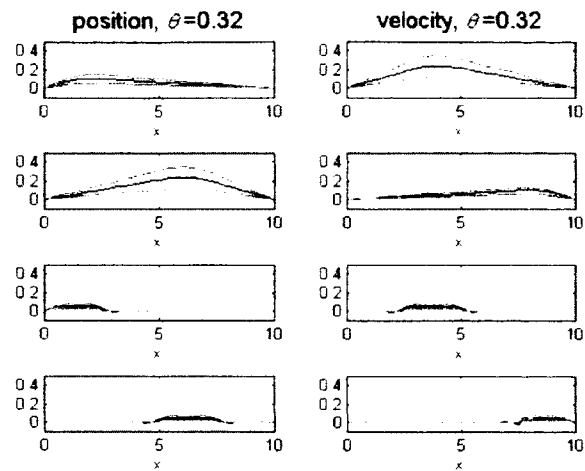


Figure 4-5: Functional gains for  $\theta = 0.32$

Figure 4-6 shows the controlled results for  $\theta = 0.04, 0.08, 0.16, 0.32$  for full-state MinMax control. These results show that the controller does a good job at driving the system faster towards equilibrium. Also, as  $\theta$  increases, the performance of the controller is virtually unchanged.



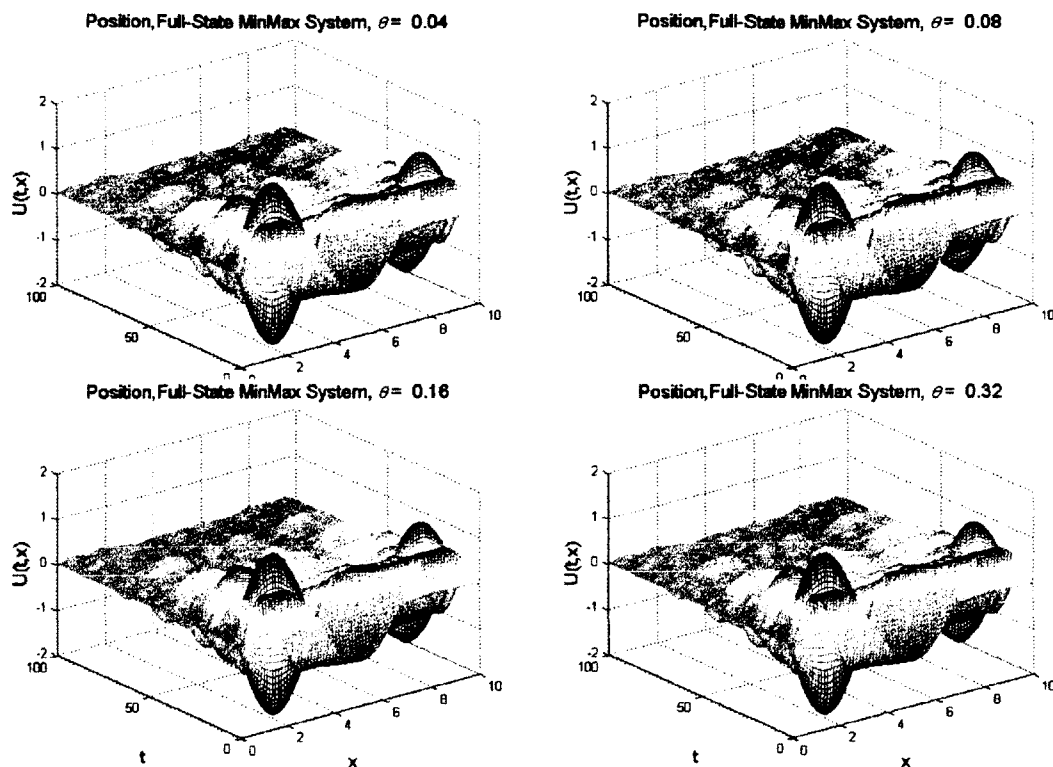


Figure 4-6: Controlled state position, full state MinMax

Figure 4-7 shows the controlled results with the use of a compensator as described in Chapter 2. The results show that the controller does a nice job at bringing the system to the desired equilibrium state. As in the case of the full-state system, the controlled results do not change with varying  $\theta$ . As a result, we conclude here that the actual value of  $\theta$  chosen is not critical with regard to controlled state performance.

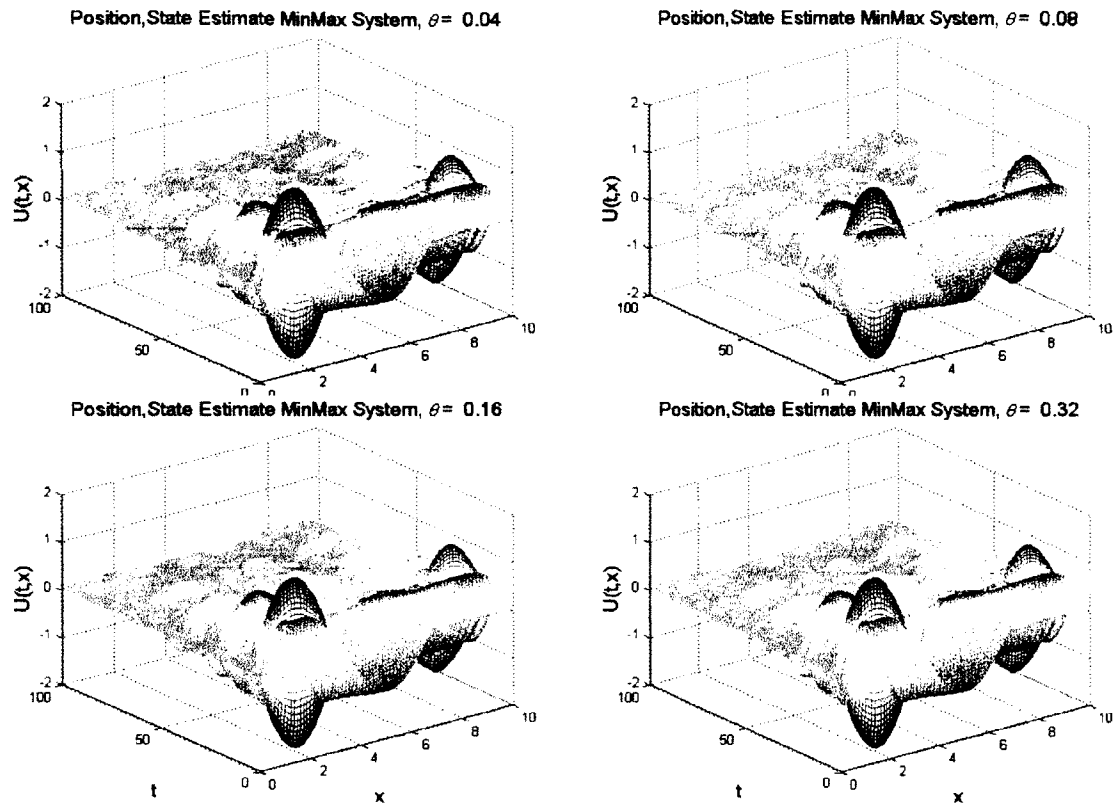


Figure 4-7: Controlled displacement, state estimate MinMax

#### 4.2.3 Stability Analysis

As stated in the previous chapter, we seek to ensure stability in the controlled system, without which our results will be invalid. As a result, we again investigate the eigenvalues of the matrix  $\begin{bmatrix} A & -Bk \\ FC & A_c \end{bmatrix}$ . Figures 4-8 and 4-9 show the eigenvalue plots for various  $\theta$  values.

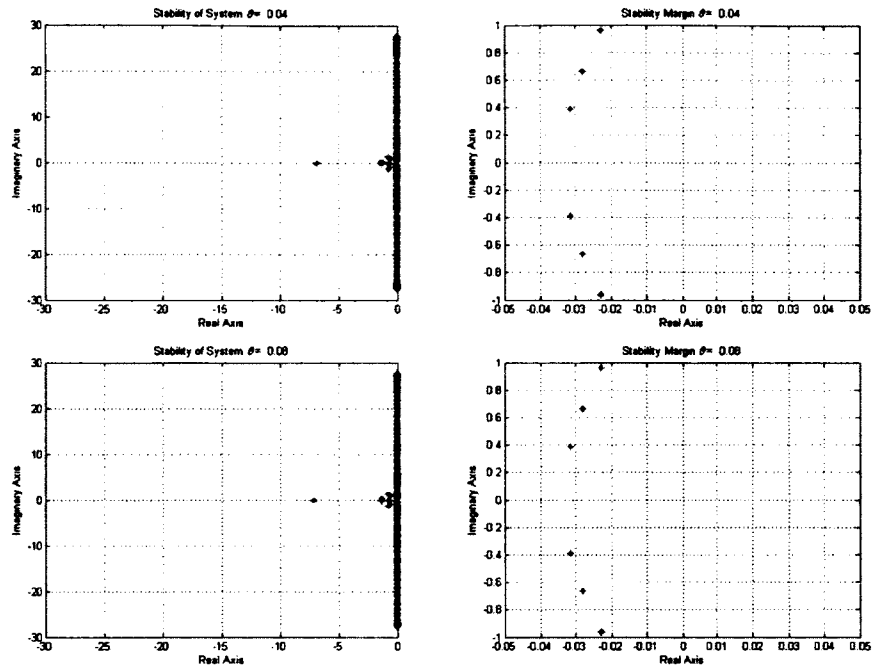


Figure 4-8: Eigenvalues of  $\begin{bmatrix} A & -BK \\ FC & A_c \end{bmatrix}$

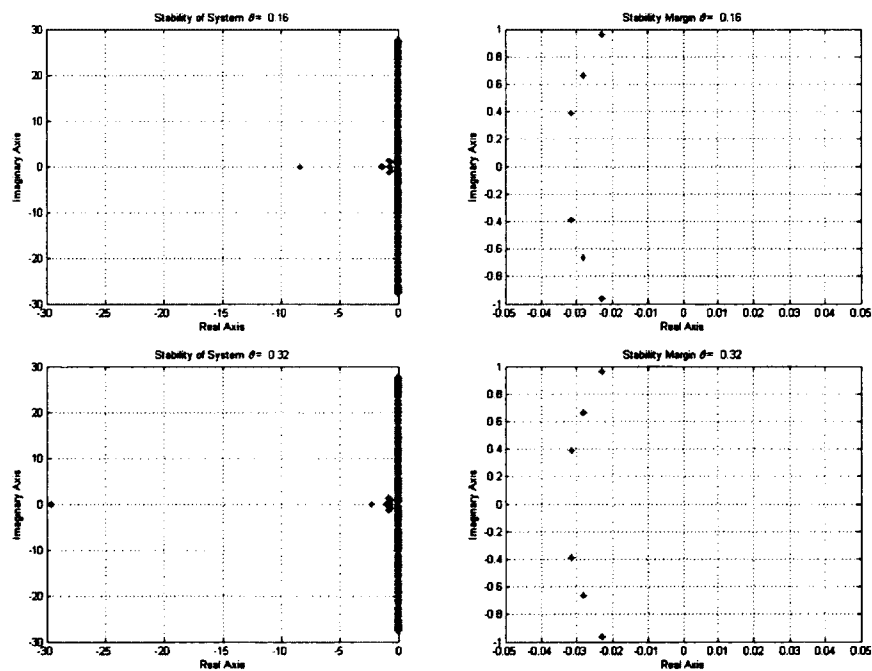


Figure 4-9: Eigenvalues of  $\begin{bmatrix} A & -BK \\ FC & A_c \end{bmatrix}$

The results conclusively show that the controlled system is stable. The graphs on the right show the closest eigenvalues from the imaginary axis. As  $\theta$  increases, the eigenvalue plots and the stability margins remain unchanged (see Table 4-1). We conclude that the choice of  $\theta$  is not critical in terms of the stability of the system. Table 4-1 shows the stability margin and radius results for varying  $\theta$  values. The results show that as  $\theta$  increases, the stability radius decreases slightly, with all the values having the same order of magnitude. The slight increases suggest that the actual value of  $\theta$  chosen is not critical in terms of the stability radii.

Table 4-1: Stability margin and radius for controlled system ( $A_{mm}$ )

$\theta$	Stability Margin	Stability Radius
0.04	0.00457127868116122	0.0735565889152003
0.08	0.00457127818031725	0.0734420137014636
0.16	0.00457127605908372	0.0729724434309744
0.32	0.00457126532342317	0.0709066557793600

#### 4.2.4 Control Effort

As has been done in Chapter 3, we investigate the control effort for the MinMax controller implemented. We therefore provide in Figures 4-10 through 4-13, the control effort for  $\theta = 0.04, 0.08, 0.16, 0.32$ . The system under investigation in these figures is the Full-State MinMax controlled system; hence no compensator/observer is used.

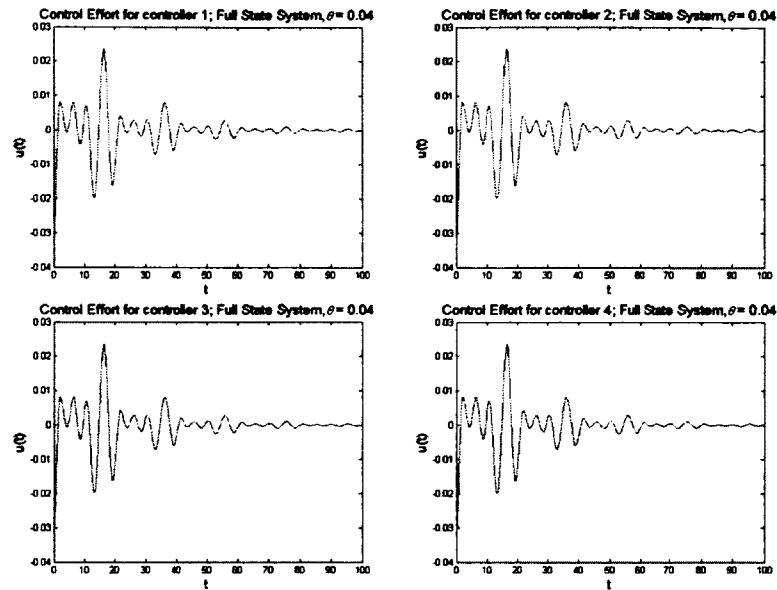


Figure 4-10: Control effort for full state MinMax system ( $\theta = 0.04$ ): controller 1 (top left), controller 2 (top right), controller 3 (bottom left), controller 4 (bottom right)

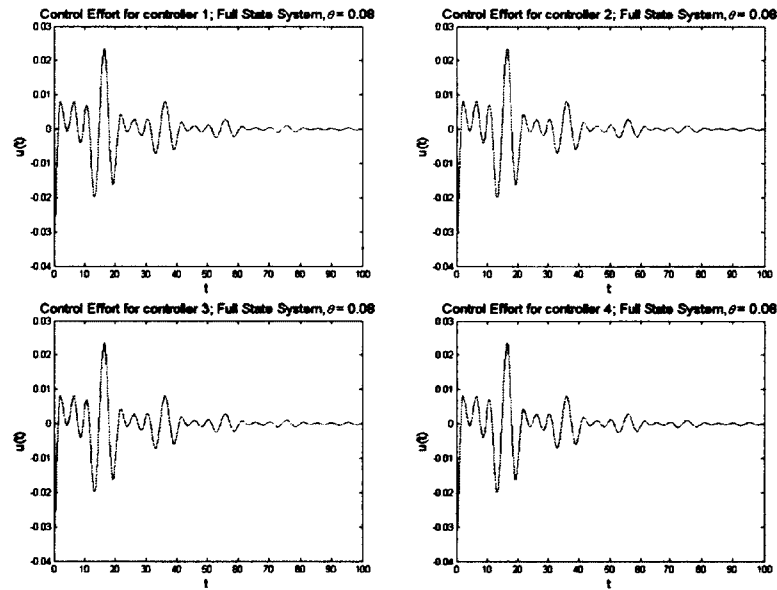


Figure 4-11: Control effort for full state MinMax system ( $\theta = 0.08$ ): controller 1 (top left), controller 2 (top right), controller 3 (bottom left), controller 4 (bottom right)

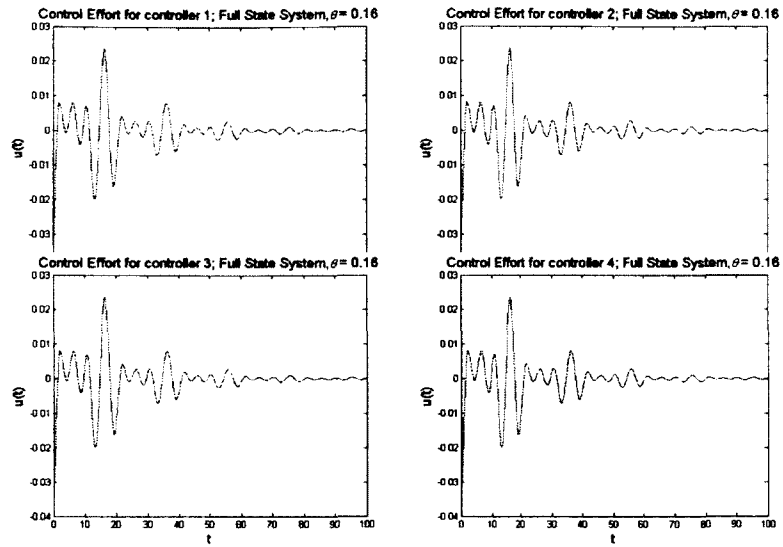


Figure 4-12: Control effort for full state MinMax System ( $\theta = 0.16$ ): controller 1 (top left), controller 2 (top right), controller 3 (bottom left), controller 4 (bottom right)

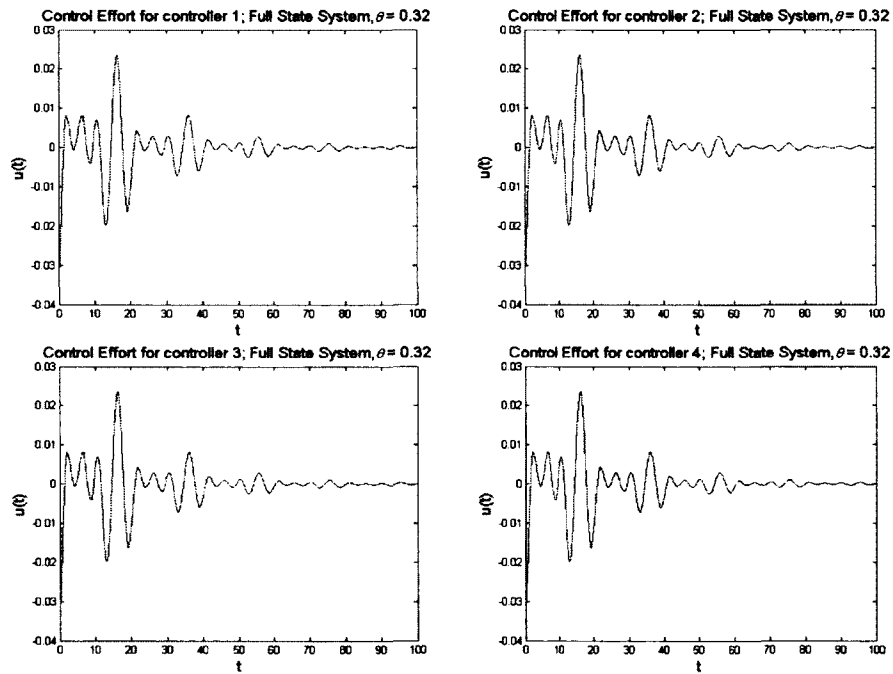


Figure 4-13: Control effort for full state MinMax system ( $\theta = 0.32$ ): controller 1 (top left), controller 2 (top right), controller 3 (bottom left), controller 4 (bottom right)

Table 4-2 shows the results for the area between the curves and the time axis using Simpson's rule. The results show that as  $\theta$  varies, the control effort is changes slightly (+1.59%), though the actual values are of the same order of magnitude. This agrees with the controlled state results of the previous section, where there was no considerable change in the results as  $\theta$  varied.

Figures 4-14 through 4-17 show the control effort results for the state estimate feedback system (i.e. a compensator/ observer is utilized). The area between the curves and the time axis are also shown in Table 4-2. One main conclusion can be made: As  $\theta$  varies from  $\theta_1$  to  $\theta_4$ , the control effort changes by approximately 11.92%, however the order of magnitude does not change. This again is similar to the results for the full-state system. As in the case of the Full State system, the actual value of  $\theta$  chosen is not critical with respect to the effort required by the controller.

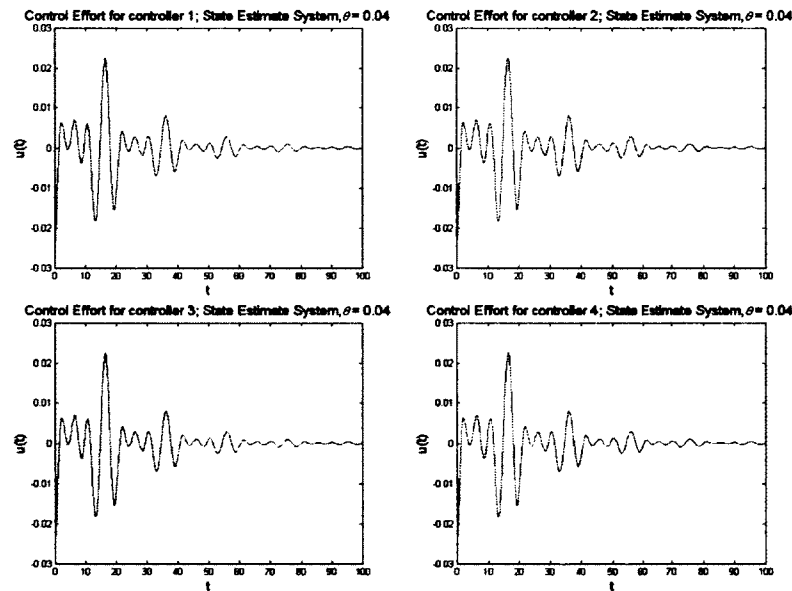


Figure 4-14: Control effort for state estimate MinMax system ( $\theta = 0.04$ ): controller 1 (top left), controller 2 (top right), controller 3 (bottom left), controller 4 (bottom right)

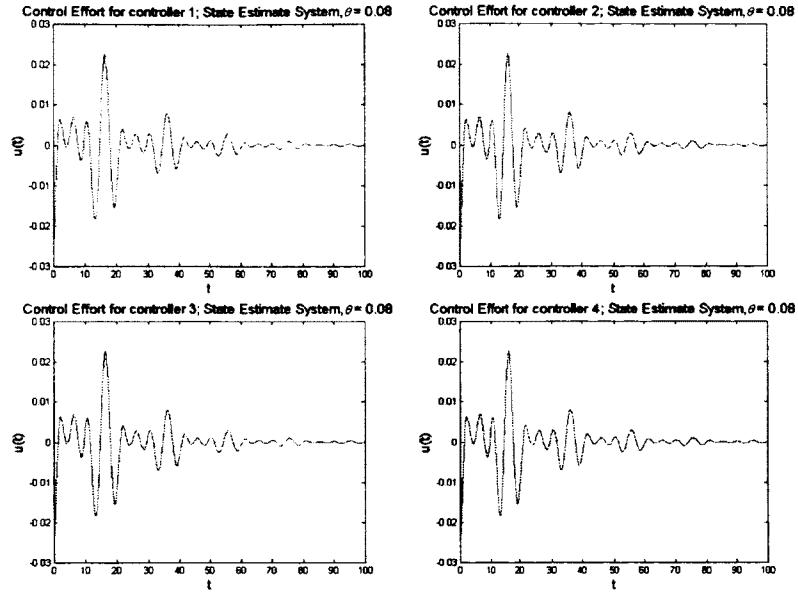


Figure 4-15: Control effort for state estimate MinMax system ( $\theta = 0.08$ ): controller 1 (top left), controller 2 (top right), controller 3 (bottom left), controller 4 (bottom right)

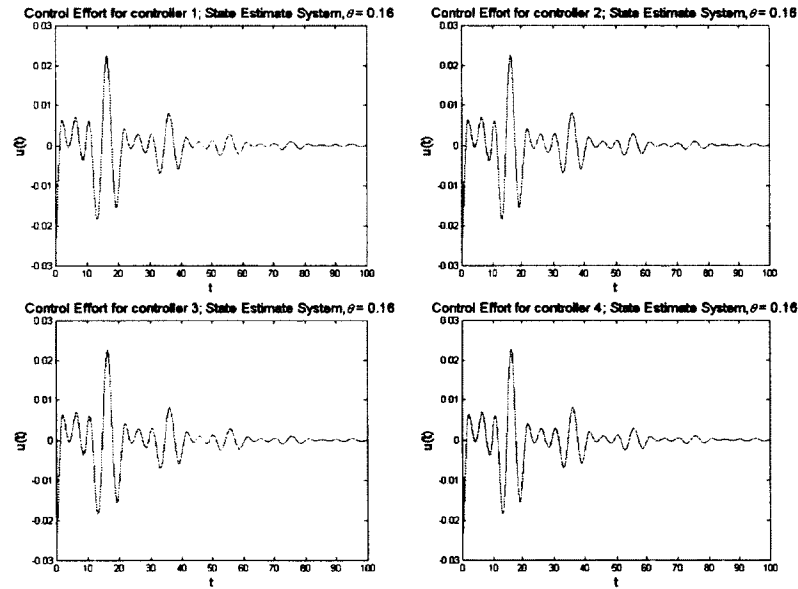


Figure 4-16: Control effort for state estimate MinMax system ( $\theta = 0.16$ ): controller 1 (top left), controller 2 (top right), controller 3 (bottom left), controller 4 (bottom right)



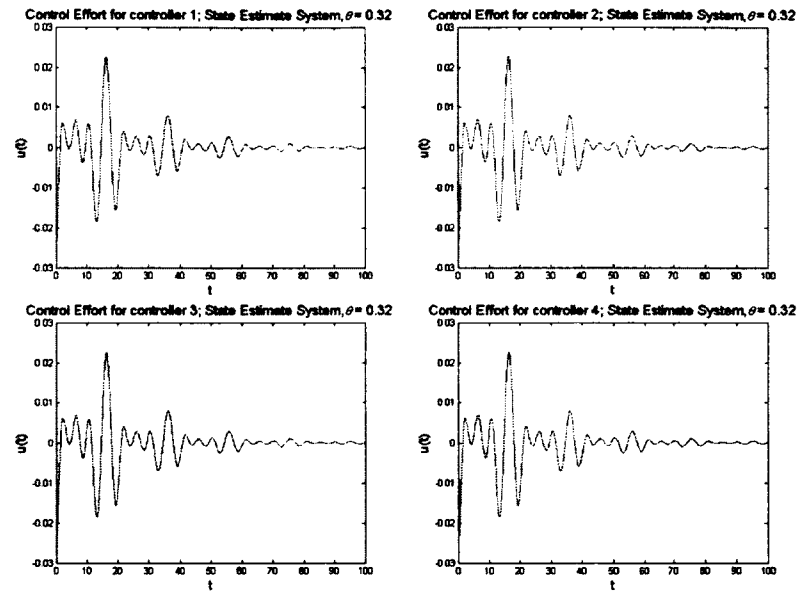


Figure 4-17: Control effort for state estimate MinMax system ( $\theta = 0.32$ ): controller 1 (top left), controller 2 (top right), controller 3 (bottom left), controller 4 (bottom right)

Table 4-2: Area under control effort curve (Simpson's rule)

<b>Area Under Curve</b>	$\theta_1 = 0.04$	$\theta_2 = 0.08$	$\theta_3 = 0.16$	$\theta_4 = 0.32$	%change from $\theta_1$ to $\theta_4$
$I_{controller\ 1}$ (full)	-0.006275	-0.006271	-0.006256	-0.006182	+1.48
$I_{controller\ 2}$ (full)	-0.006275	-0.006271	-0.006256	-0.006182	+1.48
$I_{controller\ 3}$ (full)	-0.006275	-0.006271	-0.006256	-0.006182	+1.48
$I_{controller\ 4}$ (full)	-0.006275	-0.006271	-0.006256	-0.006182	+1.48
<b>TOTAL</b>	<b>-0.0251</b>	<b>-0.0251</b>	<b>-0.0250</b>	<b>-0.0247</b>	<b>+1.59</b>
$I_{controller\ 1}$ (est.)	-0.004833	-0.004856	-0.004952	-0.005401	-11.75
$I_{controller\ 2}$ (est.)	-0.004833	-0.004856	-0.004952	-0.005401	-11.75
$I_{controller\ 3}$ (est.)	-0.004833	-0.004856	-0.004952	-0.005401	-11.75
$I_{controller\ 4}$ (est.)	-0.004833	-0.004856	-0.004952	-0.005401	-11.75
<b>TOTAL</b>	<b>-0.0193</b>	<b>-0.0194</b>	<b>-0.0198</b>	<b>-0.0216</b>	<b>-11.92</b>

#### 4.2.5 Sensitivity Analysis

In order to perform sensitivity analysis on the wave equation, we begin by differentiating the system in Eq. 4-1 with respect to the MinMax control parameter  $\theta$ .

This gives

$$U_{t\theta\theta}(t, x, \theta) - U_{xx\theta}(t, x, \theta) + \gamma U_{t\theta}(t, x, \theta) = \sum_{i=1}^m b_i(x) u_{\theta}(t, \theta). \quad \text{Eq. 4-15}$$

Again we use homogeneous Dirichlet boundary conditions,  $U_{\theta}(t, 0, \theta) = U_{\theta}(t, L, \theta) = 0$ .

Let  $\frac{\partial U(t, x, \theta)}{\partial \theta} = S_U(t, x, \theta)$  and  $\frac{\partial u(t, \theta)}{\partial \theta} = S_u(t, \theta)$ , then

$$S_{U_{tt}}(t, x, \theta) - S_{U_{xx}}(t, x, \theta) + \gamma S_{U_t}(t, x, \theta) = \sum_{i=1}^m b_i(x) S_u(t, \theta). \quad \text{Eq. 4-16}$$

The weak form of Eq. 4-16 is

$$\int_0^l \ddot{S}_U(t, x, \theta) v(x) dx - \int_0^l S_U''(t, x, \theta) v(x) dx + \int_0^l \gamma \dot{S}_U(t, x, \theta) v(x) dx, \quad \text{Eq. 4-17}$$

where  $\dot{S} = \frac{\partial S}{\partial t}$  and  $S' = \frac{\partial S}{\partial x}$ . After integration by parts, Eq. 4-17 becomes

$$\int_0^l \ddot{S}_U(t, x, \theta) v(x) dx + \int_0^l S_U'(t, x, \theta) v'(x) dx + \int_0^l \gamma \dot{S}_U(t, x, \theta) v(x) dx = \int_0^l \sum_{i=1}^m b_i(x) S_u(t, \theta) v(x) dx. \quad \text{Eq. 4-18}$$

Now let  $S_U(t, x, \theta) \approx S_U^N(t, x, \theta) = \sum_{i=1}^N e_i(t) \phi_i(x)$ , where  $\phi_i(x)$  are piecewise linear basis functions. Eq. 4-18 then becomes

$$\int_0^l \ddot{S}_U^N(t, x, \theta) v(x) dx + \int_0^l S_U'^N(t, x, \theta) v'(x) dx + \gamma \int_0^l \dot{S}_U^N(t, x, \theta) v(x) dx = \int_0^l S_u(t, \theta) \sum_{i=1}^m b_i(x) v(x) dx. \quad \text{Eq. 4-19}$$

Alternatively,

$$\int_0^l \sum_{i=1}^N \ddot{e}_i(t) \phi_i(x) v(x) dx + \int_0^l \sum_{i=1}^N e_i(t) \phi_i'(x) v'(x) dx + \quad \text{Eq. 4-20}$$

$$\gamma \int_0^l \sum_{i=1}^N \dot{e}_i(t) \phi_i(x) v(x) dx = \int_0^l S_u(t, \theta) \sum_{i=1}^m b_i(x) v(x) dx.$$

Let  $v(x)$  range over  $\phi_j(x)$  for  $j = 1, 2, \dots, N$ , then Eq. 4-20 becomes

$$\int_0^l \sum_{i=1}^N \ddot{e}_i(t) \phi_i(x) \phi_j(x) dx + \int_0^l \sum_{i=1}^N e_i(t) \phi_i'(x) \phi_j'(x) dx + \quad \text{Eq. 4-21}$$

$$\gamma \int_0^l \sum_{i=1}^N \dot{e}_i(t) \phi_i(x) \phi_j(x) dx = S_u(t, \theta) \sum_{i=1}^m b_i(x) v(x) dx.$$

This can now be rewritten as

$$M \begin{bmatrix} \ddot{e}_1(t) \\ \vdots \\ \ddot{e}_N(t) \end{bmatrix} + K \begin{bmatrix} e_1(t) \\ \vdots \\ e_N(t) \end{bmatrix} + \gamma M \begin{bmatrix} \dot{e}_1(t) \\ \vdots \\ \dot{e}_N(t) \end{bmatrix} = S_u(t, \theta) B_0, \quad \text{Eq. 4-22}$$

where,

$$M = \left[ \int_0^l \phi_i(x) \phi_j(x) dx \right]_{i,j=1}^N, \quad K = \left[ \int_0^l \phi_i'(x) \phi_j'(x) dx \right]_{i,j=1}^N \quad \text{and} \quad B_0 = \left[ \int_0^l \sum_{i=1}^m b_i(x) \phi_j(x) dx \right]_{j=1}^N.$$

Rearranging Eq. 4-22 gives

$$\begin{bmatrix} \ddot{e}_1(t) \\ \vdots \\ \ddot{e}_N(t) \end{bmatrix} = -M^{-1}K \begin{bmatrix} e_1(t) \\ \vdots \\ e_N(t) \end{bmatrix} - \gamma I \begin{bmatrix} \dot{e}_1(t) \\ \vdots \\ \dot{e}_N(t) \end{bmatrix} + S_u(t, \theta) M^{-1} B_0. \quad \text{Eq. 4-23}$$

Recall that the derivation of  $S_u(t, \theta)$  is done in Chapter 2. It is necessary to formulate the system in Eq. 4-23 as a first order system of differential equations so that the MinMax controller can be successfully implemented as stated in Chapter 2. We therefore define  $X_{1\theta}(t) = e(t)$  so that  $\dot{X}_{1\theta}(t) = \dot{e}(t)$ , and  $X_{2\theta}(t) = \dot{e}(t) = \dot{X}_{1\theta}(t)$  so that  $\dot{X}_{2\theta}(t) = \ddot{e}(t)$ . The system in Eq. 4-23 then becomes

$$\begin{bmatrix} \dot{X}_{1\theta}(t) \\ \dot{X}_{2\theta}(t) \end{bmatrix} = \begin{bmatrix} 0 & I \\ -M^{-1}K & -\gamma I \end{bmatrix} \begin{bmatrix} X_{1\theta}(t) \\ X_{2\theta}(t) \end{bmatrix} + \begin{bmatrix} 0 \\ M^{-1}B_0 \end{bmatrix} S_u(t, \theta). \quad \text{Eq. 4-24}$$

The final complete system of equations (controlled and sensitivity equations) becomes

$$\begin{bmatrix} \dot{X}(t) \\ \dot{X}_c(t) \\ \dot{S}_X(t) \\ \dot{S}_{X_c}(t) \end{bmatrix} = \begin{bmatrix} A & -BK & 0 & 0 \\ FC & A_c & 0 & 0 \\ 0 & -BK_\theta & A & -BK \\ A_{c1} & A_{c2} & A_{c3} & A_{c4} \end{bmatrix} \begin{bmatrix} X(t) \\ X_c(t) \\ S_X(t) \\ S_{X_c}(t) \end{bmatrix} \quad \text{Eq. 4-25}$$

where  $K_\theta, A_{c1}, A_{c2}, A_{c3}$ , and  $A_{c4}$  are derived and defined in Chapter 2. In order to perform the simulations, we use the following initial conditions

$$U_\theta(0, x, \theta) = 0.75 \sin x, \dot{U}_\theta(0, x, \theta) = 0.75 \cos x. \quad \text{Eq. 4-26}$$

Figure 4-18 shows that the sensitivity of the state position with respect to  $\theta$  does not vary much as  $\theta$  varies. This suggests that the MinMax control parameter's actual value may not be critical in the performance of the state. This result is in agreement with the results of the previous section where it was seen that the actual  $\theta$  value does not affect the control effort.

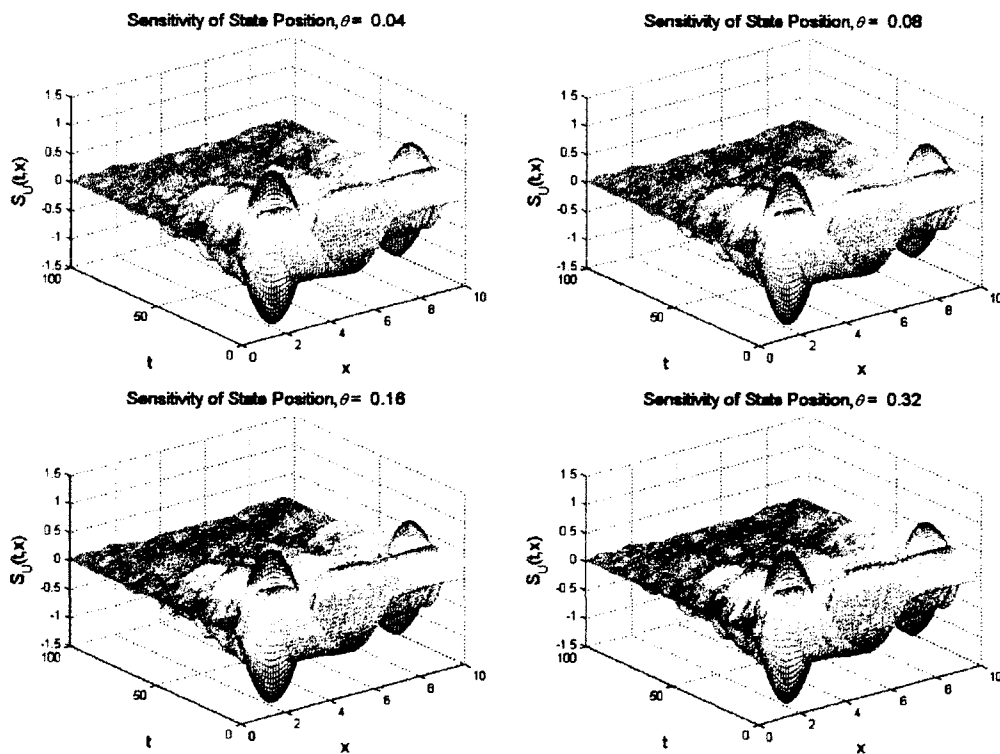


Figure 4-18: Sensitivity of state position

#### 4.2.6 Controller Sensitivity

The sensitivity of the controller with respect to  $\theta$ ,  $S_u(t, \theta)$ , was investigated. The results are shown in Figures 4-19 through 4-26 for both the full state and state estimate control systems. Table 4-3 shows the area between the curves and the time axis, giving the total controller sensitivity. The results show that the controller implemented is not very sensitive to variations in  $\theta$  since the order of magnitude is the same, despite the significant percentage increase from  $\theta_1$  to  $\theta_4$ . This is in agreement with the results in previous sections that show that the choice in  $\theta$  is not very critical to the overall performance of the controller.

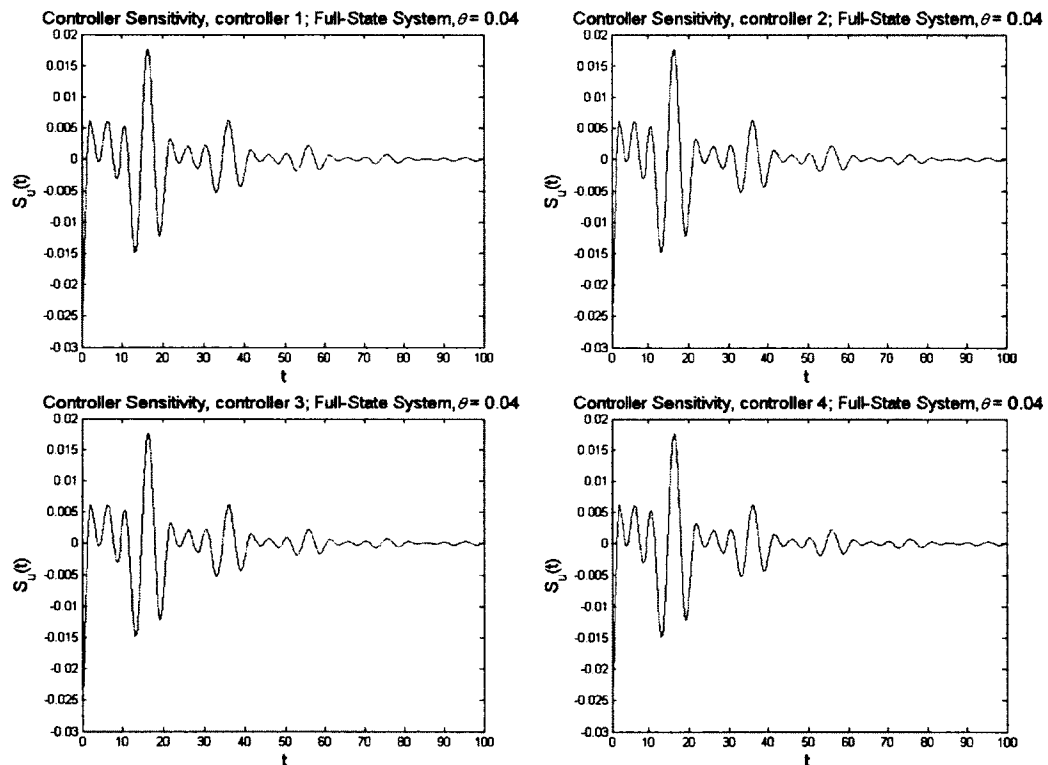


Figure 4-19: Controller sensitivity for full state MinMax system ( $\theta = 0.04$ ): controller 1 (top left), controller 2 (top right), controller 3 (bottom left), controller 4 (bottom right)

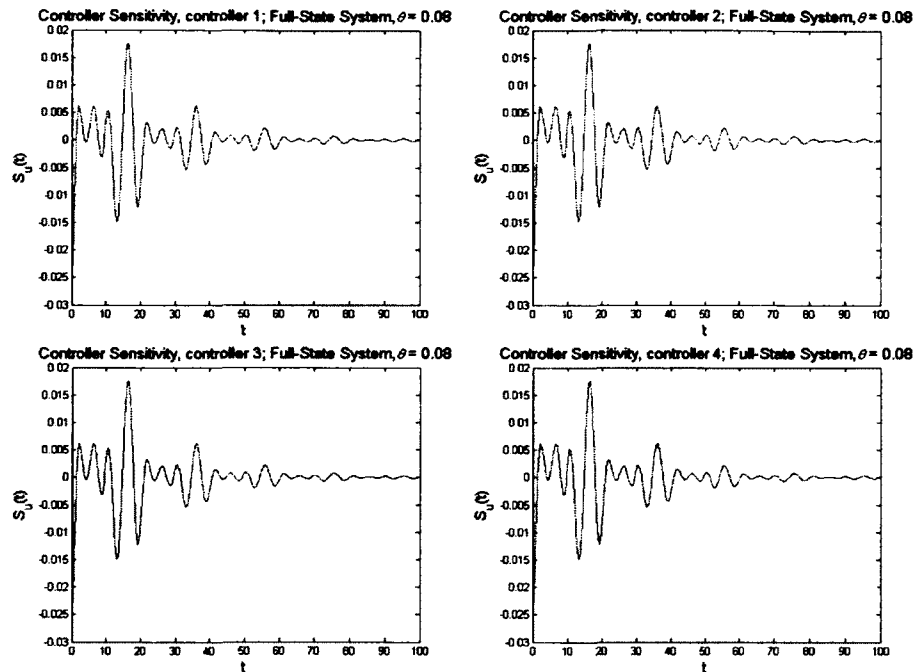


Figure 4-20: Controller sensitivity for full state MinMax system ( $\theta = 0.08$ ): controller 1 (top left), controller 2 (top right), controller 3 (bottom left), controller 4 (bottom right)

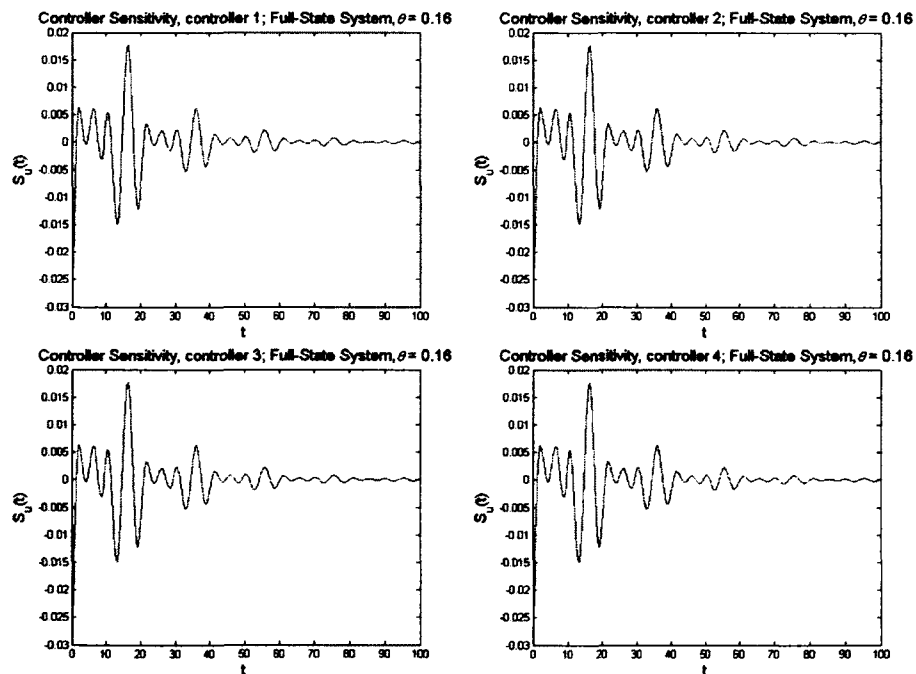


Figure 4-21: Controller sensitivity for full state MinMax system ( $\theta = 0.16$ ): controller 1 (top left), controller 2 (top right), controller 3 (bottom left), controller 4 (bottom right)

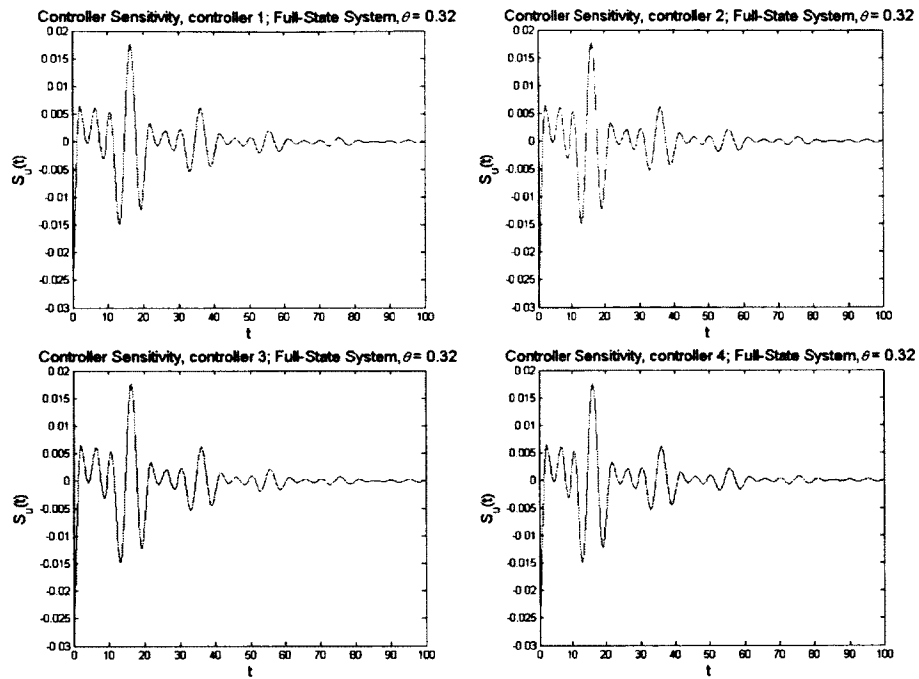


Figure 4-22: Controller sensitivity for full state MinMax system ( $\theta = 0.32$ ): controller 1 (top left), controller 2 (top right), controller 3 (bottom left), controller 4 (bottom right)

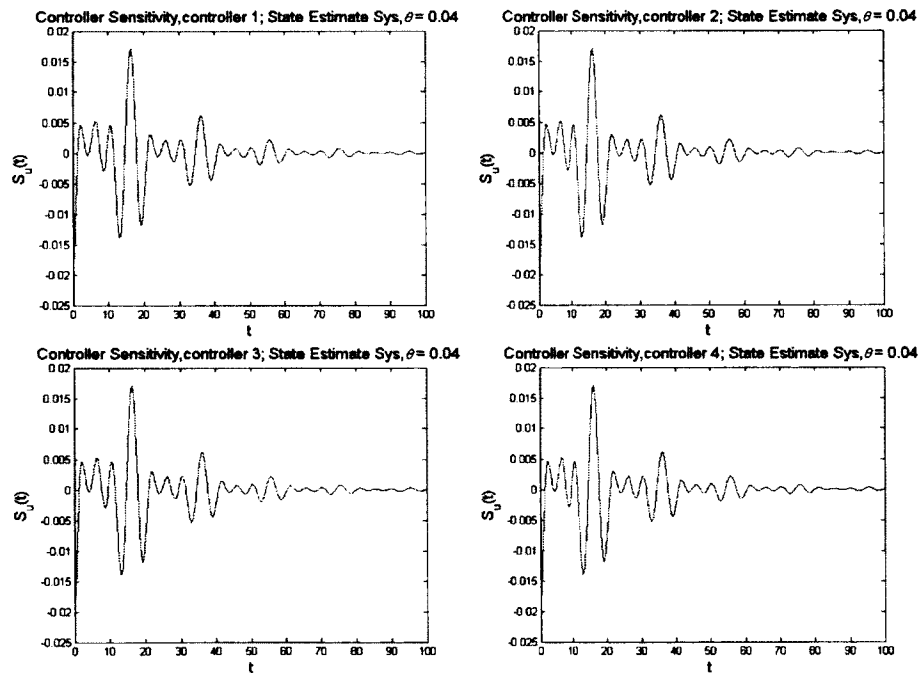


Figure 4-23: Controller sensitivity for state est. MinMax system ( $\theta = 0.04$ ): controller 1 (top left), controller 2 (top right), controller 3 (bottom left), controller 4 (bottom right)



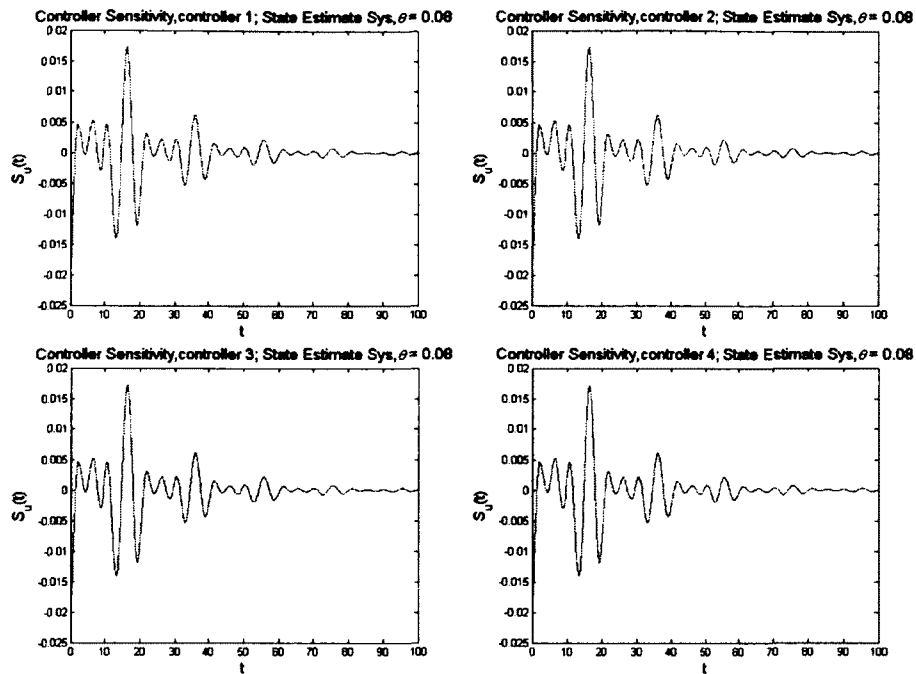


Figure 4-24: Controller sensitivity for state est. MinMax system ( $\theta = 0.08$ ): controller 1 (top left), controller 2 (top right), controller 3 (bottom left), controller 4 (bottom right)

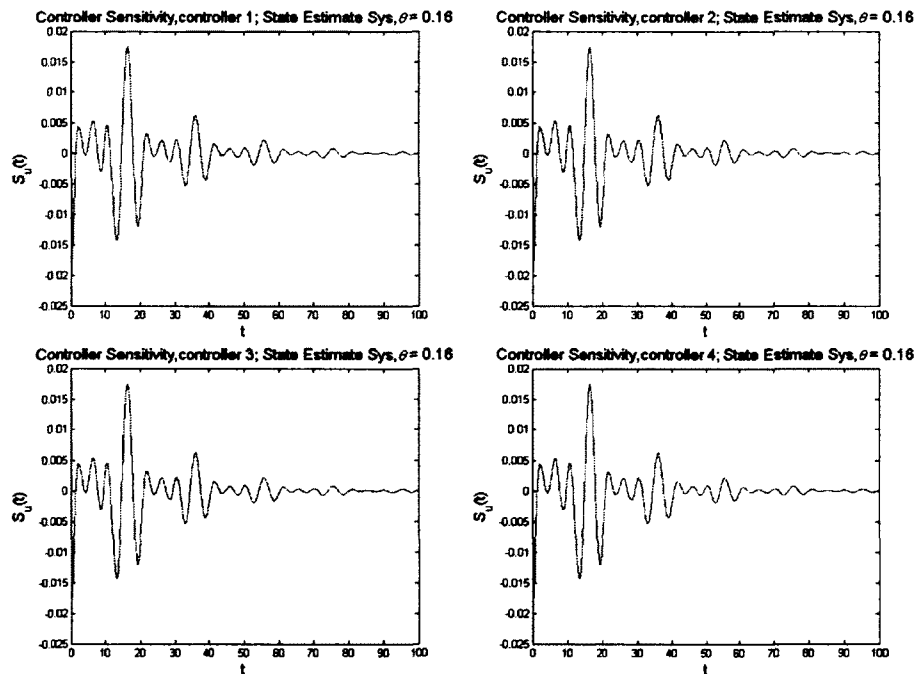


Figure 4-25: Controller sensitivity for state est. MinMax system ( $\theta = 0.16$ ): controller 1 (top left), controller 2 (top right), controller 3 (bottom left), controller 4 (bottom right)

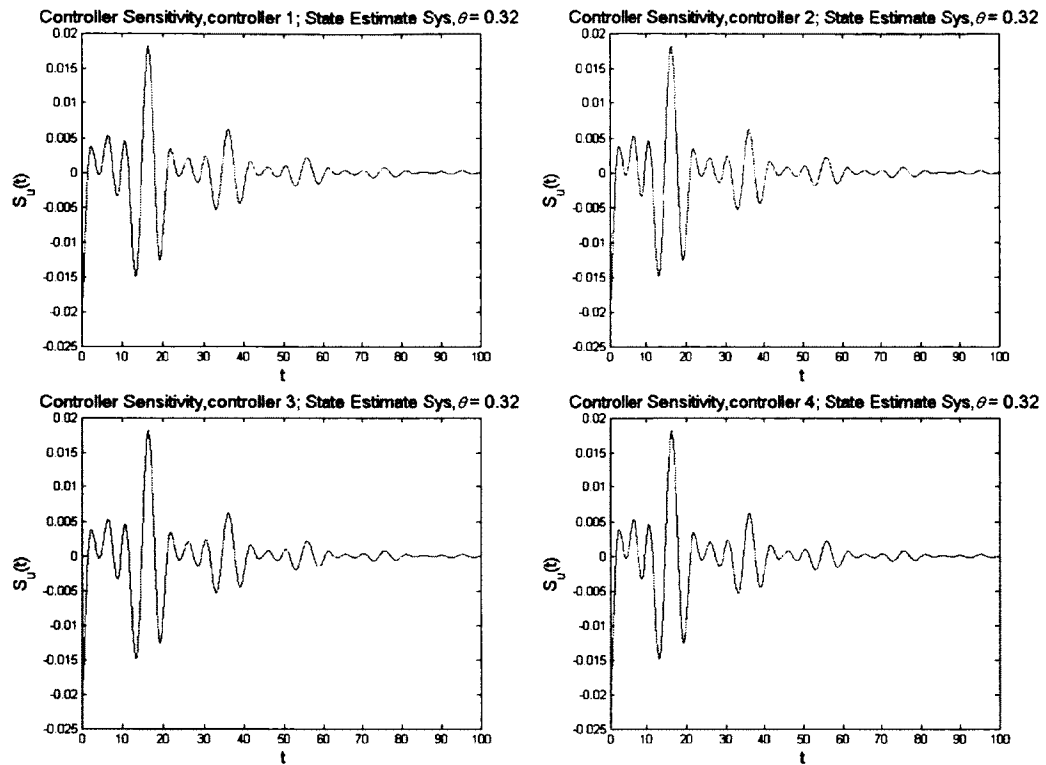


Figure 4-26: Controller sensitivity for state est. MinMax system ( $\theta = 0.32$ ): controller 1 (top left), controller 2 (top right), controller 3 (bottom left), controller 4 (bottom right)

Table 4-3: Area under controller sensitivity curve (Simpson's rule)

<b>Area Under Curve</b>	$\theta_1 = 0.04$	$\theta_2 = 0.08$	$\theta_3 = 0.16$	$\theta_4 = 0.32$	<b>%change from <math>\theta_1</math> to <math>\theta_4</math></b>
$I_{controller\ 1}$ (full)	-0.004635	-0.004559	-0.004383	-0.003816	+17.67
$I_{controller\ 2}$ (full)	-0.004635	-0.004559	-0.004383	-0.003816	+17.67
$I_{controller\ 3}$ (full)	-0.004635	-0.004559	-0.004383	-0.003816	+17.67
$I_{controller\ 4}$ (full)	-0.004635	-0.004559	-0.004383	-0.003816	+17.67
<b>TOTAL</b>	<b>-0.0185</b>	<b>-0.0182</b>	<b>-0.0175</b>	<b>-0.0153</b>	<b>+17.29</b>
$I_{controller\ 1}$ (est.)	-0.004053	-0.004514	-0.005587	-0.009029	-122.77
$I_{controller\ 2}$ (est.)	-0.004053	-0.004514	-0.005587	-0.009029	-122.77
$I_{controller\ 3}$ (est.)	-0.004053	-0.004514	-0.005587	-0.009029	-122.77
$I_{controller\ 4}$ (est.)	-0.004053	-0.004514	-0.005587	-0.009029	-122.77
<b>TOTAL</b>	<b>-0.0162</b>	<b>-0.0181</b>	<b>-0.0224</b>	<b>-0.0316</b>	<b>-95.06</b>

Figures 4-27 and 4-28 show the maximum absolute sensitivity values with respect to  $\theta$ . The results are in agreement with the other sensitivity results:

- The full state sensitivities are slightly higher in amplitude than the state estimate sensitivities
- The variations in the maximum controller sensitivities as the MinMax parameter  $\theta$  changes are small.

The conclusion therefore is the same as previous conclusions, i.e., the value of  $\theta$  chosen is not critical with respect to controller sensitivity.

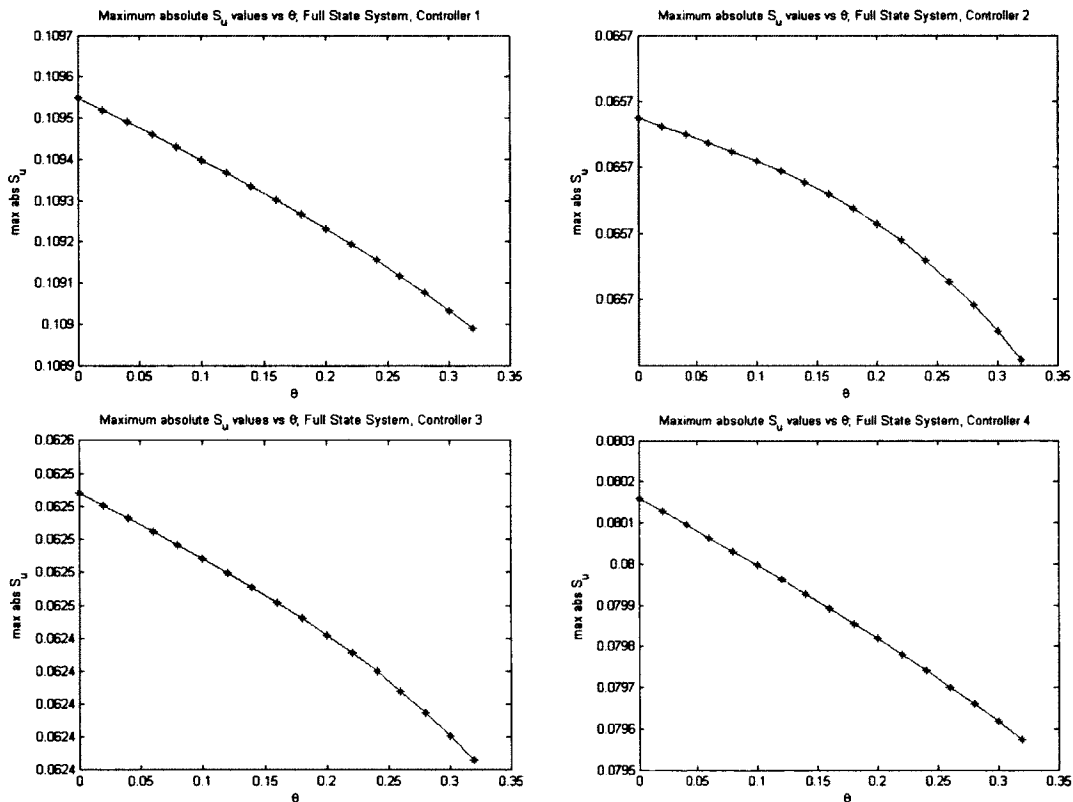


Figure 4-27: Maximum absolute controller sensitivity for full state MinMax system: controller 1 (top left), controller 2 (top right), controller 3 (bottom left), controller 4 (bottom right)

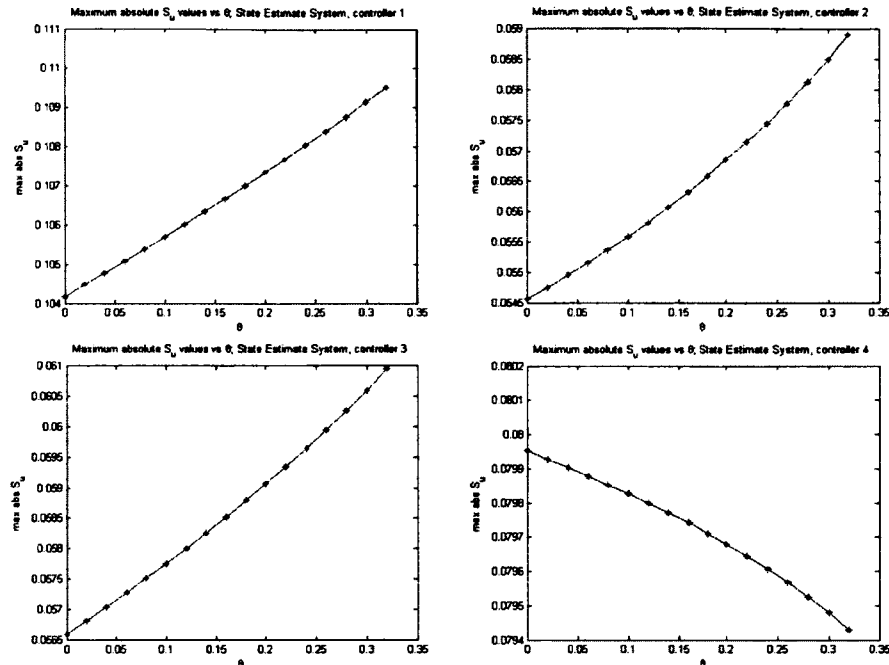


Figure 4-28: Maximum absolute controller sensitivity for state est. MinMax system: controller 1 (top left), controller 2 (top right), controller 3 (bottom left), controller 4 (bottom right)

#### 4.2.7 Riccati Sensitivity

As stated previously, the Algebraic Riccati Equations are a key component in the design of the controller as shown in Chapter 2. As a result we investigated the sensitivity of the Riccati equations with respect to  $\theta$ .

Figures 4-29 and 4-30 show plots of the maximum values of the sensitivities of the Riccati equations' solutions ( $P$  and  $\Pi$ , described fully in Chapter 2) to the MinMax parameter  $\theta$ . The results show that both maximum sensitivities increase with increasing  $\theta$ . The order of magnitude for the  $\Pi_\theta$  values does not change with respect to changes in  $\theta$ . Since  $\Pi$  directly affects the controller performance ( $u(t) = -R^{-1}B^T\Pi x_c$ ), the small variations in  $\Pi$  with respect to variations in  $\theta$  explains the unchanged controller

performance as  $\theta$  changes. These results are in agreement with previous results and hence the same conclusion can be drawn: the actual value of  $\theta$  chosen is not critical.

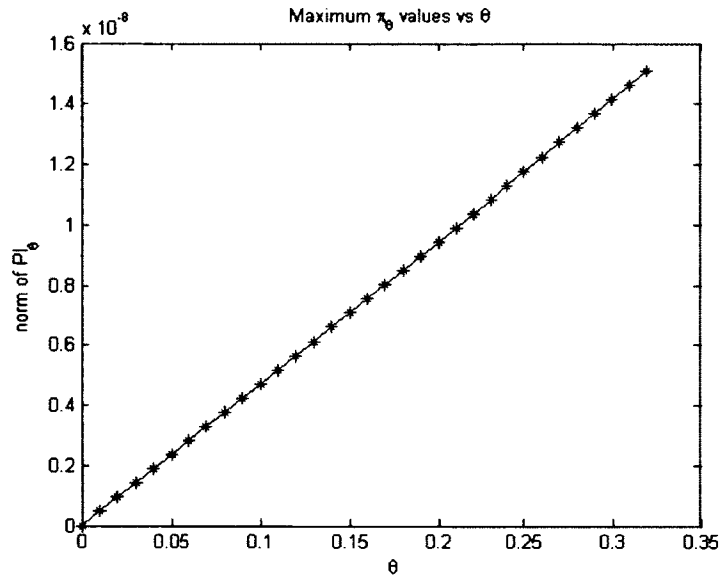


Figure 4-29: Norm of  $\Pi_\theta$  versus  $\theta$

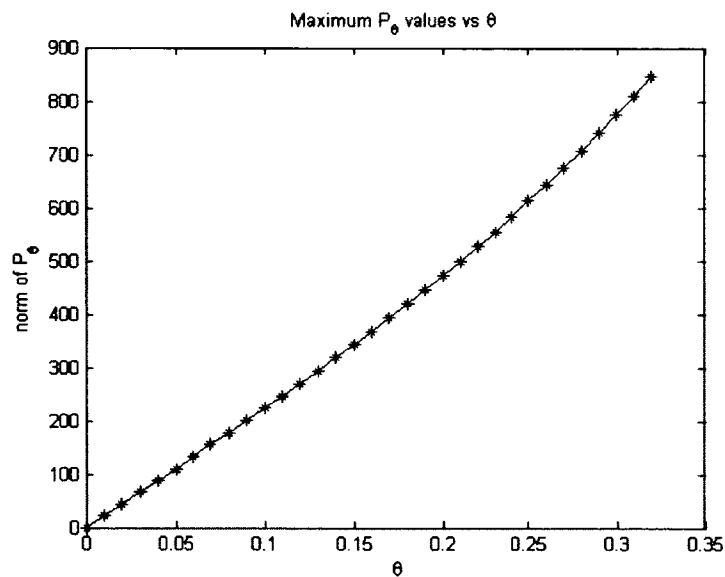


Figure 4-30: Norm of  $P_\theta$  versus  $\theta$

# CHAPTER 5

## EULER BERNOULLI CANTILEVER WITH A ROTATING HUB

### 5.1 Problem Formulation

In this Chapter, we implement the MinMax controller and apply Continuous Sensitivity Equation Methods (as described in Chapter 2) to the Euler-Bernoulli Cantilever Beam with a rotating hub. Control of this system has been investigated by several authors before e.g. [1; 28; 37; 38].

Figure 5-1 shows the system under investigation is a slight modification of the system in [39] where a tip mass was included. In this diagram  $\omega(t) = \dot{\Theta}(t)$  is the angular velocity of the hub.

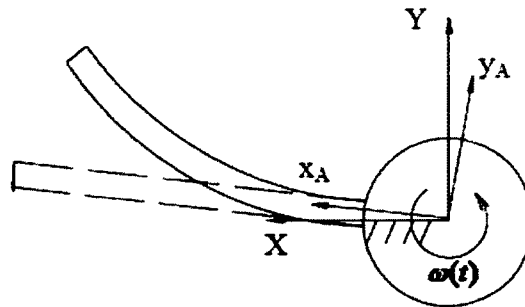


Figure 5-1: Euler-Bernoulli cantilever beam with a rotating hub

The equation of motion for this system, including Kelvin-Voigt and viscous damping is

$$\rho A \frac{\partial^2 d(t,x)}{\partial t^2} + \rho A x \frac{\partial^2 \Theta(t)}{\partial t^2} + \gamma I \frac{\partial^2 d(t,x)}{\partial t^2} + \gamma_1 \frac{\partial d(t,x)}{\partial t} + EI \frac{\partial^4 d(t,x)}{\partial t^4} = 0, \quad \text{Eq. 5-1}$$

where  $\rho$  is the density of the beam material in  $\text{kg/m}^3$ ,  $A$  is the cross-sectional area of the beam in  $\text{m}^2$ ,  $\gamma$  is the Kelvin-Voigt damping coefficient,  $\gamma_1$  is the viscous damping coefficient,  $d(t,x)$  is the displacement of the beam at time,  $t$ , and position,  $x$ ,  $E$  is Young's modulus,  $I$  is the moment of inertia,  $\Theta$  is the hub's angular position,  $x$  is the position along the beam, and  $0 \leq x \leq L$ . We apply the following boundary conditions to this system:

$$\begin{aligned} d(t,0) &= 0 \\ \frac{\partial d(t,0)}{\partial x} &= 0 \\ \gamma \frac{\partial^4 d(t,L)}{\partial t \partial x^3} + EI \frac{\partial^3 d(t,L)}{\partial x^3} &= 0 \\ \gamma \frac{\partial^3 d(t,L)}{\partial t \partial x^2} + EI \frac{\partial^2 d(t,L)}{\partial x^2} &= 0. \end{aligned} \quad \text{Eq. 5-2}$$

These boundary conditions represent:

- Clamped left-end of beam (1<sup>st</sup> two)
- No shear force at tip (3<sup>rd</sup>)
- No bending moment at tip (4<sup>th</sup>).

The model is completed by the inclusion of the hub-beam dynamics boundary condition,

$$J_0 \frac{\partial^2 \Theta(t)}{\partial t^2} - \gamma I \frac{\partial^3 d(t,0)}{\partial t \partial x^2} - EI \frac{\partial^2 d(t,0)}{\partial x^2} = u(t), \quad \text{Eq. 5-3}$$



where  $J_o$  is the hub moment of inertia and  $u(t)$  is the control input to the system via torque on the hub. We begin the finite element approximation by rewriting Eq. 5-1 as

$$\begin{aligned} \rho A \ddot{d}(t, x) + \rho A x \ddot{\Theta}(t) + E I d''''(t, x) + \gamma_1 \dot{d}(t, x) \\ + \gamma_2 \dot{d}''''(t, x) = 0, \end{aligned} \quad \text{Eq. 5-4}$$

where  $\frac{\partial d(t, x)}{\partial t} = \dot{d}(t, x)$  and  $\frac{\partial d(t, x)}{\partial x} = d'(t, x)$ . In order to determine the finite element approximation to Eq. 5-1, we first write the weak form of the PDE. In considering the weak form of the problem we seek to find a  $d(x) \in V \subseteq X = H_L^2(0, l) \cap H^4(0, l)$  such that

$$\begin{aligned} \int_0^l \rho A \ddot{d}(t, x) v(x) dx + \int_0^l \rho A x \ddot{\Theta}(t) v(x) dx + \\ \int_0^l E I d''''(t, x) v(x) dx + \int_0^l \gamma_1 \dot{d}(t, x) v(x) dx + \\ \int_0^l \gamma_2 \dot{d}''''(t, x) v(x) dx = 0, \end{aligned} \quad \text{Eq. 5-5}$$

where  $v(x) \in H_0^1(0, L)$  is a test function. Using integration by parts, we have

$$\begin{aligned} \int_0^l d''''(t, x) v(x) dx = \int_0^l d''(t, x) v''(t, x) dx, \\ \text{and } \int_0^l \dot{d}''''(t, x) v(x) dx = \int_0^l \dot{d}''(t, x) v''(x) dx. \end{aligned} \quad \text{Eq. 5-6}$$

Eq. 5-5 now becomes

$$\begin{aligned} \int_0^l \rho A \ddot{d}(t, x) v(x) dx + \\ \int_0^l \rho A x \ddot{\Theta} v(x) dx + \int_0^l E I d''(t, x) v''(x) dx + \\ \int_0^l \gamma_1 \dot{d}(t, x) v(x) dx + \int_0^l \gamma_2 \dot{d}'' v'' dx = 0. \end{aligned} \quad \text{Eq. 5-7}$$

Now we divide the spatial domain  $[0, L]$  into  $N$  equidistant subintervals and approximate

$d(t, x)$  by  $d^N(t, x) = \sum_{i=1}^N e_i(t) \phi_i(x)$ . Here  $\phi_i(x)$  are cubic b-spline basis functions and

$e_i(t)$  are their coefficients. Eq. 5-7 can then be written as

$$\begin{aligned}
& \int_0^l \rho A \ddot{d}''(t, x) v(x) dx + \int_0^l \rho A x \ddot{\Theta}(t) v(x) dx + \\
& \int_0^l EI d''''(t, x) v''(x) dx + \int_0^l \gamma_1 \dot{d}''(t, x) v(x) dx + \\
& \int_0^l \gamma_2 \dot{d}''''(t, x) v''(x) dx = 0,
\end{aligned} \tag{Eq. 5-8}$$

or alternatively,

$$\begin{aligned}
& \int_0^l \sum_{i=1}^N \ddot{e}_i(t) \phi_i(x) v(x) dx + \int_0^l \rho A x \ddot{\Theta}(t) v(x) dx + \\
& \int_0^l EI \sum_{i=1}^N e_i(t) \phi_i''(x) v''(x) dx + \int_0^l EI \sum_{i=1}^N e_i(t) \phi_i''(x) v''(x) dx + \\
& \int_0^l \gamma_1 \sum_{i=1}^N \dot{e}_i(t) \phi_i(x) v(x) dx + \int_0^l \gamma_2 \sum_{i=1}^N \dot{e}_i(t) \phi_i''(x) v''(x) dx = \\
& 0.
\end{aligned} \tag{Eq. 5-9}$$

Now we let  $v(x)$  range over  $\phi_j(x)$  for  $j = 1, 2, \dots, N$ . Eq. 5-9 then becomes

$$\int_0^l \sum_{i=1}^N \ddot{e}_i(t) \phi_i(x) \phi_j(x) dx \tag{Eq. 5-10}$$

This can now be rewritten as

$$\begin{aligned}
\rho A M \begin{bmatrix} \ddot{e}_1(t) \\ \vdots \\ \ddot{e}_N(t) \end{bmatrix} + \rho A \ddot{\Theta}(t) S + EI K \begin{bmatrix} e_1(t) \\ \vdots \\ e_N(t) \end{bmatrix} + \gamma_1 M \begin{bmatrix} \dot{e}_1(t) \\ \vdots \\ \dot{e}_N(t) \end{bmatrix} \\
+ \gamma_2 K \begin{bmatrix} \dot{e}_1(t) \\ \vdots \\ \dot{e}_N(t) \end{bmatrix} = 0,
\end{aligned} \tag{Eq. 5-11}$$

where  $M = \left[ \int_0^l \phi_i(x) \phi_j(x) dx \right]_{i,j=1}^N$ ,  $K = \left[ \int_0^l \phi_i''(x) \phi_j''(x) dx \right]_{i,j=1}^N$  and  $S = \left[ \int_0^l x \phi_j(x) dx \right]_{j=1}^N$ .

Eq. 5-11 can be rearranged to give

$$\begin{aligned}
\begin{bmatrix} \ddot{e}_1(t) \\ \vdots \\ \ddot{e}_N(t) \end{bmatrix} &= -\ddot{\Theta}(t) M^{-1} S - \frac{EI}{\rho A} M^{-1} K \begin{bmatrix} e_1(t) \\ \vdots \\ e_N(t) \end{bmatrix} - \\
& \frac{\gamma_1}{\rho A} M^{-1} \begin{bmatrix} \dot{e}_1(t) \\ \vdots \\ \dot{e}_N(t) \end{bmatrix} - \frac{\gamma_2}{\rho A} M^{-1} K \begin{bmatrix} \dot{e}_1(t) \\ \vdots \\ \dot{e}_N(t) \end{bmatrix},
\end{aligned} \tag{Eq. 5-12}$$

or,

$$\begin{bmatrix} \ddot{e}_1(t) \\ \vdots \\ \ddot{e}_N(t) \end{bmatrix} = -\ddot{\Theta}(t)M^{-1}S - \frac{EI}{\rho A}M^{-1}K \begin{bmatrix} e_1(t) \\ \vdots \\ e_N(t) \end{bmatrix} -$$

**Eq. 5-13**

$$\left( \frac{\gamma_1}{\rho A}I + \frac{\gamma_2}{\rho A}M^{-1}K \right) \begin{bmatrix} \dot{e}_1(t) \\ \vdots \\ \dot{e}_N(t) \end{bmatrix}.$$

We require Eq. 5-13 to be a system of first order equations as described in Chapter 2. We therefore define  $X_1(t) = e(t)$  and  $X_2(t) = \dot{e}(t) = \dot{X}_1(t)$ . Eq. 5-13 becomes

$$\dot{X}_1(t) = X_2(t),$$

$$\begin{aligned} \dot{X}_2(t) = & -\frac{EI}{\rho A}M^{-1}KX_1(t) - \left( \frac{\gamma_1}{\rho A} + \frac{\gamma_2}{\rho A}M^{-1}K \right) X_2(t) \\ & - \ddot{\Theta}(t)M^{-1}S. \end{aligned} \quad \text{Eq. 5-14}$$

Now Eq. 5-3 can be written as

$$J_0\ddot{\Theta}(t) - \gamma I d''(t, 0) - EI d''(t, 0) = u(t). \quad \text{Eq. 5-15}$$

This can be rearranged to give

$$\ddot{\Theta}(t) = \frac{\gamma I}{J_0} d''(t, 0) + \frac{EI}{J_0} d''(t, 0) + \frac{1}{J_0} u(t). \quad \text{Eq. 5-16}$$

Eq. 5-16 can now be rewritten as

$$\begin{aligned} \ddot{\Theta}(t) = & \frac{\gamma I}{J_0} \sum_{i=1}^N \dot{e}(t) \phi_i''(0) \\ & + \frac{EI}{J_0} \sum_{i=1}^N e_i(t) \phi_i''(0) + \frac{1}{J_0} u(t). \end{aligned} \quad \text{Eq. 5-17}$$

This can be written as

$$\ddot{\Theta}(t) = \frac{\gamma I}{J_0} q X_2(t) + \frac{EI}{J_0} q X_1(t) + \frac{1}{J_0} u(t), \quad \text{Eq. 5-18}$$

where  $q = \phi''(0)$ . Substituting Eq. 5-18 into Eq. 5-14 gives

$$\begin{aligned}
\dot{X}_1(t) &= X_2(t), \\
\dot{X}_2(t) &= -\frac{EI}{\rho A} M^{-1} K X_1 - \left( \frac{\gamma_1}{\rho A} + \frac{\gamma_2}{\rho A} M^{-1} K \right) X_2(t) - \\
&\quad \left( \frac{\gamma_1 l}{J_0} q X_2(t) + \frac{EI}{J_0} q X_1(t) + \frac{1}{J_0} u(t) \right) M^{-1} S.
\end{aligned} \tag{Eq. 5-19}$$

This can be rearranged to give

$$\begin{aligned}
\dot{X}_1(t) &= X_2(t), \\
\dot{X}_2(t) &= -\left( \frac{EI}{\rho A} M^{-1} K + \frac{EI}{J_0} q M^{-1} S \right) X_1(t) - \\
&\quad \left( \frac{\gamma_1}{\rho A} + \frac{\gamma_2}{\rho A} M^{-1} K + \frac{\gamma_1 l}{J_0} q M^{-1} S \right) X_2(t) - \frac{1}{J_0} u(t) M^{-1} S.
\end{aligned} \tag{Eq. 5-20}$$

Finally, in matrix form we have

$$\begin{aligned}
&\begin{bmatrix} \dot{X}_1(t) \\ \dot{X}_2(t) \end{bmatrix} = \\
&\begin{bmatrix} 0 & I \\ -\left( \frac{EI}{\rho A} M^{-1} K + \frac{EI}{J_0} q M^{-1} S \right) & -\left( \frac{\gamma_1}{\rho A} + \frac{\gamma_2}{\rho A} M^{-1} K + \frac{\gamma_1 l}{J_0} q M^{-1} S \right) \end{bmatrix} \begin{bmatrix} X_1(t) \\ X_2(t) \end{bmatrix} + \\
&\quad M^{-1} S \begin{bmatrix} \text{zeros}(N+1, 1) \\ \frac{-1}{J_0} \times \text{ones}(N+1, 1) \end{bmatrix} u(t).
\end{aligned} \tag{Eq. 5-21}$$

In this formulation,

$$B = M^{-1} S \begin{bmatrix} \text{zeros}(N+1, 1) \\ \frac{-1}{J_0} \times \text{ones}(N+1, 1) \end{bmatrix}. \tag{Eq. 5-22}$$

Since full knowledge of the system is not available, we take measurements in the form

$$y(t) = \begin{bmatrix} X_1(t) \\ X_2(t) \end{bmatrix} \tag{Eq. 5-23}$$

where  $C$  is composed of four averaging measurements of both the position and velocity states, resulting in the following  $8 \times (2N + 2)$  matrix

$$\begin{bmatrix} \left[ \frac{4}{l} \int_0^l \phi_i^N(x) dx \right]_{i=1}^{N+1} & 0 \\ \left[ \frac{4}{l} \int_{\frac{l}{4}}^{\frac{3l}{4}} \phi_i^N(x) dx \right]_{i=1}^{N+1} & 0 \\ \left[ \frac{4}{l} \int_{\frac{l}{2}}^{\frac{3l}{2}} \phi_i^N(x) dx \right]_{i=1}^{N+1} & 0 \\ \left[ \frac{4}{l} \int_{\frac{3l}{4}}^l \phi_i^N(x) dx \right]_{i=1}^{N+1} & 0 \\ 0 & \left[ \frac{4}{l} \int_0^l \phi_i^N(x) dx \right]_{i=1}^{N+1} \\ 0 & \left[ \frac{4}{l} \int_{\frac{l}{4}}^{\frac{3l}{4}} \phi_i^N(x) dx \right]_{i=1}^{N+1} \\ 0 & \left[ \frac{4}{l} \int_{\frac{l}{2}}^{\frac{3l}{2}} \phi_i^N(x) dx \right]_{i=1}^{N+1} \\ 0 & \left[ \frac{4}{l} \int_{\frac{3l}{4}}^l \phi_i^N(x) dx \right]_{i=1}^{N+1} \end{bmatrix} \quad \text{Eq. 5-24}$$

## 5.2 Numerical Results

For all simulations in this section,  $N = 40$ ,  $l = 5$ ,  $R = l$ . The results are presented in the following order: uncontrolled simulations, functional gains, controlled simulations, stability analysis, and sensitivity analysis.

### 5.2.1 Uncontrolled Results

For simulation purposes and to attain a solution to the system in Eq. 5-22 and Eq. 5-23, we apply the following initial conditions

$$\begin{aligned} X_0 &= \left[ X(0, x), \frac{\partial X(0, x)}{\partial t} \right] = [2 \sin 2x, 4 \cos 2x], X_{c0} \\ &= \left[ X_c(0, x), \frac{\partial X_c(0, x)}{\partial t} \right] = 0.75X_0. \end{aligned} \quad \text{Eq. 5-25}$$

The following parameters were used:  $\rho = 2700$ ,  $E = 7 \times 10^{10}$ ,  $A = 8.0 \times 10^{-5}$ ,  $J_0 = 0.01$ , and  $I = 6.7746 \times 10^{-11}$ . Figure 5-2 shows the uncontrolled state displacement.

### Position, Uncontrolled System

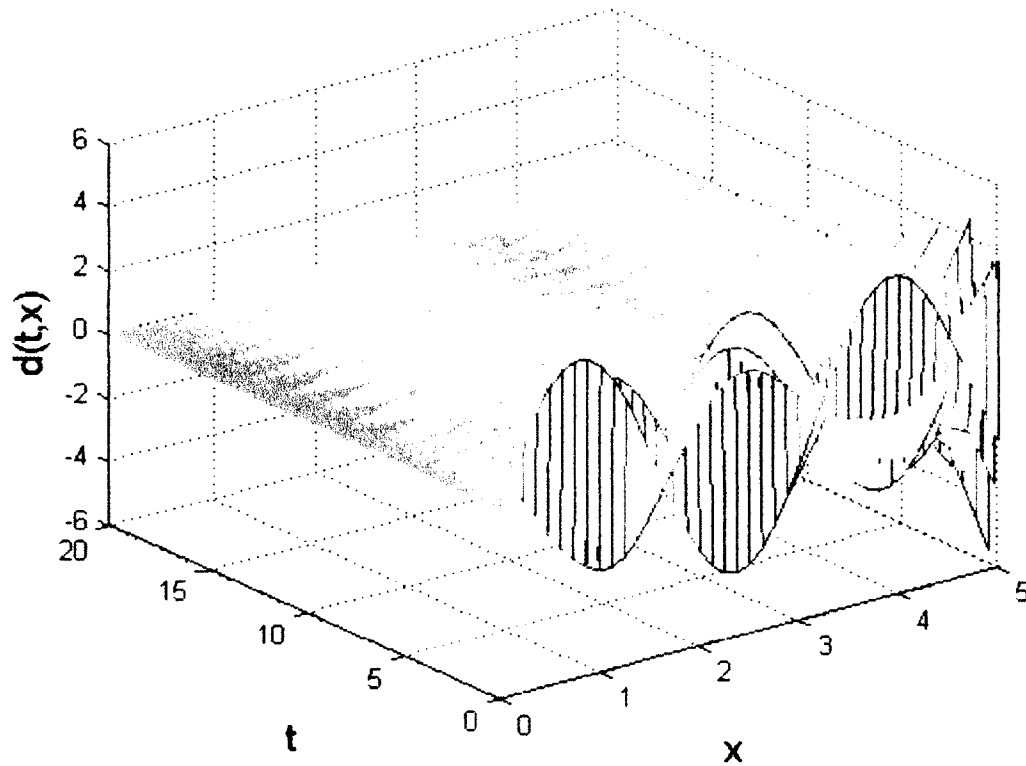


Figure 5-2: Uncontrolled displacement

#### 5.2.2 Controlled Results

Figures 5-3 through 5-5 show the functional gains for the system for  $\theta = 0.05, 0.4, 0.6$ . The color legend in this plot is as follows:  $N = 10$  blue,  $N = 20$  red,  $N = 30$  black,  $N = 40$  magenta,  $N = 50$  cyan. The results are similar to that of the wave equation: the functional gains show convergence and do not vary with varying  $\theta$ , meaning controller convergence is not affected by  $\theta$  value.

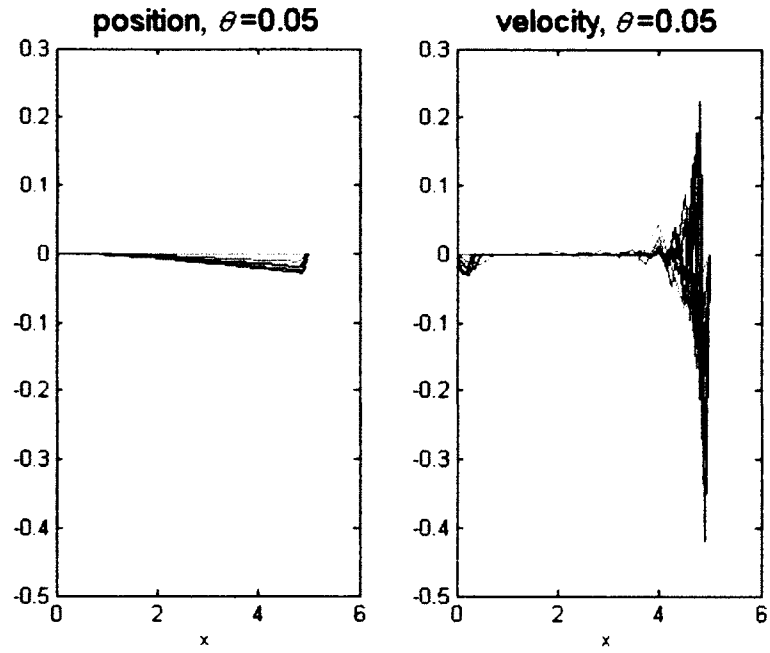


Figure 5-3: Functional gains

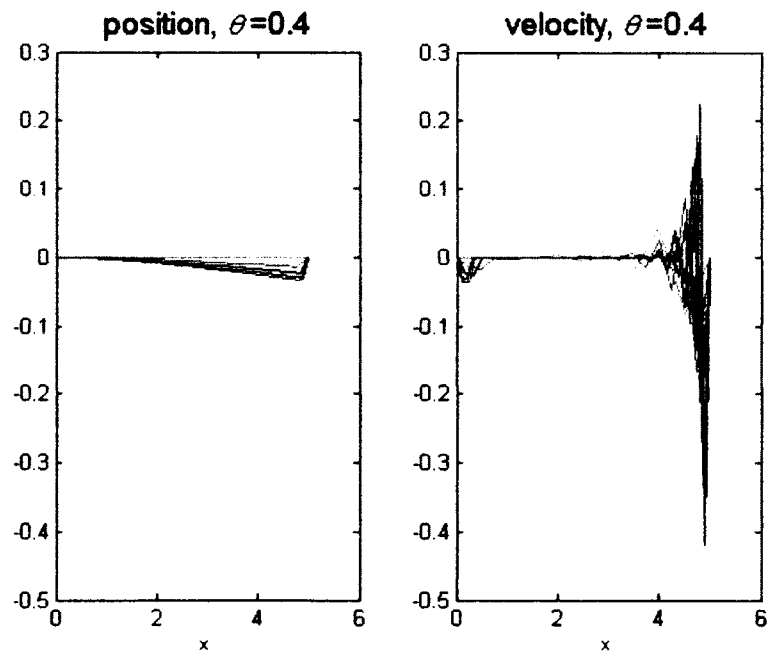


Figure 5-4: Functional gains

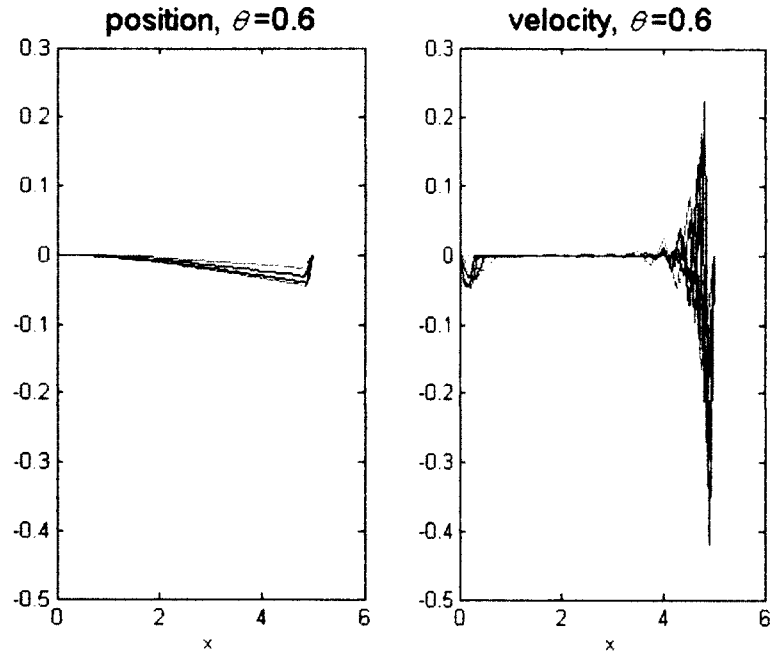


Figure 5-5: Functional gains

Figures 5-6 and 5-7 show the controlled displacement values along the beam for the full state values ( $u(t) = -KU(t)$ ) and for the state estimate system ( $u(t) = -KU_c(t)$ ) respectively. In each figure, the top left result is for  $\theta = 0.05$ , top right is for  $\theta = 0.5$ , and bottom left is for  $\theta = 0.6$ . The value 0.6 is the maximum  $\theta$  value that still results in  $[I - \theta^2 P\Pi] > 0$  and eigenvalues of  $\begin{bmatrix} A & -BK \\ FC & A_c \end{bmatrix}$  being in the left two quadrants of the complex plane as described in Chapter 2.



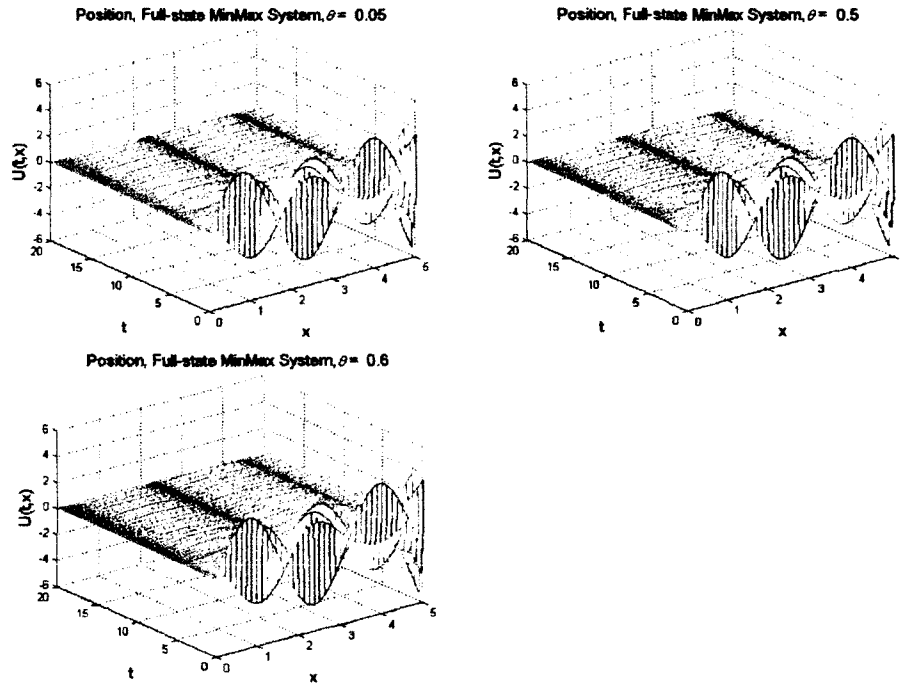


Figure 5-6: Controlled state position, full state MinMax

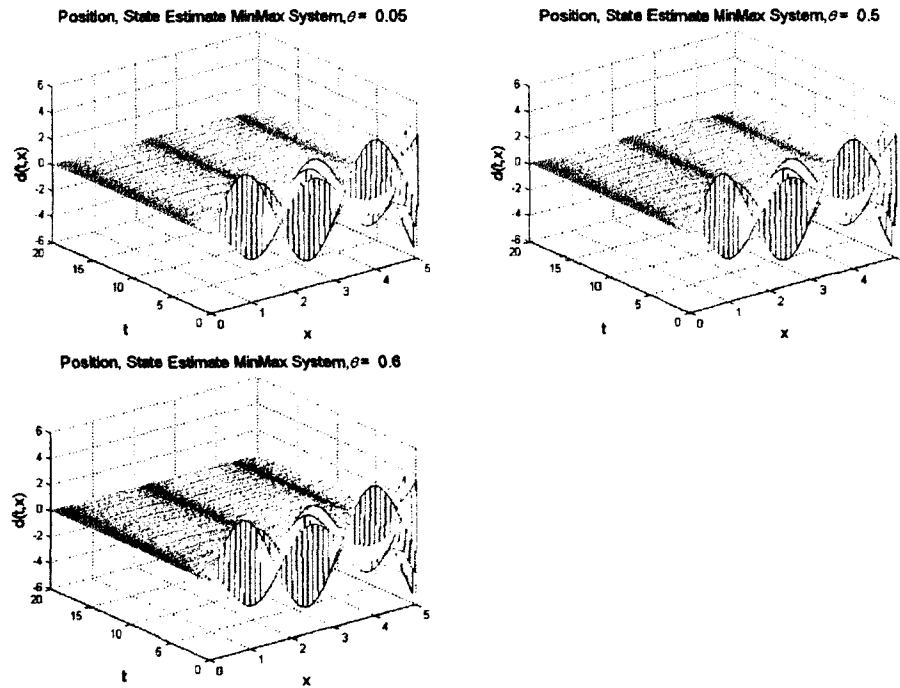


Figure 5-7: Controlled state position, state estimate MinMax

Two key points can be made:

1. The difference in the controller performance for the full state and the state estimate systems are imperceptible in this case.
2. As  $\theta$  increases, there is virtually no difference in the performance of the controller. This would suggest that the choice of  $\theta$  in terms of performance is not critical. This result is in agreement with our previous results.

### 5.2.3 Stability Analysis

As in the case of the previous two chapters, we seek to ensure stability in the control system without which our results will be invalid. As a result, we again investigate the eigenvalues of the matrix  $\begin{bmatrix} A & -BK \\ FC & A_c \end{bmatrix}$ .

Figures 5-8 and 5-9 show the eigenvalue plots for various  $\theta$  values. The graphs on the right side of each figure are a zoomed view showing the closest eigenvalues to the imaginary axis. The results conclusively show that the controlled system is stable. Furthermore the stability margin remains unchanged with changing  $\theta$  (see the stability margin results in Table 5-1). The conclusion here is that the value of  $\theta$  chosen is not relevant with respect to the stability of the system.

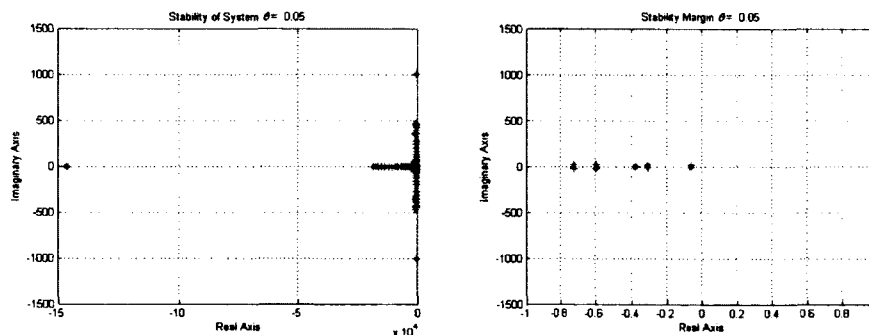


Figure 5-8: Eigenvalues of  $\begin{bmatrix} A & -BK \\ FC & A_c \end{bmatrix}$

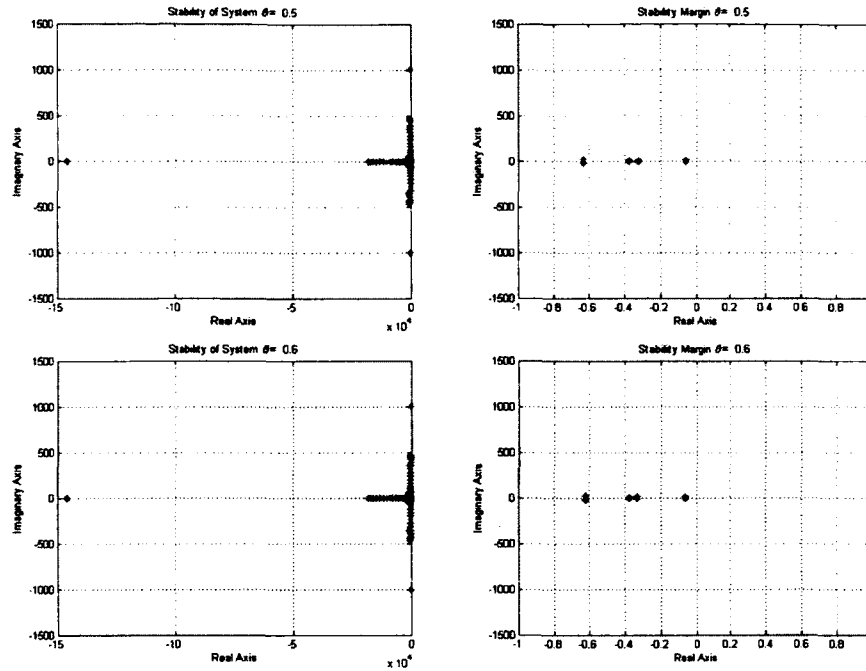


Figure 5-9: Eigenvalues of  $\begin{bmatrix} A & -BK \\ FC & A_C \end{bmatrix}$

Table 5-1 shows the stability margin and radius results for various  $\theta$  values. The table shows that as  $\theta$  increases, the stability radius decreases, hence the system becomes less stable. The difference between the smallest radius and the largest is only about 0.1. The conclusion here is that the value of the MinMax parameter chosen is not critical based on the stability radius.

Table 5-1: Stability margin and radius for controlled system ( $A_{mm}$ )

$\theta$	Stability Margin	Stability Radius
0.05	0.0582554157489640	0.627864455774280
0.2	0.0590110193003510	0.616994500302368
0.5	0.0632578775179432	0.556667853290953
0.6	0.0655009976716679	0.526411275631653

### 5.2.4 Control Effort

As has been done in the previous two chapters, we present the control effort for the MinMax controller. In this case  $\theta = 0.05, 0.5, 0.6$ . In Figure 5-10, the system under investigation is the full state MinMax controlled system where no compensator/observer is used. In Figure 5-11 a compensator is implemented. Table 5-2 shows the results for the area between the curves and the time axis, hence the total control effort. The results show that as  $\theta$  varies, the control effort does not change much. This result agrees with the controlled state results of the previous section, where there was no considerable change in the results as  $\theta$  varied. We conclude that the actual value of  $\theta$  employed is not critical with respect to the effort required by the controller.

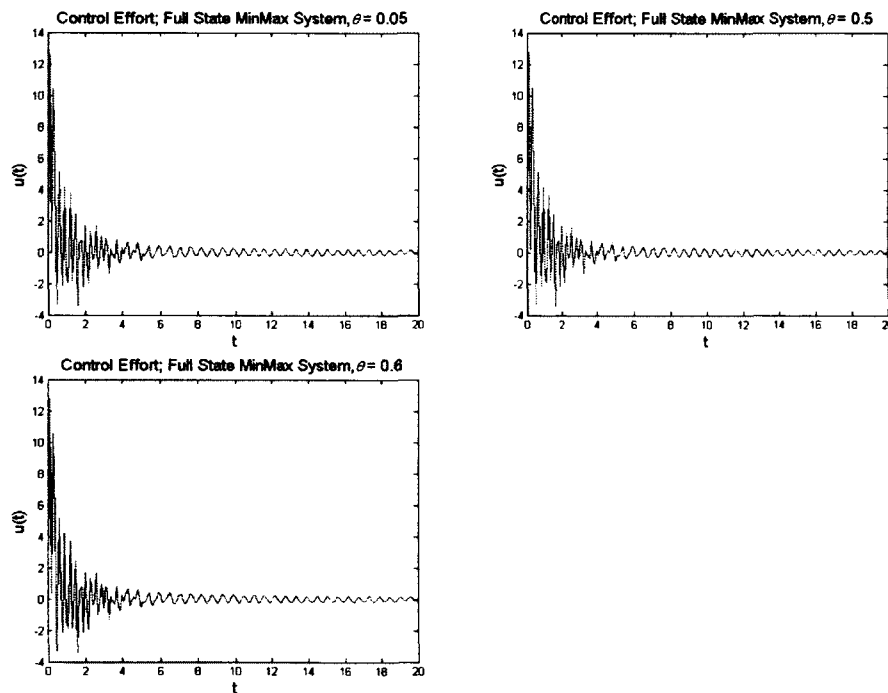


Figure 5-10: Control effort, full state MinMax

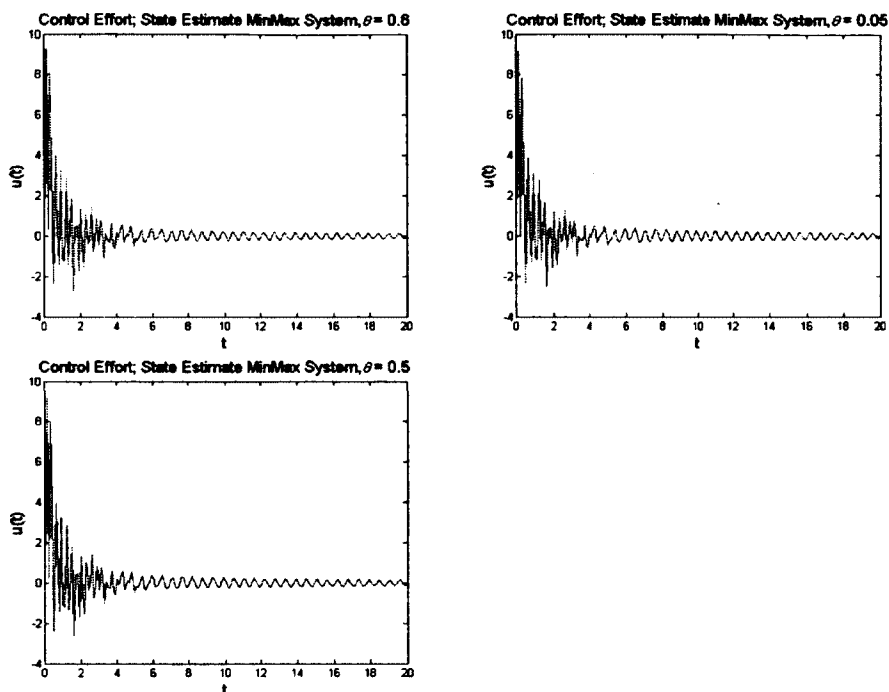


Figure 5-11: Control effort, state estimate MinMax

Table 5-2: Area under control effort curve (Simpson's rule)

Area Under Curve	$\theta_1 = 0.05$	$\theta_2 = 0.5$	$\theta_3 = 0.6$	% change bet. $\theta_1$ and $\theta_3$
$I_{controller_1}(\text{full})$	3.514129	3.557756	3.584119	1.95
$I_{controller_1}(\text{est.})$	2.643727	2.705612	2.735693	3.36

### 5.2.5 Sensitivity Analysis

In order to perform sensitivity analysis, we begin by differentiating Eq. 5-1 with respect to  $\theta$ , resulting in

$$\begin{aligned} \rho A d_{\theta\theta}(t, x, \theta) + \rho A x \Theta_{\theta\theta}(t, \theta) + \gamma_2 I d_{xxxx\theta}(t, x, \theta) + \gamma_1 d_{t\theta}(t, x, \theta) \\ + E I d_{xxxx\theta}(t, x, \theta) = 0, \end{aligned} \quad \begin{array}{l} \text{Eq.} \\ \text{5-26} \end{array}$$

where  $\Theta(t)$  is used here to represent the hub's angular position in order to avoid confusion with the MinMax parameter  $\theta$ . Here  $\frac{\partial d(t, x, \theta)}{\partial \theta} = d_{\theta}(t, x, \theta)$ . Now let  $d_{\theta}(t, x, \theta) = S_d(t, x, \theta)$  and  $\Theta_{\theta}(t, \theta) = S_{\Theta}(t, \theta)$ . We then have

$$\begin{aligned} \rho A \ddot{S}_d(t, x, \theta) + \rho A x \ddot{S}_{\Theta}(t, \theta) + \gamma_2 I \dot{S}_d''''(t, x, \theta) + \\ \gamma_1 \dot{S}_d(t, x, \theta) + E I S_d''''(t, x, \theta) = 0. \end{aligned} \quad \text{Eq. 5-27}$$

The weak form of Eq. 5-27 is

$$\begin{aligned} \rho A \int_0^l \ddot{S}_d(t, x, \theta) v(x) dx + \rho A \int_0^l x \ddot{S}_{\Theta}(t, \theta) v(x) dx + \\ \gamma_2 I \int_0^l \dot{S}_d''''(t, x, \theta) v(x) dx + \gamma_1 \int_0^l \dot{S}_d(t, x, \theta) v(x) dx + \\ E I \int_0^l S_d''''(t, x, \theta) v(x) dx = 0. \end{aligned} \quad \text{Eq. 5-28}$$

Using integration by parts,  $\int_0^l S_d''''(t, x, \theta) v(x) dx = \int_0^l S_d''(t, x, \theta) v''(x) dx$  and  $\int_0^l \dot{S}_d''''(t, x, \theta) v(x) dx = \int_0^l \dot{S}_d'' v''(x) dx$ .

Substituting this into Eq. 5-28 gives

$$\begin{aligned} \rho A \int_0^l \ddot{S}_d(t, x, \theta) v(x) dx + \rho A \int_0^l x \ddot{S}_{\Theta}(t, \theta) v(x) dx + \\ \gamma_2 I \int_0^l \dot{S}_d''(t, x, \theta) v''(x) dx + \gamma_1 \int_0^l \dot{S}_d(t, x, \theta) v(x) dx + \\ E I \int_0^l S_d''(t, x, \theta) v''(x) dx = 0. \end{aligned} \quad \text{Eq. 5-29}$$

Let  $S_d(t, x, \theta) \approx S_d^N(t, x, \theta) = \sum_{i=1}^N e_i(t) \phi_i(x)$  so that Eq. 5-29 becomes

$$\begin{aligned} \rho A \int_0^l \ddot{S}_d(t, x, \theta) v(x) dx + \rho A \int_0^l x \ddot{S}_{\Theta}(t, \theta) v(x) dx + \\ \gamma_2 I \int_0^l \dot{S}_d''(t, x, \theta) v''(x) dx + \gamma_1 \int_0^l \dot{S}_d(t, x, \theta) v(x) dx + \\ E I \int_0^l S_d''(t, x, \theta) v''(x) dx = 0, \end{aligned} \quad \text{Eq. 5-30}$$

or

$$\begin{aligned} & \rho A \int_0^l \sum_{i=1}^N \ddot{e}_i(t) \phi_i(x) v(x) dx + \rho A x \int_0^l \ddot{S}_\Theta(t, \theta) v(x) dx + \\ & \gamma_2 I \int_0^l \sum_{i=1}^N \dot{e}_i(t) \phi_i''(x) v''(x) dx + \\ & \gamma_1 \int_0^l \sum_{i=1}^N \dot{e}_i(t) \phi_i(x) v(x) dx + EI \int_0^l e_i(t) \phi_i''(x) v''(x) dx = 0. \end{aligned} \quad \text{Eq. 5-31}$$

Now let  $v(x)$  range over  $\phi_j(x)$  for  $j = 1, 2, \dots, N$ , hence

$$\begin{aligned} & \rho A \int_0^l \sum_{i=1}^N \ddot{e}_i(t) \phi_i(x) \phi_j(x) dx + \rho A x \int_0^l \ddot{S}_\Theta(t, \theta) \phi_j(x) dx + \\ & \gamma_2 I \int_0^l \sum_{i=1}^N \dot{e}_i(t) \phi_i''(x) \phi_j''(x) dx + \\ & \gamma_1 \int_0^l \sum_{i=1}^N \dot{e}_i(t) \phi_i(x) \phi_j(x) dx + EI \int_0^l e_i(t) \phi_i''(x) \phi_j''(x) dx = 0. \end{aligned} \quad \text{Eq. 5-32}$$

Eq. 5-32 can be rewritten as

$$\begin{aligned} & \rho A M \begin{bmatrix} \ddot{e}_1(t) \\ \vdots \\ \ddot{e}_N(t) \end{bmatrix} + \rho A \ddot{S}_\Theta(t, \theta) S + EI K \begin{bmatrix} e_1(t) \\ \vdots \\ e_N(t) \end{bmatrix} + \gamma_1 M \begin{bmatrix} \dot{e}_1(t) \\ \vdots \\ \dot{e}_N(t) \end{bmatrix} + \\ & \gamma_2 K \begin{bmatrix} \dot{e}_1(t) \\ \vdots \\ \dot{e}_N(t) \end{bmatrix} = 0, \end{aligned} \quad \text{Eq. 5-33}$$

where  $M = \left[ \int_0^l \phi_i(x) \phi_j(x) dx \right]_{i,j=1}^N$ ,  $K = \left[ \int_0^l \phi_i''(x) \phi_j''(x) dx \right]_{i,j=1}^N$  and  $S = \left[ \int_0^l x \phi_j(x) dx \right]_{j=1}^N$ .

Rearranging Eq. 5-33 gives

$$\begin{aligned} \begin{bmatrix} \ddot{e}_1(t) \\ \vdots \\ \ddot{e}_N(t) \end{bmatrix} &= -\ddot{S}_\Theta(t, \theta) M^{-1} S - \frac{EI}{\rho A} M^{-1} K \begin{bmatrix} e_1(t) \\ \vdots \\ e_N(t) \end{bmatrix} - \frac{\gamma_1}{\rho A} \begin{bmatrix} \dot{e}_1(t) \\ \vdots \\ \dot{e}_N(t) \end{bmatrix} \\ &\quad - \frac{\gamma_2}{\rho A} M^{-1} K \begin{bmatrix} \dot{e}_1(t) \\ \vdots \\ \dot{e}_N(t) \end{bmatrix}. \end{aligned} \quad \text{Eq. 5-34}$$

Now, recall Eq. 5-16,

$$\ddot{\Theta}(t) = \frac{\gamma I}{J_0} \dot{d}'''(t, 0) + \frac{EI}{J_0} d'''(t, 0) + \frac{1}{J_0} u(t).$$

Now differentiating this with respect to the MinMax parameter  $\theta$  gives

$$\ddot{S}_{\Theta}(t, \theta) = \frac{\gamma I}{J_0} \dot{S}_d''(t, 0, \theta) + \frac{EI}{J_0} S_d''(t, 0, \theta) + \frac{1}{J_0} S_u(t). \quad \text{Eq. 5-35}$$

The derivation and definition of  $S_u(t, \theta)$  is given in Chapter 2.

Eq. 5-35 can be rewritten as

$$\ddot{S}_{\Theta}(t, \theta) = \frac{\gamma I}{J_0} \dot{S}_d''^N(t, 0, \theta) + \frac{EI}{J_0} S_d''^N(t, 0, \theta) + \frac{1}{J_0} S_u(t). \quad \text{Eq. 5-36}$$

or

$$\ddot{S}_{\Theta}(t, \theta) = \frac{\gamma I}{J_0} \sum_{i=1}^N \dot{e}_i(t) \phi_i''(0) + \frac{EI}{J_0} \sum_{i=1}^N e_i(t) \phi_i''(0) + \frac{1}{J_0} S_u(t, \theta). \quad \text{Eq. 5-37}$$

This equation can now be written as

$$\ddot{S}_{\Theta}(t, \theta) = \frac{\gamma I}{J_0} q \begin{bmatrix} \dot{e}_1(t) \\ \vdots \\ \dot{e}_N(t) \end{bmatrix} + \frac{EI}{J_0} q \begin{bmatrix} e_1(t) \\ \vdots \\ e_N(t) \end{bmatrix} + \frac{1}{J_0} S_u(t, \theta). \quad \text{Eq. 5-38}$$

Substituting this into Eq. 5-34 gives

$$\begin{bmatrix} \ddot{e}_1(t) \\ \vdots \\ \ddot{e}_N(t) \end{bmatrix} = - \left( \frac{\gamma I}{J_0} q \begin{bmatrix} \dot{e}_1(t) \\ \vdots \\ \dot{e}_N(t) \end{bmatrix} + \frac{EI}{J_0} q \begin{bmatrix} e_1(t) \\ \vdots \\ e_N(t) \end{bmatrix} + \frac{1}{J_0} S_u(t, \theta) \right) M^{-1} S - \frac{EI}{\rho A} M^{-1} K \begin{bmatrix} e_1(t) \\ \vdots \\ e_N(t) \end{bmatrix} - \frac{\gamma_1}{\rho A} \begin{bmatrix} \dot{e}_1(t) \\ \vdots \\ \dot{e}_N(t) \end{bmatrix} - \frac{\gamma_2}{\rho A} M^{-1} K \begin{bmatrix} \dot{e}_1(t) \\ \vdots \\ \dot{e}_N(t) \end{bmatrix}. \quad \text{Eq. 5-39}$$

Regrouping this equation gives

$$\begin{bmatrix} \ddot{e}_1(t) \\ \vdots \\ \ddot{e}_N(t) \end{bmatrix} = \left( -\frac{\gamma I}{J_0} q M^{-1} S - \frac{\gamma_1}{\rho A} - \frac{\gamma_2}{\rho A} M^{-1} K \right) \begin{bmatrix} \dot{e}_1(t) \\ \vdots \\ \dot{e}_N(t) \end{bmatrix} + \left( \frac{EI}{J_0} q M^{-1} S - \frac{EI}{\rho A} M^{-1} K \right) \begin{bmatrix} e_1(t) \\ \vdots \\ e_N(t) \end{bmatrix} + \frac{1}{J_0} S_u(t, \theta) M^{-1} S. \quad \text{Eq. 5-40}$$

We desire Eq. 5-40 to be a system of first order differential equations and so we define,

$S_{X_1}(t) = e(t)$  and  $S_{X_2}(t) = \dot{e}(t)$ . Eq. 5-40 now becomes



$$\begin{aligned}\dot{S}_{X_1}(t) &= S_{X_2} \\ \dot{S}_{X_2}(t) &= \left(-\frac{\gamma I}{J_0} q M^{-1} S - \frac{\gamma_1}{\rho A} - \frac{\gamma_2}{\rho A} M^{-1} K\right) S_{X_2}(t) + \left(\frac{EI}{J_0} q M^{-1} S + \right. \\ &\quad \left. \frac{EI}{\rho A} M^{-1} K\right) S_{X_1}(t) + \frac{1}{J_0} S_u(t, \theta) M^{-1} S.\end{aligned}\tag{Eq. 5-41}$$

The final complete system of equations (controlled and sensitivity equations) becomes

$$\begin{bmatrix} \dot{X}(t) \\ \dot{X}_c(t) \\ \dot{S}_X(t) \\ \dot{S}_{X_c}(t) \end{bmatrix} = \begin{bmatrix} A & -BK & 0 & 0 \\ FC & A_c & 0 & 0 \\ 0 & -BK_\theta & A & -BK \\ A_{c_1} & A_{c_2} & A_{c_3} & A_{c_4} \end{bmatrix} \begin{bmatrix} X(t) \\ X_c(t) \\ S_X(t) \\ S_{X_c}(t) \end{bmatrix},\tag{Eq. 5-42}$$

where  $K_\theta$ ,  $A_{c_1}$ ,  $A_{c_2}$ ,  $A_{c_3}$ , and  $A_{c_4}$  are derived and defined in Chapter 2.

Figure 5-12 shows the sensitivity results for the Euler Bernoulli Cantilevered beam with a rotating hub for varying  $\theta$ . The following initial conditions were used:

$$\begin{aligned}S_X(0, x, \theta) &= 0.75X(0, x), \text{ and} \\ S_{X_c}(0, x, \theta) &= 0.75X_c(0, x).\end{aligned}\tag{Eq. 5-43}$$

The results show that the sensitivity of the state is initially high then decreases rapidly with increasing time. This suggests that the system is closer to its desired equilibrium state as time elapses. The results for higher  $\theta$  values show slightly lower sensitivity than for lower  $\theta$ . The conclusion here is that the actual value of  $\theta$  chosen is not critical based on the sensitivity analysis.

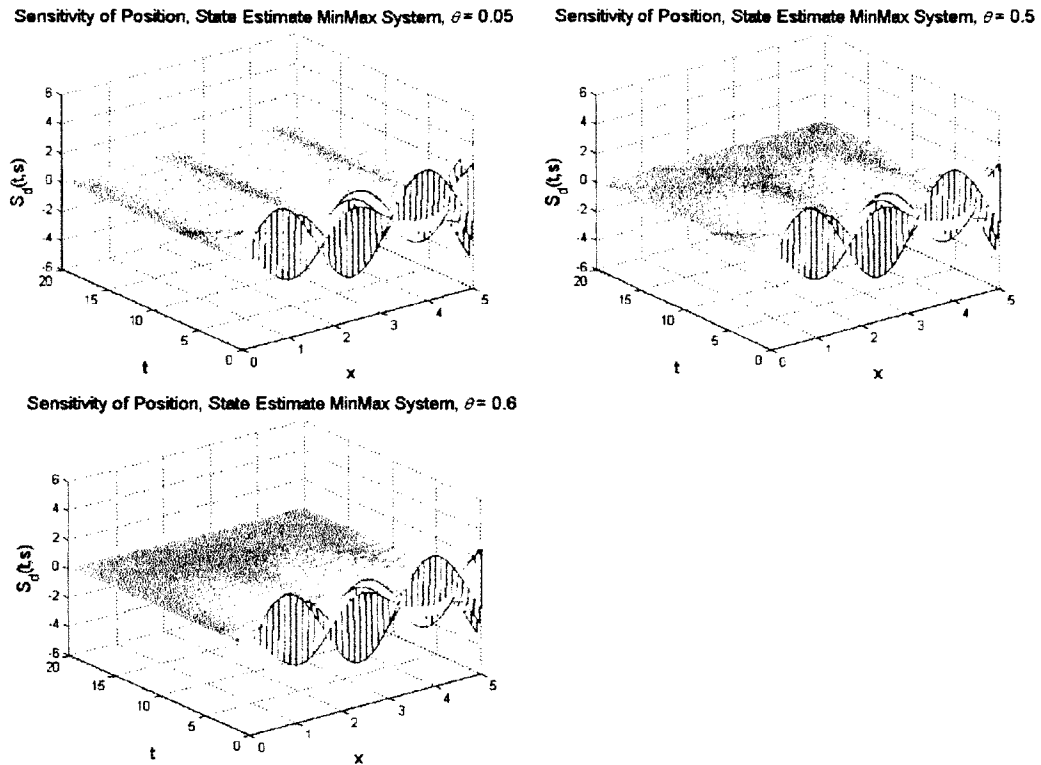


Figure 5-12: Sensitivity of state

Figure 5-13 shows the results for the controller sensitivity for various  $\theta$  values. As was done in the case of the control effort, we employ Simpson's rule to determine the area between the curve and the time axis. This area gives us the total sensitivity of the controller. Table 5-3 summarizes the results, where  $I$  gives the area obtained by Simpson's rule. The total area is calculated for each  $\theta$  value and recorded in the table.

As in the case of the control effort, the table shows that the change in the sensitivity results as  $\theta$  increases is not significant. The order of magnitude is the same. We draw the same conclusion, the actual value of  $\theta$  chosen is not critical based on these sensitivity results.

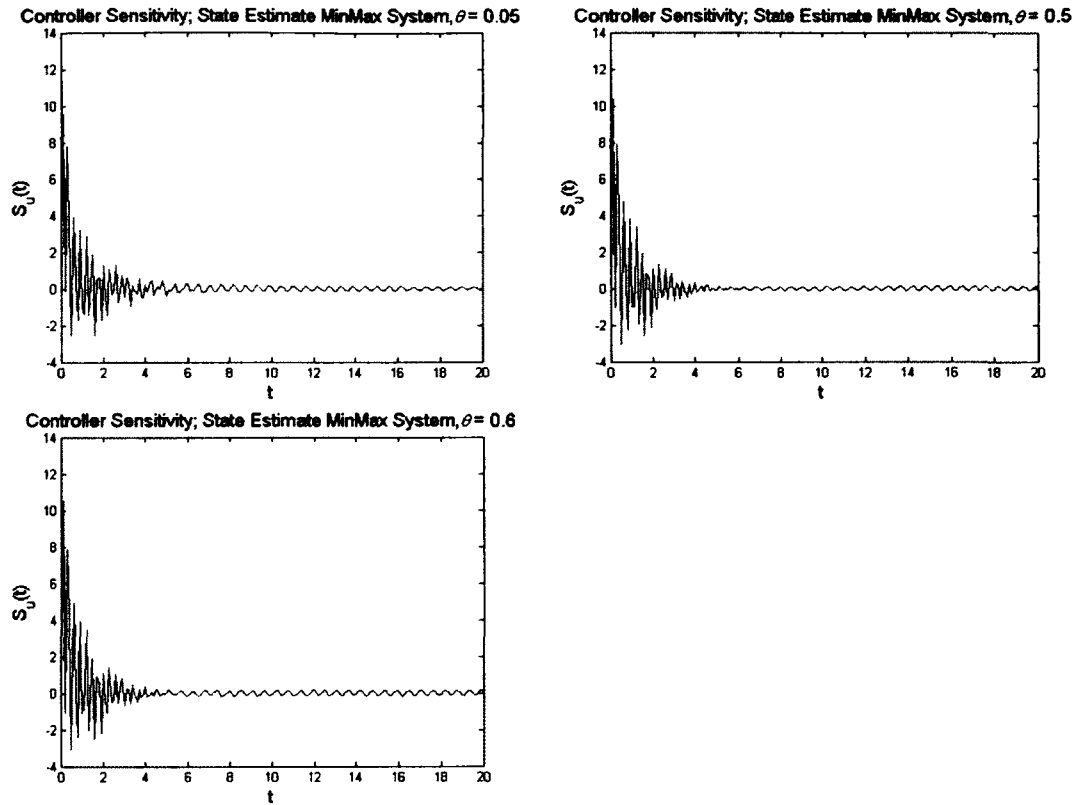


Figure 5-13: Controller sensitivity, state estimate MinMax

Table 5-3: Area under controller sensitivity curve (Simpson's rule)

Area Under Curve	$\theta_1 = 0.05$	$\theta_2 = 0.5$	$\theta_3 = 0.6$	% change from $\theta_1$ to $\theta_3$
$I_{controller}(full)$	2.650461	2.785177	2.809907	5.67
$I_{controller}(est)$	2.007114	2.171982	2.123014	5.46

Figures 5-14 and 5-15 show the maximum absolute controller sensitivity values with respect to  $\theta$  for both the full-state and the state estimate MinMax systems, respectively. In the case of the full-state system, as  $\theta$  increases, the maximum sensitivity slightly increases. In the case of the state estimate system, the maximum sensitivity increases gradually, then decreases. The overall change in maximum controller

sensitivity values for both cases is insignificant. This is in agreement with the previous results which show that the controller performance changes only slightly with changing  $\theta$ .

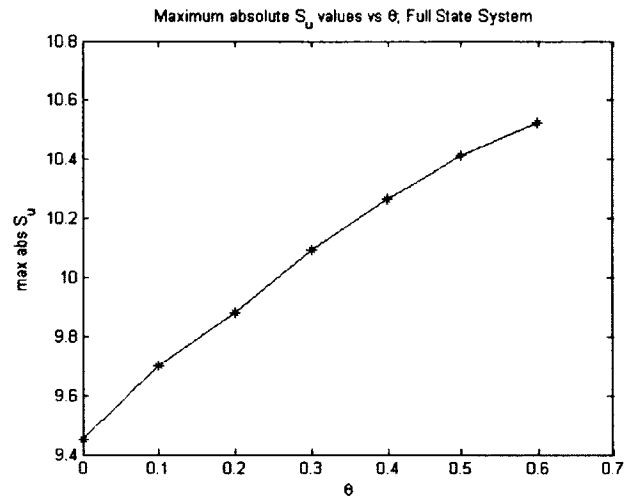


Figure 5-14: Maximum  $S_u(t)$  values, full state system

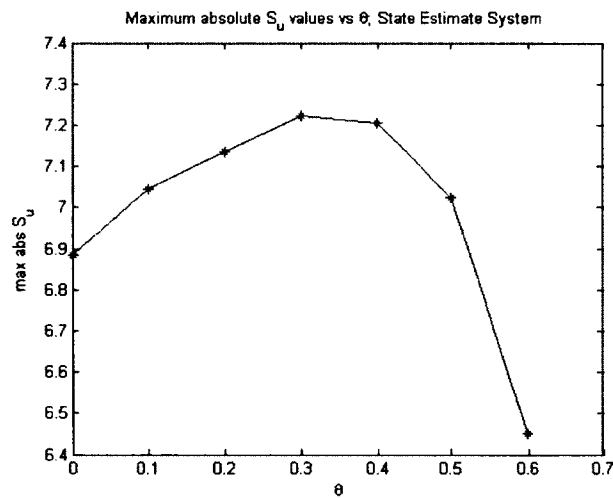


Figure 5-15: Maximum  $S_u(t)$  values, state estimate system

### 5.2.6 Riccati Sensitivity

As stated previously, the Algebraic Riccati Equations are a key component in the design of the controller as shown in Chapter 2. As a result we investigated the sensitivity of the Riccati equations with respect to  $\theta$ .

Figures 5-16 and 5-17 are plots of the maximum values of the sensitivities of the Riccati equations' solutions ( $P$  and  $\Pi$ , described fully in Chapter 2) to the MinMax parameter  $\theta$ . The results show that both maximum sensitivities increase with increasing  $\theta$ . The order of magnitude for the  $\Pi_{\theta}$  values does not change with respect to changes in  $\theta$ . Since  $\Pi$  directly affects the controller performance ( $u(t) = -R^{-1}B^T\Pi x_c$ ), the minimal variations in  $\Pi$  with respect to variations in  $\theta$  explains the unchanged controller performance as  $\theta$  changes. These results are in agreement with previous results and hence the same conclusion can be drawn: the actual value of  $\theta$  chosen is not critical regarding Riccati solution sensitivity.

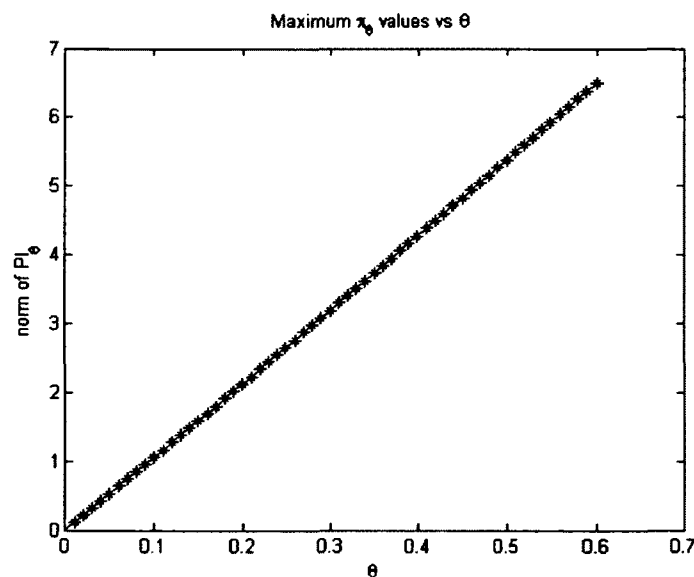


Figure 5-16: Norm of  $\Pi_{\theta}$  versus  $\theta$

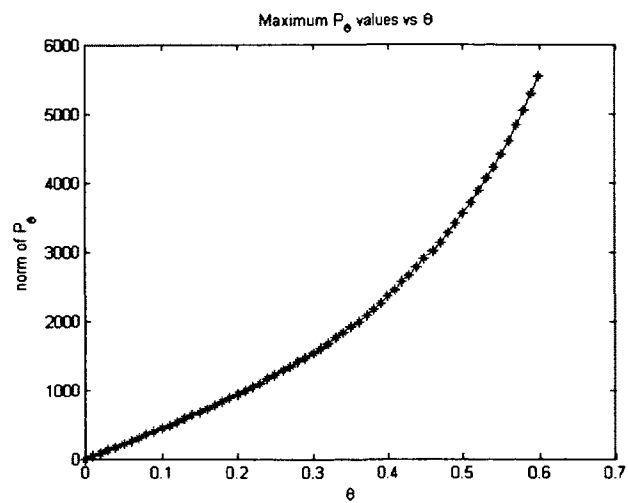


Figure 5-17: Norm of  $P_\theta$  versus  $\theta$

## CHAPTER 6

### CONCLUSIONS AND FUTURE WORK

#### 6.1 Conclusions

In this work, we have successfully computed an optimal MinMax controller using a Galerkin finite element scheme for the 1 and 2-dimensional heat equations, 1-dimensional wave equation with viscous damping, and the cantilevered Euler-Bernoulli beam with a torque control through a hub, including both Kelvin-Voigt and viscous damping. We then investigated the effects of variations in the MinMax parameter on control effort, controlled system stability (stability margin and radius), functional gains, and state position and/or velocity. We then applied Continuous Sensitivity Equation Methods to each finite dimensional approximation of the original four (4) infinite-dimensional PDEs. This was done in order to investigate the effects of variations in the MinMax parameter on the sensitivity of state position and/or velocity, controller sensitivity, and Riccati sensitivity. The results for all four sets of equations modeled in this work are conclusive. For each case the conclusions were similar:

1. Controller Performance

We found that varying  $\theta$  does not significantly affect the performance of the controller. In virtually all the cases, the system is driven towards equilibrium in about the same time.

## 2. Functional Gains

As mentioned in Chapter 2, the functional gains tell us whether the Galerkin finite element schemes, employed in this work to approximate the various infinite-dimensional Partial Differential Equations, are convergent as well as whether the controller employed is convergent. As a result, we plotted the functional gains for varying  $\theta$  values for each system. The results in each case showed that the functional gains were convergent for each  $\theta$  value for the given  $N$  values (where  $N$  is number of discretization intervals). More importantly, the gains were similar for the different  $\theta$  values. We therefore concluded that, in terms of functional gains and thus controller convergence, the actual value of  $\theta$  chosen is not critical.

## 3. Controlled System Stability

As previously stated, the controlled system must be stable in order for the other controlled results to be useful. We investigated the stability margin and stability radius for each system as  $\theta$  varied. We found that for all cases of  $\theta$ , the stability margin and radii were both similar or of the same order of magnitude. We therefore concluded that the actual value of  $\theta$  chosen had no significant effect on the stability of the system and thus was not critical.

## 4. Control Effort

We investigated the control effort  $u(t)$  for each controller implemented for varying  $\theta$ . In order to better analyze the results, we employed Simpson's rule for numerical integration to each graph. The results for each system showed that the control efforts were similar or of the same order of magnitude for varying  $\theta$  values. We therefore



concluded in the case of each system, that the actual value of  $\theta$  chosen was not critical in terms of control effort required for each particular design.

#### 5. Sensitivity of State

We employed Continuous Sensitivity Equation Methods, as outlined in Chapter 2, to each system under investigation. The results for the sensitivity of the state with respect to  $\theta$  showed similar state sensitivities for each control design with varying  $\theta$  values.

#### 6. Controller Sensitivity

We investigated the sensitivity of the controller with respect to varying  $\theta$  values. In order to better analyze the results, we employed Simpson's rule for numerical integration to each graph. In each case, we found that the controller sensitivities were all either similar or of the same order of magnitude. Surprisingly, the MinMax controller, which depends on  $\theta$ , was not significantly sensitive to different  $\theta$  values.

#### 7. Riccati Sensitivity

We investigated the sensitivity of the solution so the Riccati equations to variations in  $\theta$ . In particular, we were interested in the  $\Pi_\theta$  values since  $u(t) = -R^{-1}B^*\Pi x_c(t)$  suggesting that  $\Pi$  directly influences the control effort. Generally, the results showed that as  $\theta$  varies the sensitivities had similar orders of magnitude. We concluded therefore, that the actual value of  $\theta$  was not critical.

Although we have not obtained an explicit formula for the optimal  $\theta$  value, we have provided both quantitative and qualitative results that suggest that the optimal value in terms of stability, performance, and controller convergence is any  $\theta$  that satisfies the positive definite condition in the  $[I - \theta^2 P \Pi] > 0$ . This further suggests that there is no need to expend computational costs on choosing a  $\theta$  value. A low  $\theta$  value close to 0, such

as 0.05, can be chosen and the controlled system would exhibit excellent performance and stability properties, along with controller convergence.

## 6.2 Future Work

In [35], the conditioning of the MinMax Riccati Equations, the sensitivity of the eigenvalues of  $[I - \theta^2 P \Pi]$ , as well as the robustness of the controller with respect to variations in  $\theta$ . It was concluded that the optimal value of the MinMax parameter  $\theta$  was not necessarily crucial. In order to further the investigation, the systems in this dissertation would be analyzed using the methods in [35].

**APPENDIX A**  
**NUMERICAL MODELING OF EXACT**  
**SOLUTIONS**

## A.1 Exact Solutions

### A.1.1 Uncontrolled 1-dimension Heat Equation

The equation for the exact solution of the 1-dimensional Heat Equation is [40]:

$$U(t, x) = \sum_{m=1}^{\infty} a_m e^{-\left(\frac{m^2 \pi^2}{L^2}\right)kt} \sin\left(\frac{m\pi x}{L}\right),$$

$$a_m = \frac{2}{L} \int_0^L U^0(x) \sin\left(\frac{m\pi x}{L}\right) dx,$$

Eq. A-1

$$U^0(x) = 100.$$

Figure A-1 shows the simulation of the exact solution for the uncontrolled 1-dimensional heat equation. This result is similar to that of Figure 3-2, where a Galerkin finite element scheme was employed.

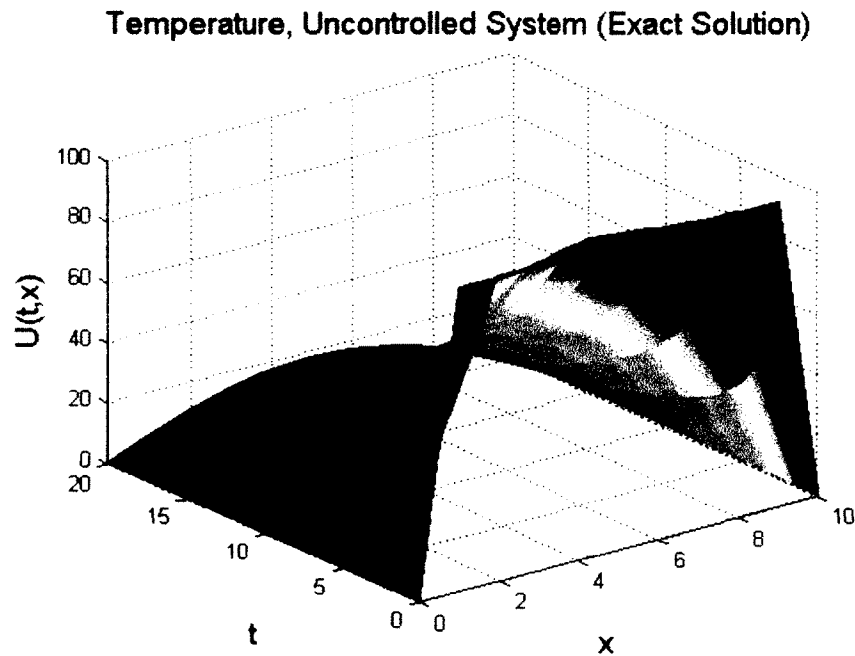


Figure A-1: Exact solution of uncontrolled heat in 1-d rod

### A.1.2 2-Dimensional Heat Equation

The equation for the exact solution of the uncontrolled 2-dimensional heat equation is [41]:

$$U(t, x, y) = \sum_0^{\infty} \sum_0^{\infty} A_m \sin\left(\frac{n\pi x}{L_x}\right) \sin\left(\frac{m\pi y}{L_y}\right) e^{-\left(\frac{n^2\pi^2 kt}{L_x} + \frac{m^2\pi^2 kt}{L_y}\right)},$$

$$U(t, 0, y) = U(t, L, y) = U(t, x, 0) = U(t, x, L) = 0,$$

Eq. A-2

$$U(0, x, y) = 100,$$

$$A_{mn} = \frac{4}{L^2} \int_0^{L_x} \int_0^{L_y} U(0, x, y) \sin\left(\frac{n\pi x}{L_x}\right) \sin\left(\frac{m\pi y}{L_y}\right) dx.$$

Figure A-2 shows the simulation of the exact solution for the 2-dimensional heat equation. This result is similar to that of Figure 3-33, where a Galerkin finite element scheme was employed.

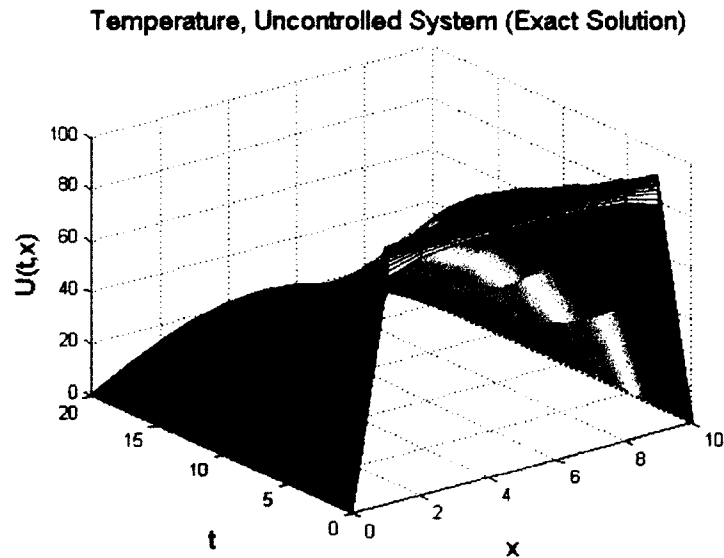


Figure A-2: Exact solution of uncontrolled heat on 2-d surface (along horizontal center)

### A.1.3 1-Dimensional Wave Equation

The equation for the exact solution of the 1-dimensional wave equation with viscous damping is [42]:

$$U(t, x) = \sum_{n=1}^{\infty} \sin\left(\frac{n\pi x}{L}\right) e^{-\frac{c^2 \gamma}{2} t} (a_n \sin(\mu_n t) + b_n \cos(\mu_n t))$$

$$U(t, 0) = 0$$

$$U(0, x) = f(x) = \sin x$$

$$\frac{\partial U(0, x)}{\partial x} = g(x) = \cos(x)$$

$$\gamma = 0.01.$$

Eq. A-3

$$\mu_n \equiv \frac{c\sqrt{4n^2\pi^2 - b^2L^2c^2}}{2L},$$

$$b_n = \frac{2}{L} \int_0^L \sin\left(\frac{n\pi x}{L}\right) f(x) dx,$$

$$a_n = \frac{2}{L\mu_n} \int_0^L \sin\left(\frac{n\pi x}{L}\right) \left( g(x) + \frac{c^2\gamma}{2} f(x) \right) dx.$$

Figure A-3 shows the simulation of the exact solution for the uncontrolled 1-dimensional wave equation with viscous damping. This result is similar to that of Figure 4-1, where a Galerkin finite element scheme was employed.

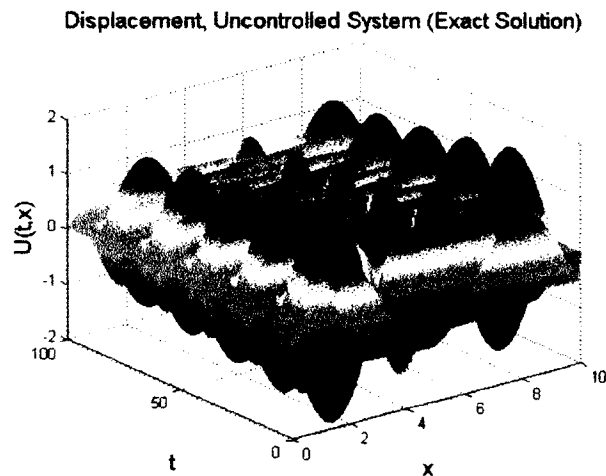


Figure A-3: Exact solution of displacement for 1-d wave equation

**APPENDIX B**

**FINITE DIFFERENCE SOLUTIONS**

## B.1 Finite Difference Solutions

In order to further verify the accuracy of the simulations in this work, we present the uncontrolled simulations of the heat and wave equations using the explicit Finite Difference scheme.

### B.1.1 1-dimensional heat equation

We used the explicit Finite Difference scheme to approximate the solution to the uncontrolled 1-dimensional heat equation

$$U_t(t, x) = kU_{xx}(t, x). \quad \text{Eq. B-1}$$

The resulting model formulation is

$$X_{t+1} = AX_t, \text{ where} \quad \text{Eq. B-2}$$

$$\begin{bmatrix} 1-2v & v & 0 & 0 & 0 & 0 & 0 & 0 & 0 & 0 \\ v & 1-2v & v & 0 & \cdot & \cdot & \cdot & 0 & 0 & 0 \\ 0 & v & 1-2v & v & \cdot & \cdot & \cdot & \cdot & \cdot & 0 \\ 0 & 0 & v & \cdot & v & 0 & \cdot & \cdot & \cdot & \cdot \\ 0 & 0 & 0 & \cdot & \cdot & \cdot & 0 & \cdot & \cdot & \cdot \\ \cdot & \cdot & 0 & 0 & \cdot & \cdot & \cdot & 0 & 0 & \cdot \\ \cdot & \cdot & \cdot & 0 & 0 & \cdot & \cdot & \cdot & 0 & \cdot \\ \cdot & \cdot & \cdot & \cdot & \cdot & 0 & \cdot & \cdot & v & 0 \\ \cdot & \cdot & \cdot & \cdot & \cdot & \cdot & 0 & v & 1-2v & v \\ 0 & 0 & 0 & 0 & 0 & \cdot & 0 & 0 & v & 1-2v \end{bmatrix} \quad \text{Eq. B-3}$$

The result is shown in Figure B-1. This is similar to the original result in Figure 3-2.



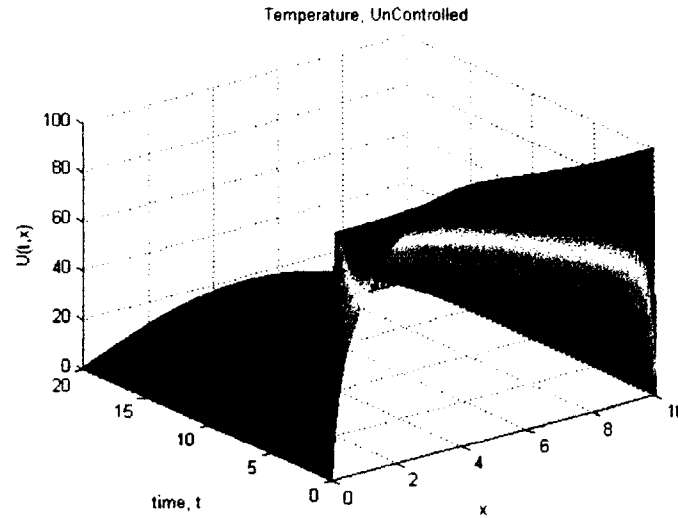


Figure B-1: Uncontrolled heat in 1-dimensional rod (explicit finite difference)

### B.1.2 2-Dimensional Heat Equation

In this section, the explicit scheme was used to simulate the uncontrolled 2-dimensional heat equation

$$\frac{\partial U(x, y, t)}{\partial t} = k \left[ \frac{\partial^2 U(x, y, t)}{\partial x^2} + \frac{\partial^2 U(x, y, t)}{\partial y^2} \right]. \quad \text{Eq. B-4}$$

This was modeled as

$$X_{t+1} = AX_t, \quad \text{Eq. B-5}$$

where



Figure B-3 shows the results. It is clear that this is similar to Figure 3-33.

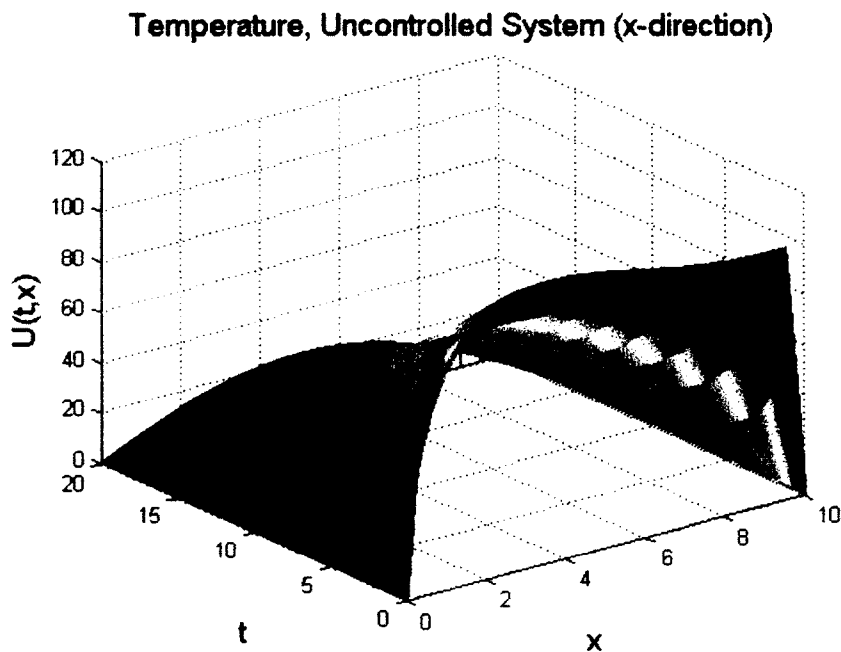


Figure B-3: Uncontrolled heat distribution across horizontal center of 2-dimensional square plate

### B.1.3 1-Dimensional Wave Equation

In this section we use the explicit scheme to solve the 1-dimensional uncontrolled wave equation with viscous damping,

$$\frac{\partial U(t,x)}{\partial x} = c^2 \frac{\partial^2 U(t,x)}{\partial x} - \gamma \frac{\partial U(t,x)}{\partial t}. \quad \text{Eq. B-7}$$

We formulate Eq. B-7 as

$$X_{t+1} = AX_t, \quad \text{Eq. B-8}$$

where

$$\begin{bmatrix}
 1 & 0 & 0 & 0 & 0 & \Delta t & 0 & 0 & 0 & 0 \\
 0 & 1 & 0 & 0 & 0 & 0 & \Delta t & 0 & 0 & 0 \\
 0 & 0 & 1 & 0 & 0 & 0 & 0 & \Delta t & 0 & 0 \\
 0 & 0 & 0 & 1 & 0 & 0 & 0 & 0 & \Delta t & 0 \\
 0 & 0 & 0 & 0 & 1 & 0 & 0 & 0 & 0 & \Delta t \\
 -2v & v & 0 & 0 & 0 & 1-\gamma & 0 & 0 & 0 & 0 \\
 v & -2v & v & 0 & 0 & 0 & 1-\gamma & 0 & 0 & 0 \\
 0 & v & -2v & v & 0 & 0 & 0 & 1-\gamma & 0 & 0 \\
 0 & 0 & v & -2v & v & 0 & 0 & 0 & 1-\gamma & 0 \\
 0 & 0 & 0 & v & -2v & 0 & 0 & 0 & 0 & 1-\gamma
 \end{bmatrix} \cdot \quad \text{Eq. B-9}$$

The matrix of Eq. B-9 was computed for a spatial discretization of  $N = 5$  intervals. The actual simulation was obtained with  $N = 40$  intervals. Figure B-4 shows the resulting simulation. The figure is similar to Figure 4-2.

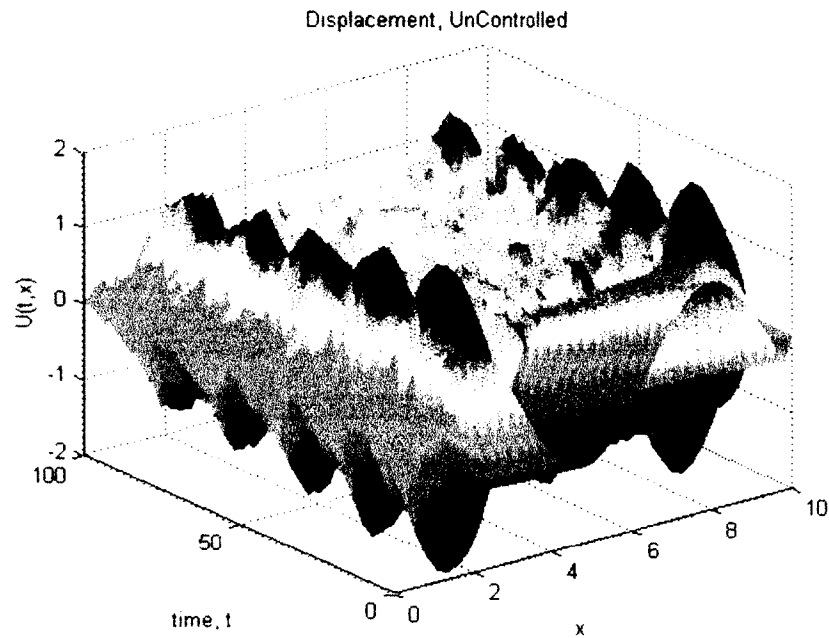


Figure B-4: Uncontrolled displacement (explicit finite difference scheme)

## BIBLIOGRAPHY

1. Gibson, J. S. and Adamian, A. *Approximation theory for linear quadratic gaussian control of flexible structures*. 1991. pp. 1-37. Vol. 29.
2. Kwakernaak, Huibert and Sivan, Raphael. *Linear Optimal Control Systems*. First Edition: Wiley-Interscience, 1972.
3. Sontag, Eduardo. *Mathematical Control Theory: Deterministic Finite Dimensional Systems*. second: Springer, 1998.
4. Skogestad, S and Postlethwaite, I. *Multivariable Feedback Control*. Chichester : John Wiley and Sons, 1996.
5. Curtain, R. F. and Zwart, H. J. *An Introduction to Infinite-Dimensional Systems Theory*. New York : Springer-Verlag, 1995.
6. Rhee, I and Speyer, J. *A game theoretic controller and its relationship to h-infinity and linear-exponential-gaussian synthesis*. 1989. pp. 909-915.
7. Chung, Walter H. and Speyer, Jason L. *A Game Theoretic Fault Detection Filter*. 1998. Vol. 43.
8. King, Belinda B. and Ou, Yuh-Roung. *Nonlinear Dynamic Compensator Design for FLOW Control in a Driven Cavity*. New Orleans : s.n., 1995.
9. Evans, K. A. *Sensitivity Analysis for control parameter determination for a Nonlinear Cable-Mass System*. St. Louis : s.n., 2009. pp. 4091-4096.
10. Yaesh, I. and Shaked, U. *Discrete-Time Min-Max Tracking*. 2006.
11. Witsenhausen, Hans S. *A Minmax Control Problem for Sampled Linear Systems*. 1968. Vol. AC013.
12. Bemporad, Alberto, Borrelli, Francesco and Morari, Manfred. *Min-Max Control of Constrained Uncertain Discrete-Time Linear Systems*. 2003. Vol. 48.
13. Blondel, Vincent D. and Megretski, Akexandre. *Unsolved Problems in Mathematical Systems and Control Theory*. Princeton and Oxford : Princeton University Press.

15. Hammer, P. Parameter Identification in Parabolic Partial Differential Equations Using Quasilinearization. *Ph.D Thesis*. Blackburg, Virginia, USA : Virginia Polytechnic Institute and State University, 1995.
16. Coleman, T., Santosa, F. and Verma, A. *semi-automatic differentiation*. Birkhauser, Boston:1998. pp. 113-126.
17. Hovland, P., Mohammadi, B. and Bischof, C. *Automatic differentiation and navier-stokes computations*. Birkhauser, Boston:1998. pp. 265-284.
18. Borggaard, J. T. *The Sensitivity Equation Method for Optimal Design*. Blackburg : Virginia Polytechnic Institute and State University, 1994.
19. Borggaard, J. T. and Burns, J. A. *A sensitivity equation approach to optimal design of nozzles*. 1994. pp. 232-241.
20. Borggaard, J. T. *A PDE sensitivity equation method for optimal aerodynamic design*. 1997. pp. 366-384.
21. Stanley, Lisa G. Computational Methods for Sensitivity Analysis with Applications to Elliptic Boundary Value Problems. *Ph.D. Dissertation*. s.l., Virginia, USA : Virginia Polytechnic Institute and State University, July 8, 1999.
22. Wolka, J. *Partial Differential Equations*. Cambridge : Cambridge University Press, 1987.
23. Pazy, A. *Semigroups of Linear Operators and Applications to Partial Differential Equations*. New York : Springer-Verlag, 1983.
24. Bernal, Anibal Rodriguez. *Introduction to semigroup theory for partial differential equations*. Madrid : Universidad Complutense de Madrid.
25. Phillips, Ralph S. *Semigroup methods in the theory of partial differential equations. Modern Mathematics for the engineer. Second series*. New York : McGraw-Hill, 1961. pp. 100-132.
26. Mizohata, Sigeru. *The theory of partial differential equations*. Tokyo : Iwanami Shoton, 1965.
27. Hernandez, Erwin and Otarola, Enrique. *Numerical approximation of the LQR problem in a strongly damped wave equation*. 2008.
28. Fahroo, F. and Wang, Yun. *Optimal location of piezoceramic actuators for vibration suppression of a flexible structure*. 1997.
29. Salmon, D. M. *MinMax Controller Design*. 1968. Vols. AC-13, No. 4. 4.
30. Bubnicki, Zdzislaw. *Modern Control Theor.* : Springer-Verlag, 2005.

31. Engelberg, Shlomo. *A Mathematical Introduction to Control Theory*. s.l. : Imperial College Press, 2005.
32. Evans, Katie A. *Reduced Order Controllers for Distributed Parameter Systems*. *Ph.D Dissertation*. Virginia Polytechnic Institute and State University, Virginia, USA : 2003. Ph.D. Dissertation.
33. Hinrichsen, D. and Pritchard, A. J. *Stability radii of linear systems*. 1986. Vol. 1.
34. Ruggiero, Eric J. *LQR control and judicious sensor placement derived from functional gain analysis for a 1D active membrane*. 2007.
35. Zietsman, L, et al. *Riccati Conditioning and Sensitivity for a MinMax Controlled Cable-Mass Systems*. 2008.
36. Dai, Weizhong, Kaliq, Abdul and Nassar, Raja. *An Introduction to Finite Element Method*. Ruston : Louisiana Tech University. 2010
37. Ray, Cody W. *Modeling and Control of a Biologically inspired Compliant Structure*. *Master's Thesis*, Oregon, USA : Oregon State University, April 2009.
38. King, Belinda B. *Modeling and Control of Multiple Control Component Structures*. s.l. : Clemson University, 1991.
39. Yuksel, Sefaaddin and Aksoy, Taylan Mete. *Flexural Vibrations of a Rotating Beam Subjected to Different Base Excitations*. Ankara, Turkey : G.U. Journal of Science, 2009. pp. 33-40. Vol. 22.
40. Abrahamson, Adam and Richards, David. *The One Dimensional Heat Equation*. 2002.
41. Hancock, Matthew J. *The heat and wave equations in 2D and 3D*. MIT : Fall, 2006.
42. <http://mathworld.wolfram.com/WaveEquation1-Dimensional.html>.
43. Inman, D. J. *Engineering vibration* : Prentice-Hall, 1994.
44. Kim, Ki Baek, Lee, Jae-Won and Kwon, Wook Hyun. *Interval Receding Horizon H-infinity Tracking Control for Discrete Linear Periodic Systems*. 2002
45. Lions, J. L. *Optimal Control of Systems Governed by Partial Differential Equations*. Berlin : Springer-Verlag, 1971.
46. Morton, K W and Mayers, D F. *Numerical Solution of Partial Differential Equations* : Cambridge University Press, 1994.
47. Ganesan, K. *On Some Properties of Interval Matrices*. 2007. Vol. 1.

48. Bensoussan, A., et al. *Representation and Control of Infinite Dimensional Systems*. Birkhauser, Boston :1992. Vol. 1.
49. Zames, G. *Feedback and optimal sensitivity: model reference transformations, multiplicative seminorms and appropriate inverses*. 1981. pp. 301-320. Vol. 26.
50. Zhang, Da-Qing. *Controllability and Quadratic Stabilization of discrete-time interval systems and LMI approach*. 2006. pp. 413-431.